UNIVERSIDADE ESTADUAL PAULISTA ‘‘JÚLIO DE MESQUITA FILHO’’
FACULDADE DE ENGENHARIA
CAMPUS DE ILHA SOLTEIRA

LUIS GUSTAVO GIACON VILLANI

ROBUST DAMAGE DETECTION IN UNCERTAIN NONLINEAR SYSTEMS

ILHA SOLTEIRA
2019

LUIS GUSTAVO GIACON VILLANI

ROBUST DAMAGE DETECTION IN UNCERTAIN NONLINEAR SYSTEMS

Thesis presented to the Faculdade de Engenharia de Ilha Solteira - UNESP as a part of the requirements for obtaining the Doctorate in Mechanical Engineering.
Knowledge area: Solid Mechanics.

Advisor: Prof. Dr. Samuel da Silva
Co-advisor: Prof. Dr. Americo Barbosa da Cunha Junior

ILHA SOLTEIRA

2019

FICHA CATALOGRÁFICA
Desenvolvido pelo Serviço Técnico de Biblioteca e Documentação

Villani, Luis Gustavo Giacon.
V716R Robust damage detection in uncertain nonlinear systems =Detecção robusta de danos em sistemas não lineares incertos / Luis Gustavo Giacon Villani. -- Ilha Solteira: [s.n.], 2019
139 f. : il.

Tese (doutorado) - Universidade Estadual Paulista. Faculdade de Engenharia de Ilha Solteira. Área de conhecimento: Mecânica dos Sólidos, 2019

Orientador: Samuel da Silva
Co-orientador: Americo Barbosa da Cunha Junior
Inclui bibliografia

1. Stochastic volterra series. 2. Uncertainty quantification. 3. Nonlinear systems. 4. Robust damage detection.

João Josué Barbosa
Serviço Técnico de Biblioteca e Documentação

unesp

UNIVERSIDADE ESTADUAL PAULISTA

Câmpus de Ilha Solteira

CERTIFICADO DE APROVAÇÃO

TÍTULO DA TESE: Robust Damage Detection in Uncertain Nonlinear Systems

AUTOR: LUIS GUSTAVO GIACON VILLANI
ORIENTADOR: SAMUEL DA SILVA
COORIENTADOR: AMERICO BARBOSA DA CUNHA JUNIOR

Aprovado como parte das exigências para obtenção do Título de Doutor em ENGENHARIA MECÂNICA, área: Mecânica dos Sólidos pela Comissão Examinadora:

Prof. Dr. SAMUEL DA SILVA
Departamento de Engenharia Mecânica / Faculdade de Engenharia de Ilha Solteira - UNESP

Prof. Dr. JOAO ANTONIO PEREIRA
Departamento de Engenharia Mecânica / Faculdade de Engenharia de Ilha Solteira - UNESP

Prof. Dr. JOSÉ MARIA CAMPOS DOS SANTOS
Departamento de Mecânica Computacional / Universidade Estadual de Campinas - UNICAMP

Prof. Dr. MÁRIO ANDERSON DE OLIVEIRA
Departamento de Eletroeletrônica / Instituto Federal de Educação, Ciência e Tecnologia de Mato Grosso - IFMT

Prof. Dr. THIAGO GAMBOA RITTO
Departamento de Engenharia Mecânica / Universidade Federal do Rio de Janeiro - UFRJ

Ilha Solteira, 10 de dezembro de 2019

To my parents and my wife.

ACKNOWLEDGMENTS

I would like to thank my advisor Prof. Samuel da Silva for the last 7 years of mentoring and friendship. For all motivation, help, and guidance during this research. I am sure that this work would not be possible without his support.

I would like to say thanks to my co-advisor Prof. Americo Cunha Jr for helping me with the uncertainty analysis topic and Prof. Michael Todd for the support during my internship at the University of California San Diego.

My thanks in particular to my parents, Sueli and Giovanni, for all support given during my whole life, I am sure that this victory is more theirs than mine. To my wife, Adriana, for all the patience, partnership, and care; her courage to leave everything and follow me is, and always will be, my inspiration to look for my dreams. To my sister, Lais, and all my family for always wish the best for me.

My sincere thanks to all my friends from my "República", friends of the Group of Intelligent Materials and Systems (GMSINT), Department of Mechanical Engineering, and University of California San Diego.

Finally, I would also like to thank the financial support provided by the São Paulo Research Foundation (FAPESP) during the direct doctorate (grant number 2015/25676-2[1]), internship at University of California San Diego (2017/24977-4[2]), scientific initiation (grant numbers 2012/25483-1[3] and 2014/03179-4[4]) and research aid (grant number 2012/09135-3[5]). I also acknowledge the Coordenação de Aperfeiçoamento de Pessoal de Nível Superior - Brasil (CAPES) - Finance Code 001.

[1]https://bv.fapesp.br/pt/bolsas/163108
[2]https://bv.fapesp.br/pt/bolsas/176101
[3]https://bv.fapesp.br/pt/bolsas/140752
[4]https://bv.fapesp.br/pt/bolsas/151042
[5]https://bv.fapesp.br/pt/auxilios/55159

ABSTRACT

Structural Health Monitoring (SHM) methodologies aim to develop techniques able to detect, localize, quantify and predict the progress of damages in civil, aerospatial and mechanical structures. In the hierarchical process, the damage detection is the first and most important step. Despite the existence of numerous methods of damage detection based on vibration signals, two main problems can complicate the application of classical approaches: the *nonlinear phenomena* and the *uncertainties*. This thesis demonstrates the importance of the use of a stochastic nonlinear model in the damage detection problem considering the intrinsically nonlinear behavior of mechanical structures and the measured data variation. A new stochastic version of the Volterra series combined with random Kautz functions is proposed to predict the behavior of nonlinear systems, considering the presence of uncertainties. The stochastic model proposed is used in the damage detection process based on hypothesis tests. Firstly, the method is applied in a simulated study assuming a random Duffing oscillator exposed to the presence of a breathing crack modeled as a bilinear oscillator. Then, an experimental application considering a nonlinear beam subjected to the presence of damage with linear characteristics (loss of mass in a bolted connection) is performed, with the direct comparison between the results obtained using a deterministic and a stochastic model. Finally, an experimental application considering a nonlinear beam subjected to the presence of nonlinear damage (a breathing crack) is carried out. In all the applications, the comparison between the use of linear and nonlinear models is held, revealing the better results obtained when one considers the nonlinearities in the analysis. Furthermore, although the reference stochastic model is always the same, the methodology to detect the damage changes from one application to another, showing the evolution of the proposed approach during the research. The method presented satisfactory results in all the conditions studied, representing an improvement in the damage detection area considering nonlinearities and uncertainties at the same time.

Keywords: Stochastic Volterra series. Uncertainty quantification. Nonlinear systems. Robust damage detection.

RESUMO

As metodologias de Monitoramento da Integridade Estrutural (SHM[1]) visam desenvolver técnicas capazes de detectar, localizar, quantificar e prever o progresso de danos em estruturas civis, aeroespaciais e mecânicas. Nesse processo hierárquico, a detecção de danos é o primeiro e mais importante passo. Apesar da existência de inúmeros métodos de detecção de danos baseados em sinais de vibração, dois problemas principais podem complicar a aplicação de abordagens clássicas: os *fenômenos não lineares* e as *incertezas*. Esta tese demonstra a importância do uso de um modelo não linear estocástico no problema de detecção de danos, considerando o comportamento intrinsecamente não linear de estruturas mecânicas e a variação dos dados medidos. Uma nova versão estocástica das séries de Volterra, combinada com funções aleatórias de Kautz, é proposta para prever o comportamento de sistemas não lineares, considerando a presença de incertezas. O modelo estocástico proposto é utilizado no processo de detecção de danos com base em testes de hipótese. Primeiramente, o método é aplicado em um estudo simulado, assumindo um oscilador Duffing aleatório exposto à presença de uma trinca respiratória modelada como um oscilador bilinear. Em seguida, uma aplicação experimental é realizada considerando uma viga não linear sujeita à presença de um dano com características lineares (perda de massa em uma conexão parafusada), com a comparação direta entre os resultados obtidos utilizando um modelo determinístico e um estocástico. Por fim, uma aplicação experimental considerando uma viga não linear sujeita à presença de um dano não linear (uma trinca respiratória) é realizada. Em todas as situações, a comparação entre o uso de modelos lineares e não lineares é mostrada, revelando os melhores resultados obtidos quando as não linearidades são consideradas. Além disso, embora o modelo estocástico de referência seja sempre o mesmo, a metodologia para detectar os danos muda de uma aplicação para outra, mostrando a evolução da abordagem proposta durante a pesquisa. O método apresentou resultados satisfatórios em todas as situações estudadas, representando uma melhoria na área de detecção de danos, considerando não linearidades e incertezas ao mesmo tempo.

Palavras-Chave: Séries de Volterra estocásticas. Quantificação de incertezas. Sistemas não lineares. Detecção robusta de danos.

[1]do inglês, *Structural Health Monitoring*

LIST OF FIGURES

LIST OF TABLES

LIST OF ACRONYMS

ANN	-	Artificial Neural Network
FRF	-	Frequency Response Function
GP-NARX	-	Gaussian Process - Nonlinear Autoregressive with Exogenous input model
HB	-	Harmonic Balance
HOFRFs	-	High-Order Frequency Response Functions
MC	-	Monte Carlo
MCMC	-	Monte Carlo Markov Chain
MM	-	Multiple Models
PCA	-	Principal Component Analysis
PCE	-	Polynomial Chaos Expansion
PDF	-	Probability Density Function
POD	-	Proper Orthogonal Decomposition
RSF	-	Restoring Force Surface
SDoF	-	Single-Degree-of-Freedom
DoFs	-	Degrees-of-Freedom
SHM	-	Structural Health Monitoring

LIST OF SYMBOLS

a_η	-	Parameter of the Kautz orthonormal function
$\mathcal{B}_\eta$	-	Deterministic η-order Volterra kernel in the orthonormal basis
$\mathbb{B}_\eta$	-	Random η-order Volterra kernel in the orthonormal basis
b_η	-	Parameter of the Kautz orthonormal function
$\mathbb{C}$	-	Principal components in the reference condition
$\mathcal{C}$	-	Principal components in an unknown condition
c_1	-	Deterministic damping coefficient
$\mathbb{c}_1$	-	Random damping coefficient
$conv(.)$	-	Monte Carlo convergence function
$\mathcal{D}^2$	-	Mahalanobis squared distance calculated in an unknown condition
$\mathbb{D}^2$	-	Mahalanobis squared distance calculated in the reference condition
$\mathcal{D}$	-	Standardized Euclidean distance calculated in an unknown condition
$\mathbb{D}$	-	Standardized Euclidean distance calculated in the reference condition
d^2	-	A realization of the Mahalanobis squared distance in the reference condition
d	-	A realization of the standardized Euclidian distance in the reference condition
$\exp(.)$	-	Exponential function
$e_{\eta,ref}$	-	Prediction error calculated in the reference condition
$e_{\eta,unk}$	-	Prediction error calculated in an unknown condition
F_s	-	Sampling frequency
g	-	Three-dimensional surface
$\mathcal{F}$	-	Deterministic restoring force
$\mathbb{F}$	-	Random restoring force
$\mathcal{G}$	-	Deterministic bilinear force
$\mathbb{G}$	-	Random bilinear force
H_0	-	Null hypothesis
H_1	-	Alternative hypothesis
$\mathcal{H}_\eta$	-	η-order deterministic Volterra kernel in the discrete-time formulation
h	-	Impulse response function
$\mathbb{I}$	-	Damage index calculated in the reference condition

$\mathcal{I}$ - Damage index calculated in an unknown condition

$\mathbf{J}$ - Objective function

J_η - Number of orthonormal functions to represent the η-th Volterra kernel

K - Kernel used in the density estimation

k - Discrete-time

k_1 - Deterministic linear stiffness

$\mathbb{k}_1$ - Random linear stiffness

k_2 - Deterministic quadratic stiffness

$\mathbb{k}_2$ - Random quadratic stiffness

k_3 - Deterministic cubic stiffness

$\mathbb{k}_3$ - Random cubic stiffness

$\boldsymbol{L}$ - Cholesky decomposed matrix

l - Deterministic input signal filtered by the orthonormal function

$\mathbb{l}$ - Random input signal filtered by the orthonormal function

m_1 - Deterministic input equivalent mass

$\max(.)$ - Maximum operator

$\mathbb{m}_1$ - Random equivalent mass

N_s - Number of Monte Carlo simulations

N_η - Memory length of the η-order Volterra kernel in the discrete-time formulations

n_1 - First-order sample delay in the discrete-time formulation of Volterra series

n_η - η-order sample delay in the discrete-time formulation of Volterra series

n_{pca} - Number of the PCA component

$\mathbb{P}$ - Probability measure

$P_{\mathbb{V}}(dv)$ - Probability distribution of $\mathbb{V}$

p_1 - Coefficient of second kernel frequency

p_2 - Coefficient of second kernel damping

p_3 - Coefficient of third kernel frequency

p_4 - Coefficient of third kernel damping

P_c - Percentile

p - Probability measure

$\mathbb{q}$ - Generic random variable

q - Generic variable

$\mathcal{S}_\eta$ - Kautz pole in the continuous-frequency domain

$p_V(v)$ - Probability density function of $\mathbb{V}$

$\mathbb{R}$ - Real numbers set

$\boldsymbol{R}$ - Correlation matrix

r - Smoothing parameter

$\boldsymbol{S}$ - Matrix of random variables

$\tilde{\boldsymbol{S}}$ - Normalized matrix of random variables

s - Integration variable

$\boldsymbol{T}$ - Matrix of correlated random variables

$\tilde{\boldsymbol{T}}$ - Normalized matrix of correlated random variables

t - Time

U - External force

u - Volterra model input

V - Matrix with the standard deviations

$\mathcal{X}^2$ - Chi-square distribution

x - Deterministic displacement of the Duffing oscillator

$\mathbb{x}$ - Random displacement of the Duffing oscillator

$\dot{x}$ - Deterministic velocity of the Duffing oscillator

$\dot{\mathbb{x}}$ - Random velocity of the Duffing oscillator

$\ddot{x}$ - Deterministic acceleration of the Duffing oscillator

$\ddot{\mathbb{x}}$ - Random acceleration of the Duffing oscillator

y_{exp} - Experimental output

y_{exp}^{ref} - Experimental output measured in the reference condition

y_{exp}^{unk} - Experimental output measured in an unknown condition

y - Deterministic Volterra model output

$\mathbb{y}$ - Random Volterra model output

y_{lin} - First-order Volterra model output in an unknown condition

$\mathbb{y}_{lin}$ - Random first-order Volterra model output in the reference condition

y_{quad} - Second-order Volterra model output in an unknown condition

$\mathbb{y}_{quad}$ - Random quadratic-order Volterra model output in the reference condition

y_{cub} - Third-order Volterra model output in an unknown condition

$\mathbb{y}_{cub}$ - Random third-order Volterra model output in the reference condition

y_{nl} - Nonlinear contribution to the total Volterra model output in an unknown condition

$\mathbb{y}_{nl}$ - Random nonlinear contribution to the total Volterra model output in the reference condition

y_η - Deterministic η-order Volterra model output

$\mathbb{y}_\eta$ - Random η-order Volterra model output

$\mathbb{Z}_+$ - Nonnegative integers numbers set

$\mathcal{Z}_\eta$ - Kautz pole in the discrete-frequency domain

$\bar{\mathcal{Z}}_\eta$ - Complex conjugate of the Kautz pole in the discrete-frequency domain

z - complex variable in the discrete-frequency domain

GREEK LETTERS

β - Probability of false alarms

$\mathbf{\Gamma}$ - Matrix containing the regressors terms $l_{i_j}(k)$ of inputs filtered by Kautz functions

Γ - Gamma distribution

$\mathbf{\Phi}$ - Vector with the coefficients of the orthonormal Volterra kernels

$\mathbf{\Phi}_1$ - Vector with the coefficients of the first orthonormal Volterra kernel

$\mathbf{\Phi}_2$ - Vector with the coefficients of the second orthonormal Volterra kernel

$\mathbf{\Phi}_3$ - Vector with the coefficients of the third orthonormal Volterra kernel

$\mathbf{\Upsilon}$ - Matrix with regressors $[x\ x^2\ x^3]$

$\mathbf{\Xi}$ - Vector with estimated parameters $\{k_1\ k_2\ k_3\}^{\mathrm{T}}$

$\delta_{(.)}$ - Dispersion operator

η - Order of the Volterra series expansion

Λ - Threshold value

λ_{lin} - Linear Volterra kernels' coefficients estimated in an unknown condition

$\mathbb{\lambda}_{lin}$ - Random linear Volterra kernels' coefficients estimated in the reference condition

λ_{quad} - Quadratic Volterra kernels' coefficients estimated in an unknown condition

$\mathbb{\lambda}_{quad}$ - Random quadratic Volterra kernels' coefficients estimated in the reference condition

λ_{cub} - Cubic Volterra kernels' coefficients estimated in an unknown condition

$\mathbb{\lambda}_{cub}$ - Random cubic Volterra kernels' coefficients estimated in the reference condition

λ_{nl} - Nonlinear Volterra kernels' coefficients estimated in an unknown condition

$\mathbb{\lambda}_{nl}$ - Random nonlinear Volterra kernels' coefficients estimated in the reference condition

$\mu_{(.)}$ - Mean operator

Ψ - Orthonormal function in the discrete-frequency domain

ψ - Deterministic orthonormal function in the discrete-time domain

$\mathbb{\psi}$ - Random orthonormal function in the discrete-time domain

Θ - Sample space

θ - random realization

$\mathbf{\Sigma}$ - Covariance matrix

$\mathbb{\Sigma}$ - σ-algebra

$\sigma_{(.)}$ - Standard deviation operator

ζ - Deterministic damping ratio of the equivalent linear system

$\mathfrak{\zeta}$ - Random damping ratio of the equivalent linear system

ω_d - Deterministic damped natural frequency of the equivalent linear system

ω_n - Deterministic natural frequency of the equivalent linear system

$\mathfrak{\omega}_n$ - Random natural frequency of the equivalent linear system

ω_η - Deterministic frequency representing the η-order Volterra kernel in the orthonormal basis

ξ_η - Deterministic damping representing the η-order Volterra kernel in the orthonormal basis

$\mathfrak{\omega}_\eta$ - Random frequency representing the η-order Volterra kernel in the orthonormal basis

$\mathfrak{\xi}_\eta$ - Random damping representing the η-order Volterra kernel in the orthonormal basis

γ_η - Deterministic damage index

ν - Degrees-of-freedom of the chi-square distribution

CONTENTS

1 INTRODUCTION

This chapter regards the introduction of the thesis. Section 1.1 shows the motivation and challenges of the work, aiming the Structural Health Monitoring (SHM) problems applied in initially nonlinear systems, considering the presence of uncertainties. Section 1.2 presents the main objectives of the research. Section 1.3 shows the main contributions of this thesis and, finally, section 1.4 presents the outline.

1.1 MOTIVATION

The process of damage detection in mechanical, aerospace and civil systems and structures, based on damage features and the statistical analysis of them, is commonly called Structural Health Monitoring (SHM) (FARRAR; WORDEN, 2007). The study and application of SHM techniques are motivated by the potential life-safety and economic impact of their implementation, which contributes to the development of new approaches (FARRAR; WORDEN, 2012). Moreover, within the hierarchy of complexity that SHM methodologies may achieve, damage detection is the first step, and its performance is fundamental to the success of the subsequent application of higher forms of SHM in the hierarchy (RYTTER, 1993).

As it is widely known, the damage detection features can be sensitive to confounding effects such as environmental or operating conditions, temperature and humidity changes, sensors bonding conditions, and others (WORDEN; CROSS, 2018). Also, real systems and structures are subject to the presence of uncertainties, mostly related to noise in the measurements, geometric imperfections, manufacturing irregularities, environmental conditions, or even, lack of knowledge about the system physics (SOIZE, 2012; SOIZE, 2013; SOIZE, 2017). These uncertainties can complicate the damage detection problem and have to be considered in the SHM applications, reducing the occurrence of false alarms and improving the positive detections as well (MAO; TODD, 2013). Aiming to overcome this issue, the damage detection can be done based on statistical procedures, taking into account confidence limits to the dynamic behavior of the systems and structures. Thus, structural monitoring can be done, usually, based on (WORDEN *et al.*, 2015):

- Novelty detection: detection of discrepant responses of the structure compared with

a normal condition, that is previously known. In most cases, statistical thresholds are established using the system's behavior in a normal condition of operation;

- Classification: all the structural states are previously known and the condition of the structure is classified into labels of different damage stages and health condition;
- Regression algorithms: a variable or process that can represent the system's behavior is monitored with confidence limits. Regression methods can also be defined as classification algorithms with continuous labels.

The choice of the more interesting approach to be used depends on the specific problem and the level of knowledge about the damage (detection, localization, assessment, prognosis) desired. In this sense, many methods can be used, such as linear and nonlinear Principal Component Analysis (PCA - NPCA) (PAVLOPOULOU; WORDEN; SOUTIS, 2016) , Extreme Value Statistics (EVS) (SOHN *et al.*, 2005), Peaks Over Threshold (POT) (RÉBILLAT *et al.*, 2018), machine learning algorithms (SANTOS *et al.*, 2016), neural network (WORDEN; MANSON; ALLMAN, 2003), Bayesian approaches (FIGUEIREDO *et al.*, 2014; LEBEL *et al.*, 2017; LEBEL *et al.*, 2019), Mahalanobis distance (WORDEN; MANSON; FIELLER, 2000; FIGUEIREDO *et al.*, 2010), probabilistic model selection approaches (VAMVOUDAKIS-STEFANOU; SAKELLARIOU; FASSOIS, 2018; AVENDAÑO-VALENCIA; FASSOIS, 2017b; POULIMENOS; SAKELLARIOU, 2019), big data based methods (LESTOILLE; SOIZE; FUNFSCHILLING, 2016), stochastic damage models (SUDRET, 2008; LESTOILLE; SOIZE; FUNFSCHILLING, 2016), and others. In all these applications, the final objective of the methods' implementation is the same, to become clear the difference between the presence of uncertainties and the variations caused by the damages.

Furthermore, many otherwise-linear structures can exhibit nonlinear phenomena induced by the presence of damage, and in this situation, any form of nonlinearity detector is akin to detecting damage (WORDEN *et al.*, 2008). Such damage that produces nonlinear behavior, for example, delamination (MANDAL; WADADAR; BANERJEE, 2015; GHRIB *et al.*, 2018), rubbing and unbalance in rotor systems (TANG *et al.*, 2010; ZENG *et al.*, 2015; XIA *et al.*, 2016), and opening cracks (ANDREAUS; BARAGATTI, 2012; LIM *et al.*, 2014; RÉBILLAT; HAJRYA; MECHBAL, 2014) may be detected through the observation of nonlinear behavior in the measured responses. All of these approaches are powerful tools used to detect the presence of damage that induces nonlinear effects on the system's behavior. However, a more significant problem is encountered when the structure presents nonlinear effects even in the healthy condition, making the classical

approaches fail to distinguish the variation related to the nonlinear phenomena from the variation caused by the occurrence of damage (BORNN; FARRAR; PARK, 2010). Moreover, many mechanical systems and structures can operate with nonlinear behavior, that makes them exhibit complex responses containing subharmonic and superharmonic resonances, jumps, modal interactions, bifurcation, quasi-periodicity, and possible chaos (VIRGIN, 2000; NOËL; KERSCHEN, 2016). In this situation, the nonlinear behavior of the system in the reference condition needs to be considered.

In this regard, many approaches, in time and frequency domain, can be used to describe the nonlinear behavior, such as Hilbert transform, Narmax Models, High-Order FRFs (KERSCHEN *et al.*, 2007; WORDEN *et al.*, 2007), restoring force surface methods (RFS) (MASRI; CAUGHEY, 1979; NOËL; KERSCHEN; NEWERLA, 2012), harmonic balance method (TANG *et al.*, 2016) and others. Unfortunately, these nonlinearities have many individualities, in way that it is difficult to obtain a general model that describes all the structures of interest. Among the different methods for nonlinearities identification, the Volterra series stands out, because it is a generalization of the linear convolution concept, allowing the separation of the system response in linear and nonlinear components (SCHETZEN, 1980). The main procedure to estimate the Volterra kernels is the Harmonic Probing method, that was extensively used in system identification problems (CHATTERJEE, 2010a; SCUSSEL; SILVA, 2017) and damage characterization (CHATTERJEE, 2010b). The limitation of the approach is the dependence of a parametric model of the system.

Another possible formulation is the direct use of input/output signals to estimate the Volterra kernels. Shiki, Silva and Todd (2017) have used this formulation, based on input/output signals, to detect structural variations related to the occurrence of damage, in a beam presenting nonlinear behavior even in the reference condition. The authors have shown the use of Volterra series expanded through the Kautz functions, as a reference model to predict the nonlinear system's response and to monitor the structure of interest. A statistical study of the damage index proposed was done with satisfactory results, but only the variation related to measurement noise was taken into account. The authors have not considered the possible system's response variation related to uncertainties, like environmental and operating conditions, and others as reported before. The interesting results obtained and the absence of a probabilistic analysis of the formulation used motivated the development of this thesis.

Thus, it is proposed to use a stochastic version of the Volterra series approach, expanded using random Kautz functions, as a stochastic reference model to be used in

the damage detection procedure based on novelty detection. The Volterra kernels are estimated in a probabilistic framework, considering the data variation, to construct a set of reference models. To allow the description of the response variability, the Kautz parameters are treated as random variables and the Kautz functions used to reduce the number of terms of the Volterra kernels, as random processes. This methodology allows to include in the proposed model the capability to describe the system nonlinear behavior and the data variation, simultaneously. Different damage-sensitive features based on the Volterra kernels estimated are explored during the work, showing the improvement of the damage detection performance when we compare with previously developed methods.

1.2 OBJECTIVES

Based on the issues presented in the motivation, the main goal of the present thesis is to propose an original methodology to detect damage in systems with intrinsically nonlinear behavior, considering the presence of uncertainties through data variation. The damage detection procedure must be based on a stochastic nonlinear model and will be applied using experimental data measured considering nonlinear structures, data variation and the presence of damages with different effects in the structures' behavior.

1.3 MAIN CONTRIBUTIONS OF THE THESIS

The main contributions of the present thesis are:

- Proposition of a new stochastic formulation, grounded in the idea of Multiple Models (MM) identification, for the input/output based Volterra series model (VILLANI; SILVA; CUNHA JUNIOR, 2017a; VILLANI; SILVA; CUNHA JUNIOR, 2019b);
- Development of a damage detection methodology, based on the random Volterra kernels' features, to be applied in problems where the intrinsically nonlinear behavior and data variation are complicating factors (VILLANI; SILVA; CUNHA JUNIOR, 2019b; VILLANI *et al.*, 2019a; VILLANI *et al.*, 2019b);
- Comparison between results obtained in the process of damage detection using a deterministic and a stochastic reference model when the uncertainties are considered (VILLANI *et al.*, 2019a);
- Application of the proposed methodology considering different kinds of damage and variabilities to test its performance, including the situation of an intrinsically

nonlinear structure subject to the presence of damage that induces nonlinear phenomena to the system's response (VILLANI *et al.*, 2019b).

1.4 OUTLINE

This work is organized as follows:

- **Chapter 1 - INTRODUCTION -** The motivation of the research, the main objectives and contributions of the thesis;
- **Chapter 2 - PARAMETERS ESTIMATION OF AN UNCERTAIN NONLINEAR SYSTEM -** Description of the identification of a random version of the Duffing oscillator model to describe the dynamic behavior of a structure that presents nonlinear behavior for large displacements. This chapter shows the importance of considering the presence of uncertainties in the problem of models' parameters estimation, even when the experiments are conducted in laboratory conditions;
- **Chapter 3 - FROM THE DETERMINISTIC TO THE STOCHASTIC VERSION OF VOLTERRA SERIES -** Development of a stochastic version of the Volterra series model to be used with a random version of the Kautz functions to describe uncertain nonlinear system's output. The stochastic model proposed will be used as reference model in the problems of damage detection presented in this thesis;
- **Chapter 4 - SIMULATED DAMAGE DETECTION BASED ON STOCHASTIC VOLTERRA SERIES: A NONLINEAR DAMAGE -** Application of the approach proposed based on stochastic Volterra series in a simulated damage detection problem. A random version of the Duffing oscillator is assumed as the system to be monitored and the damage emulated (a breathing crack model) induces a nonlinear effect on the system's output. Different levels of damage are considered and the main results of the damage detection procedure applied are shown;
- **Chapter 5 - EXPERIMENTAL DAMAGE DETECTION BASED ON STOCHASTIC VOLTERRA SERIES: A LINEAR DAMAGE -** Experimental application of the approach based on stochastic Volterra series to detect damage, a mass reduction in a bolted connection with linear characteristic, in

an initially nonlinear system, considering the presence of uncertainties. Again, different levels of damage are emulated and the performance of the approach is discussed. Additionally, this chapter presents an interesting comparison between the use of deterministic and stochastic models in the damage detection process when the system is exposed to data variation;

- **Chapter 6 - ON THE DETECTION OF A NONLINEAR DAMAGE IN AN UNCERTAIN NONLINEAR BEAM USING STOCHASTIC VOLTERRA SERIES -** Experimental application of the methodology considering an intrinsically nonlinear system subject to the presence of a breathing crack that induces nonlinear phenomenon to the system's output. This chapter shows the proposition of a hybrid damage index to be used in real applications and the main results obtained;
- **Chapter 7 - FINAL REMARKS -** Presentation of the main conclusions obtained and discussion about the future works and the continuity of the research.

2 PARAMETERS ESTIMATION OF AN UNCERTAIN NONLINEAR SYSTEM

This chapter deals with the approximation of a random nonlinear system by a stochastic version of the classical Duffing oscillator, using the restoring force surface method and Monte Carlo simulations. The identification procedure proposed, considering the data variation related to the presence of uncertainties in the experimental measurement procedure, aims to show that, even in laboratory conditions, the estimation of parameters is susceptible to the presence of uncertainties. The results of this chapter can be found in Villani, Silva and Cunha Junior (2019a).

The chapter is organized as follows: section 2.1 shows the motivation; section 2.2 shows the experimental apparatus used to emulate a nonlinear mechanical system undergoing large displacements; section 2.3 presents the mechanical-mathematical model used to describe the nonlinear system dynamics; section 2.4 describes the identification procedure used for system parameters estimation; section 2.5 encompasses the results obtained and the model validation; and finally, in section 2.6 the main conclusions are highlighted. Worth it to point out that the random Duffing oscillator model studied in this chapter will be considered in the simulations performed to obtain the results presented in chapter 4.

2.1 IDENTIFICATION OF STOCHASTIC NONLINEAR SYSTEMS

The mathematical modeling of engineering structures is important to understand the dynamic behavior of the underlying mechanical systems, to make predictions, and to develop reliable projects. Usually, the modal analysis is employed to describe the dynamical response of mechanical systems, through the identification and validation of structural models, which are based on parameters such as natural frequencies, damping ratios, and modal shapes (SILVA; MAIA, 2012; AVITABILE, 2001; CAKIR; UYSAL; ACAR, 2016; CHANG *et al.*, 2016). This approach leads to reasonable results for structures that present linear behavior since the classical modal analysis is based on the superposition principle. However, it is known that many engineering structures can present nonlinear behavior caused by geometric effects, severe operating conditions, materials with complex structure, large amplitude excitations, etc. Therefore, to perform

a reliable analysis of a structure, and to optimize its operation, it is necessary to take these nonlinear effects into account (VIRGIN, 2000; WORDEN; TOMLINSON, 2000; KERSCHEN *et al.*, 2006). Unfortunately, these nonlinearities have many individualities, in a way that it is difficult to obtain a general identification method that is able to deal with all the structures of interest.

One of the first methodologies for the identification of nonlinear mechanical systems was proposed by Masri and Caughey (1979), which presents the method of restoring force surface (RFS). RFS is a nonparametric estimation technique where the analyst does not need to know the functional form of the nonlinear force. In several cases, for identification of single-degree-of-freedom (SDoF) models, RFS method has proven to be effective (KERSCHEN *et al.*, 2000; KERSCHEN; LENAERTS; GOLINVAL, 2003; NOËL; RENSON; KERSCHEN, 2014). For details on RFS method the reader is encouraged to see Noël, Kerschen and Newerla (2012). Another strategy of nonlinear systems identification has been proposed by Tang *et al.* (2016), where a comparison between the harmonic balance method and RFS was made. Many other approaches, in time and frequency domain, can be used to describe nonlinear systems, such as Hilbert transform, Nonlinear Autoregressive Moving Average Models with eXogenous Input (NARMAX), High-Order Frequency Response Functions (HOFRFs) (KERSCHEN *et al.*, 2007; WORDEN *et al.*, 2007), Volterra series (SCUSSEL; SILVA, 2016; SHIKI; SILVA; TODD, 2017), Harmonic Balance (HB), Proper Orthogonal Decomposition (POD), Artificial Neural Network (ANN) (BUSSETTA; SHIKI; SILVA, 2017), and others.

However, once the approaches described above are deterministic, they are not robust to variations in the system's parameters, neither offer a confidence interval to the identified parameters. Since any real system is uncertain with respect to the project nominal values, due to material imperfections, irregularities on the manufacturing process, noise in the measurements, boundary conditions, etc., it is essential for a reliable system identification technique to take into account the parameters' uncertainties (SOIZE, 2013; SOIZE, 2017; CUNHA JUNIOR, 2017; HEIDENREICH *et al.*, 2017). Techniques of stochastic system identification, that take uncertainties into account, are available in the literature, for instance, using a nonparametric probabilistic approach (CAPIEZ-LERNOUT; SOIZE, 2008; SOIZE; CAPIEZ-LERNOUT; OHAYON, 2008; BATOU; SOIZE; AUDEBERT, 2015), or Bayesian statistics (YAN; KATAFYGIOTIS, 2015; BEHMANESH *et al.*, 2015; RITTO; SAMPAIO; AGUIAR, 2016), Global sensitivity analysis (YUAN *et al.*, 2019). They are very sophisticated and powerful tools, generally used to identify complex mechanical systems with a large number of degrees-of-freedom

(DoFs) and parameters. Although these stochastic techniques can be used to identify systems with one or a few DoFs, the low dimension of some systems allows one to develop a simpler framework for stochastic identification.

Therefore, it is proposed to use a stochastic version of the RSF method to identify a SDoF system, developed in a probabilistic framework, which models the system parameters as random variables in order to take into account the underlying uncertainties (SOIZE, 2017). The variability in system parameters is related not only to their variation with respect to the nominal values but also to the identification techniques sensitivity to noise in the system's observations (experimental data). So, it is shown that, even for structures analyzed in controlled conditions, where the tests are conduced in the laboratory, it is essential to consider the data uncertainties in the model identification procedure, to make predictions with some kind of certification (a probabilistic envelope of reliability).

In this way, the main contribution of this chapter is to propose a stochastic version of the RFS method, where the marginal probability density functions (PDFs) and covariance matrix of the model parameters are estimated using experimental data, instead of their deterministic values, as it is made in conventional RFS applications. See, for example, Kerschen, Golinval and Worden (2001), Silva, Cogan and Foltête (2010) and Noël, Renson and Kerschen (2014), where the RFS method was used to identify nonlinear systems in a deterministic way, i.e., single values were identified for the model parameters without any probabilistic analysis or confidence bands estimation. Thus, with the aid of experimental data, this stochastic methodology is used to identify a mechanical-mathematical model that describes the dynamic behavior of a clamped-free beam, with nonlinear effects induced by the presence of a magnet near to the free end. With the stochastic model identified the uncertainties propagation is performed using Monte Carlo (MC) simulations, a Markov Chain Monte Carlo (MCMC) algorithm is adopted to generate the random numbers based on the marginal distributions of the parameters and covariance matrix, given that a projection method is implemented to consider the correlation between the parameters' marginal distributions in the analysis. The conclusions show that the method is simple and reaches effective results, so that it is suitable for application in simple systems, with low order, where more sophisticated techniques may be needless.

2.2 EXPERIMENTAL APPARATUS

The experimental setup considered is the same used in Shiki, Silva and Todd (2017). The experimental setup consists of:

- A cantilever aluminum beam with 300 × 18 × 3 [mm^3] of dimension;
- A steel mass and a magnet that interacts each other;
- A bolted connection with four nuts;
- A Modal Shop shaker (Model Number: K2004-E01);
- A vibrometer laser Polytec (Model: OFV-525/-5000-S);
- A m+p Vib Pilot data acquisition system.

The steel mass is glued in the free extremity of the beam, generating a nonlinear interaction among the beam and the magnet placed near to the free extremity (Fig. 1). The idea of the experimental setup is emulating a mechanical system with nonlinear behavior due to large displacements. In the context of future applications related to damage detection, a bolted connection is placed 150 [mm] from the beam free end with four nuts with 1 [g] each one. The shaker is located 50 mm from the clamp. The structure was excited using different levels of input amplitude 0.01 V (low), 0.10 V (medium) and 0.15 V (high). The vibrometer laser is employed to measure the beam free extremity velocity, that is admitted the system output. The input signal examined in this work is the voltage provided by the amplifier to drive the shaker. It is easier to keep this signal constant over a range of frequency, using the power amplifier in the electrical current mode, than to keep the force applied constant close to the resonance frequency of the system. The same strategy was used in Tang *et al.* (2016). All signals were measured using 1024 Hz as sampling rate and 4096 samples were collected.

Figure 1 – Illustration of the experimental apparatus used.

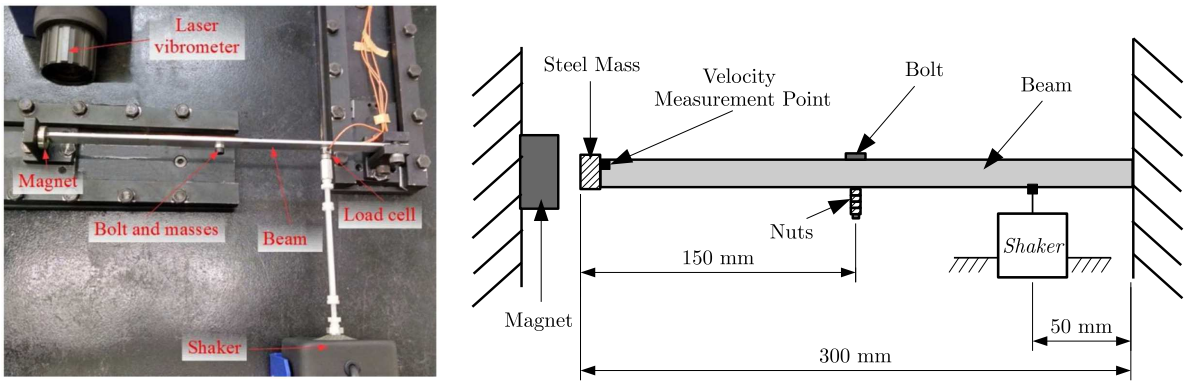

(a) Experimental apparatus. (b) Schematic representation.

Source: Adapted from Shiki, Silva and Todd (2017).

The experimental arrangement presents nonlinear behavior with hardening characteristic (KOVACIC; BRENNAN, 2011). This characteristic can be seen by the results obtained when the structure was subject to the stepped sine test (Fig. 2(a)). In this test, each sine input signal is applied, and the fundamental amplitude in the stationary state of the output is measured, thus, each point of the graphic considers the amplitude of the response obtained from a different time series caused by a sine input signal with a different fundamental frequency. The system response presents the jump phenomenon, related to the nonlinear behavior, that is a result of the large displacements achieved when a high level of input (0.15 V) is applied to the structure. The structure manifests linear behavior when a low level of input (0.01 V) is applied. Additionally, the structure has been excited applying a high level of amplitude (0.15 V) chirp signal, varying the excitation frequency from 10 to 50 Hz (the first modal shape region) in 4 seconds. The spectrogram of the system response can be viewed in Fig. 2(b). It is possible to observe the appearance of harmonics of second and third-order in the system's output. These results attest that the structure exhibits nonlinear behavior as a consequence of large displacements.

The occurrence of the multiple harmonics can suggest the use of a polynomial function to approximate the nonlinear behavior of the system, confirming the hypothesis that the system's output can be approximated, in a limited range of frequencies, by a Duffing oscillator model. It is known that non polynomial nonlinearities can also generate multiple harmonics, however the shape of the restoring force obtained experimentally, that will be shown further on, also suggests that a polynomial function can be used. Additionally, Barton, Burrow and Clare (2010) describes a similar system using a cubic term in the Duffing equation.

Figure 2 – Illustration of the system nonlinear behavior.

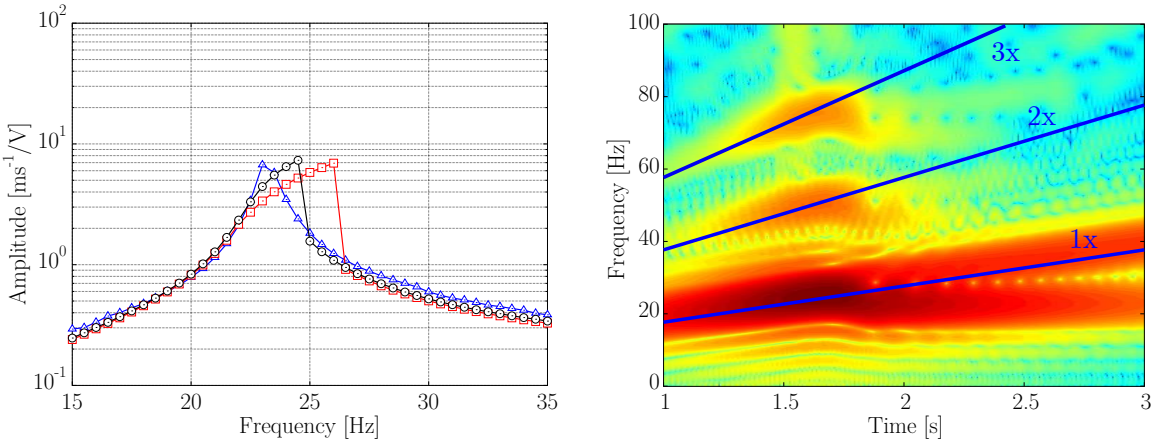

(a) Stepped sine test, where △ represents the low level of input signal (0.01 V), ∘ the medium level (0.10 V) and □ the high level (0.15 V).

(b) System response spectrogram.

Source: Villani *et al.* (2019a).

2.3 MATHEMATICAL MODELING

This section describes the Duffing oscillator equation used to approximate the behavior of the nonlinear system in this study, the explanation about the random variables considered in the model identification problem and the stochastic formulation used to make the parametrization of the nonlinear restoring force.

2.3.1 **Deterministic model**

The considered mechanical system presents nonlinear behavior only when subjected to large displacements, and its dynamic behavior can be approximated, for a limited frequency range, i.e., its first mode shape, whose amplitude evolves according to a SDoF Duffing oscillator (KOVACIC; BRENNAN, 2011). The classical Duffing oscillator, considering viscous damping, is described by the following differential equation

$$m_1\,\ddot{x}(t) + c_1\,\dot{x}(t) + k_1\,x(t) + k_2\,x(t)^2 + k_3\,x(t)^3 = U(t), \tag{1}$$

where t represents the time, m_1 is the system equivalent mass in [kg], c_1 is the damping coefficient in [Ns/m], k_1 is the linear stiffness in [N/m], k_2 is the quadratic stiffness in [N/m^2], k_3 is the cubic stiffness in [N/m^3], and $U(t)$ is the external force in [N]. The displacement, velocity and acceleration in the free extremity of the beam are represented by $x(t)$, $\dot{x}(t)$ and $\ddot{x}(t)$.

Since in the RFS method no form for the nonlinear restoring force is initially assumed, Eq. (1) is rewritten as

$$m_1\,\ddot{x}(t) + c_1\,\dot{x}(t) + \mathcal{F}(x,t) = U(t), \tag{2}$$

where

$$\mathcal{F}(x,t) = \underbrace{k_1\,x(t)}_{linear} + \underbrace{k_2\,x(t)^2 + k_3\,x(t)^3}_{nonlinear}, \tag{3}$$

is the restoring force in [N]. From now on, in order to apply the RFS method, this polynomial functional relationship is assumed to be unknown.

2.3.2 Stochastic model

A parametric probabilistic approach (SOIZE, 2012; SOIZE, 2013; SOIZE, 2017) is employed here to describe the system parameters uncertainties, induced by measurements noise, variation in the boundary conditions, position of the shaker, sensors and magnet, uncertainties related to the methods of parameters estimation. In this framework, the model parameters subjected to uncertainties are described as random variables or random processes, defined on the probability space $(\Theta, \mathbb{\Sigma}, \mathbb{P})$, where Θ is sample space, $\mathbb{\Sigma}$ is a σ-algebra over Θ, and $\mathbb{P}$ is a probability measure. It is assumed that any random variable $\theta \in \Theta \mapsto \mathbb{V}(\theta) \in \mathbb{R}$ in this probabilistic setting, with probability distribution $P_{\mathbb{V}}(dv)$ on $\mathbb{R}$, admits a probability density function (PDF) $v \mapsto p_{\mathbb{V}}(v)$ with respect to dv.

For the Duffing oscillator described in last section, the equivalent mass, the damping coefficient and the restoring force are assumed to be uncertain. In this way, the scalar values m, c are, respectively, modeled by the random variables $\theta \in \Theta \mapsto \mathbb{m}_1(\theta) \in \mathbb{R}$ and $\theta \in \Theta \mapsto \mathbb{c}_1(\theta) \in \mathbb{R}$. On the other hand, $\mathcal{F}$ is described by the random process $(\theta,t) \in \Theta \times \mathbb{R} \mapsto \mathbb{F}(\theta,t)$. Thus, the stochastic equivalent of Eq. (2) is given by

$$\mathbb{m}_1(\theta)\,\ddot{\mathbb{x}}(\theta,t) + \mathbb{c}_1(\theta)\,\dot{\mathbb{x}}(\theta,t) + \mathbb{F}(\mathbb{x}(\theta,t),t) = U(t), \tag{4}$$

where the random processes $(\theta,t) \in \Theta \times \mathbb{R} \mapsto \mathbb{x}(\theta,t)$, $(\theta,t) \in \Theta \times \mathbb{R} \mapsto \dot{\mathbb{x}}(\theta,t)$, and $(\theta,t) \in \Theta \times \mathbb{R} \mapsto \ddot{\mathbb{x}}(\theta,t)$, respectively represent the displacement, velocity and acceleration in the beam free end. The stochastic model of Eq. (4) will be used to described the nonlinear random dynamics of the mechanical system emulated by the experimental apparatus. The random parameters of this model are identified in a nonparametric way, that is explained in details in the next section.

2.4 STOCHASTIC SYSTEM PARAMETERS IDENTIFICATION

In this work, a frequentist inference is employed, i.e., the parameters' distributions are estimated based on experimental data measured repeatedly. In order to estimate the stochastic model parameters, two types of experimental tests are considered. The first one excites the structure with a low-level amplitude chirp signal, defined by a constant voltage of 0.01 V, while in the second test, the chirp signal amplitude level is high, induced by a constant voltage of 0.15 V. The frequency of the chirp excitation varies with a rate of 10 Hz/s, from 10 to 50 Hz and the two tests are performed in sequence. The result of each experimental test performed is a velocity time series, called velocity realization. From a velocity realization it is possible to obtain displacement and acceleration time series, using integration and differentiation in frequency domain, respectively. Associated to each velocity realization, there are also underlying values for the system parameters, which need to be identified. Each type of test is repeated 200 times, in different days. In fact, experimental tests reported here were conducted in different days from April to May 2015. This period helped to induce variations on experimental data, once the system was susceptible to a number of uncertainties such as: variations in boundary conditions, clamp grip, position of the shaker, sensor and magnet, and others. It is worth to note that the parameters estimation is also influence by the uncertainties in the deterministic methods used in the identification process.

2.4.1 **Linear parameters estimation**

The identification of the system's parameters m_1 and c_1 uses the underlying linear dynamics of the beam, obtained when the input signal has a low level of amplitude (0.01 V). Note that in this case, ideally, we have $\mathcal{F}(x,t) = k_1\,x(t)$ for any time t, i.e., the nonlinear behavior has no influence on the system dynamics. First of all, the analytical expression to the Impulse Response Function (IRF) of a linear SDoF system is given by

$$h(t) = \frac{1}{m_1\,\omega_d}\,e^{-\zeta\,\omega_n\,t}\,\sin\left(\omega_d\,t\right), \tag{5}$$

where $h(t)$ represents the IRF, ζ is the damping ratio of the equivalent linear system, ω_n is the natural frequency of the equivalent linear system in [rad/s], and

$$\omega_d = \omega_n\,\sqrt{1-\zeta^2} \tag{6}$$

is the damped natural frequency of the equivalent linear system in [rad/s].

To estimate the system equivalent mass and damping coefficient, the IRF is obtained from the Frequency Response Function (FRF), for each experimental realization, converting the signal from frequency to time domain. The damped natural frequency can be estimated considering the inverse of the damped period of $h(t)$. The damping ratio ζ can be estimated through the logarithmic decrement method and the equivalent mass m_1 can be obtained by comparing IRF experimental data with Eq. (5), considering just the signal envelope. With the damping ratio, natural frequency and equivalent mass estimated, the damping coefficient can be calculated as

$$c_1 = 2\,\zeta\,\omega_n\,m_1\,. \tag{7}$$

Considering that, the deterministic values of the parameters are not interesting in this work, after identifying several realizations of the modal parameters (200 in fact), the PDFs of system equivalent mass $\mathbb{m}_1$ and damping coefficient $\mathbb{c}_1$ are nonparametrically estimated, through histograms and kernel smoothed density curves (WASSERMANN, 2006).

2.4.2 **Restoring force estimation**

After the estimation of the mass and damping, the nonlinear dynamics of the beam, obtained when the input has a high level of amplitude (0.15 V), is used to estimate the restoring force $\mathbb{F}(\mathbb{x}(\theta,t),t)$ to each realization θ. In this case, the RFS method defines the nonlinear force from the equation

$$\mathbb{F}(\mathbb{x}(\theta,t),t) = U(t) - \left[\mathbb{m}_1\,\ddot{\mathbb{x}}(\theta,t) + \mathbb{c}_1\,\dot{\mathbb{x}}(\theta,t)\right], \tag{8}$$

where all objects of the equation right hand side are known. Note that the nonlinear function $\mathbb{F}$ is a stochastic process, once it is defined as the difference between the excitation $U(t)$ and the stochastic process $\mathbb{m}_1\ddot{\mathbb{x}}+\mathbb{c}_1\dot{\mathbb{x}}$. In practice, realizations of $\mathbb{F}$ are constructed by means of realizations of the system parameters as well as from velocity and acceleration time series. Additionally, the reader can observe that, for a fixed discrete-time t, each experimental realization of $\mathbb{F}$ defines a three-dimensional surface, i.e., $\mathcal{F} = g(x,\dot{x})$ for some scalar map $g:\mathbb{R}^2\to\mathbb{R}$. As the formulation of this version of the RFS method is done in terms of a stochastic process, the identification process is inherently stochastic. It is also worth mentioning that, as the estimation of the restoring force depends on acceleration, that is obtained through the derivation in the frequency domain, this procedure can generate more uncertainties that can influence in the estimation of the

nonlinear parameters. In this sense, estimating a deterministic value for the restoring force may lead to unreliable results.

Thus, the polynomial coefficients (k_1, k_2 and k_3 in Eq.(3)), to each realization, can be estimated through the polynomial regression based on the minimization of the squared error (least squares method), described by

$$\boldsymbol{\Xi} = (\boldsymbol{\Upsilon}^{\mathrm{T}}\boldsymbol{\Upsilon})^{-1}\boldsymbol{\Upsilon}^{\mathrm{T}}\mathcal{F}, \tag{9}$$

where $\boldsymbol{\Xi}$ is the vector with the estimated parameters $\{k_1\ k_2\ k_3\}^{\mathrm{T}}$ and $\boldsymbol{\Upsilon}$ is an array of dimension $N_p \times 3$, where N_p is the number of samples used, with the vectors $[x\ x^2\ x^3]$, to each realization θ. As made with the mass and damping, the PDFs of system linear $\Bbbk_1$, quadratic $\Bbbk_2$ and cubic $\Bbbk_3$ stiffness are also estimated in a nonparametric way.

2.5 MODEL IDENTIFICATION AND VALIDATION

This section presents the results obtained in the estimation of the random parameters following the methodology proposed and the validation of the stochastic model identified through Monte Carlo simulations.

2.5.1 **Linear vibration**

Figure 3 shows the mean value of the IRF, as well as a confidence band, where the probability of a realization to be contained is 99%. The realizations of the IRF used to construct this graph, are used to estimate the probability distribution of each linear parameters (m_1 and c_1), such as described in the last section. The nonparametric estimations for system mass and damping coefficient PDFs can be seen in Fig. 4. Note that the figures show PDFs of normalized random variables, i.e., random variables with zero mean and unit standard deviation, in addition to the nominal values. This normalization is used to facilitate the comparison between the different PDFs.

The PDFs show that the two parameters have unimodal behavior, i.e., the values are distributed around the mean values. It is worth to do not confuse the word *modal* used here with linear mode, in this case modal refers to the concept of mode in statistics. It is possible to observe that $\mathbb{m}_1$ has mean value of $\mu_{\mathbb{m}_1}$ = 0.233 kg with low dispersion around the nominal value, additionally, the values are concentrated between ± 3 standard deviation. The coefficient of variation, standard deviation divided by the mean, is $\delta_{\mathbb{m}_1}$ = 2.44 %. The variation in the equivalent mass is a consequence of the system's output

Figure 3 – Impulse Response Function, obtained from experimental realizations. – represents the mean value and a gray area represents the 99% confidence bands.

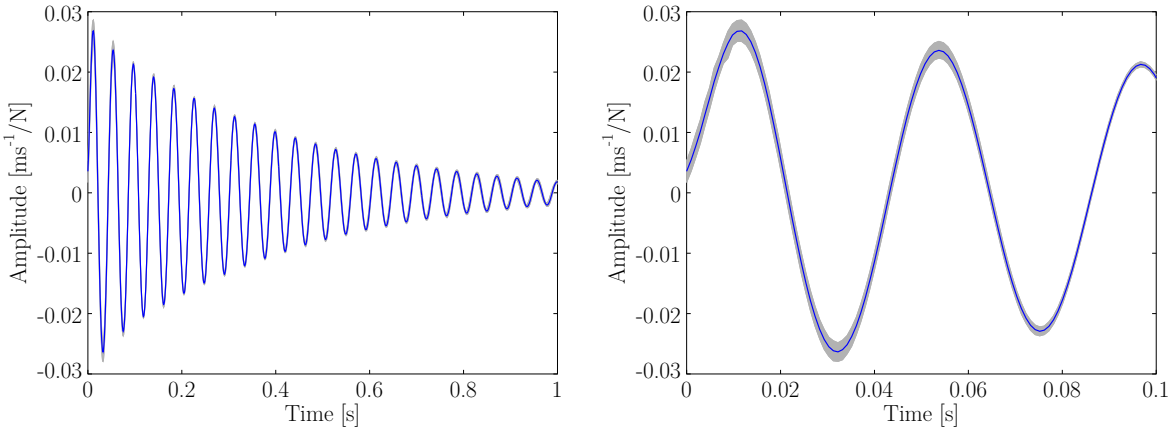

(a) Signal. (b) Zoom.

Source: Prepared by the author.

variation since the values are estimated considering the vibration measured data because they can not be directly measured. The damping coefficient $\mathbb{c}_1$ has big influence of the damping ratio in its definition, therefore presents variation related to the IRF variation, with concentration across the mean value $\mu_{\mathbb{c}_1}$ = 1.226 Ns/m and low dispersion. Again, the values are concentrated between ± 3 standard deviation and $\delta_{\mathbb{c}_1}$ = 1.77 %.

Figure 4 – Estimated PDFs for mass and damping coefficients.

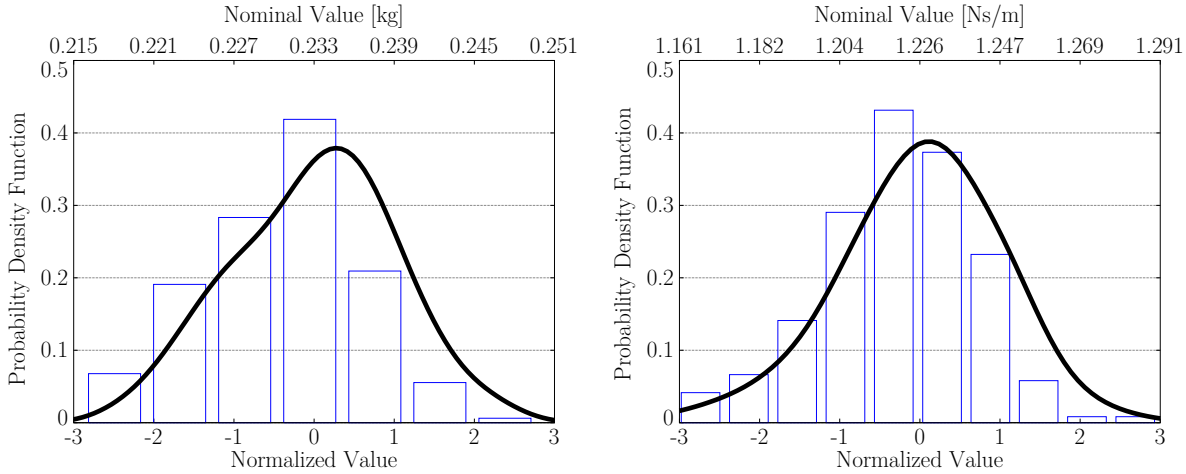

(a) Estimated PDF for $\mathbb{m}_1$. (b) Estimated PDF for $\mathbb{c}_1$.

Source: Prepared by the author.

2.5.2 **Restoring force**

With the surfaces $\mathcal{F} = g(x, \dot{x})$ estimated, some sections can be extracted between different values of velocity. Figure 5 shows the sections obtained considering $|\dot{x}| \leq 0.1$, $|\dot{x}| \leq 0.2$ and $|\dot{x}| \leq 0.3$ m/s, where it is possible to see the dispersion of restoring force. It can be also seen that the results are very similar in the three cases considered.

Figure 5 – Experimental nonlinear restoring force. The red color represents $|\dot{x}| \leq 0.1$, the blue color $|\dot{x}| \leq 0.2$ and the **black color** $|\dot{x}| \leq 0.3$ m/s.

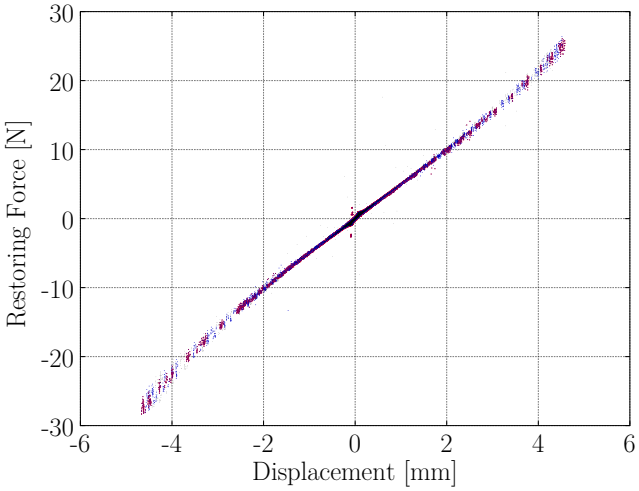

Source: Prepared by the author.

After the nonparametric estimation of $\mathcal{F}$, becomes natural to perform a parametrization of this force, trying to fit a function whose shape resembles the curve raised by RFS method. In fact, observing Fig. 5, it is very natural to infer that $\mathcal{F}$ is well represented by a polynomial function with degree 3, i.e.,

$$\mathcal{F}(x(t), t) \approx k_1\, x(t) + k_2\, x(t)^2 + k_3\, x(t)^3, \tag{10}$$

where k_1, k_2 and k_3 represent the linear, quadratic and cubic stiffness, respectively. Indeed, this is according to the Duffing oscillator equation, a fact which was assumed to be unknown previously. The stiffnesses k_1, k_2 and k_3 can be determined by adjusting Eq.(10) to the nonparametric curves obtained via RFS, considering $|\dot{x}| \leq 0.1$ m/s (cleaner results). Since the nonlinear restoring force is random, it should be assumed that the stiffnesses are also aleatory, being modeled by random variables $\theta \in \Theta \mapsto \Bbbk_1(\theta) \in \mathbb{R}$, $\theta \in \Theta \mapsto \Bbbk_2(\theta) \in \mathbb{R}$ and $\theta \in \Theta \mapsto \Bbbk_3(\theta) \in \mathbb{R}$. Nonparametric estimations for PDFs of the stiffnesses $\Bbbk$, $\Bbbk_2$ and $\Bbbk_3$ are presented in Fig. 6.

It can be seen in Fig. 6(a) the PDF of the linear stiffness. The behavior is unimodal with the values concentrated around the mean value $\mu_{\Bbbk_1} = 4.954 \times 10^3$ N/m and coefficient

of dispersion $\delta_{\mathbb{k}_1} = 2.21\%$. Fig. 6(b) shows the PDF of the quadratic stiffness. The mean value is equal to $\mu_{\mathbb{k}_2} = -30.867$ N/m^2 and dispersion $\delta_{\mathbb{k}_2} = 2.72\%$, with unimodal behavior and concentration around the mean. The quadratic term has a low contribution to the system response in the time domain (symmetric response). The PDF of the cubic stiffness, presented in Fig. 6(c), has also unimodal distribution with mean value $\mu_{\mathbb{k}_3} = 39.859 \times 10^7$ [N/m^3] and dispersion $\delta_{\mathbb{k}_3} = 4.06\%$. The large variation of these parameters is related to the uncertainties present in the RFS method applied, since the method uses time-series responses to determine the restoring force, with underlying variabilities (e.g. noise, the magnet, shaker and sensor position, etc).

Figure 6 – Estimated PDFs for the stiffnesses and the fitted restoring force.

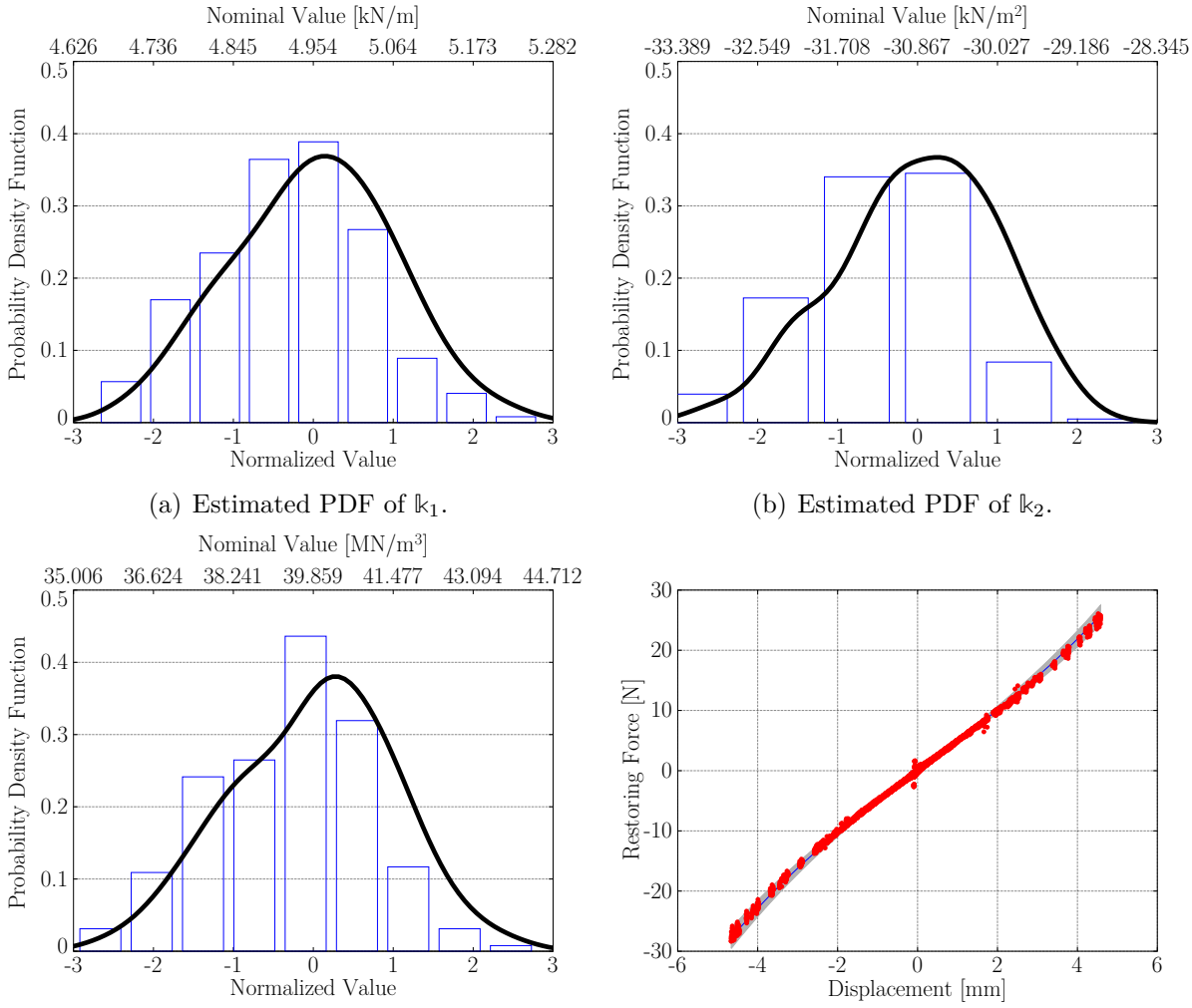

(a) Estimated PDF of $\mathbb{k}_1$.

(b) Estimated PDF of $\mathbb{k}_2$.

(c) Estimated PDF of $\mathbb{k}_3$.

(d) Fitted restoring force with 99% of confidence limits. ∘ represents the experimental data and – the mean value.

Source: Prepared by the author.

Figure 6(d) shows the experimental $\mathbb{F}$ and the polynomial modeling identified with 99% of confidence bands. The results are satisfactory considering that the model can

predict the behavior of the nonlinear force mainly when it has a high amplitude. When the nonlinear restoring force has a low amplitude (≈ 0) it is difficult to the model to describe the behavior, but how the low amplitude has a lower contribution in the model this error is considered acceptable. The variations in the system's parameters, mainly in nonlinear terms, causes large dispersion in the model's responses depending on the conditions and levels of excitation used. This results can be proven hereafter.

2.5.3 Samples generation to model validation

Once the stochastic model of Eq.(4) is identified, it can be used to make predictions about the beam nonlinear dynamic behavior, offering probabilistic limits of confidence to the response. In order to compute the mean value of $\dot{x}$, and the respective envelope of reliability, it is necessary to quantify the stochastic model's response uncertainties, i.e., to see how the model parameters uncertainties propagate through the stochastic model of Eq.(4). This calculation was done using Monte Carlo (MC) method (KROESE; TAIMRE; BOTEV, 2013; CUNHA JUNIOR *et al.*, 2014), which draws values for m_1, c_1 and $\mathcal{F}$ according to the joint-distribution of the model parameters, and then integrate Eq.(1) several times. The sampling procedure of the parameters using their PDFs is described as follow.

First of all, the experimental nonparametric marginal PDFs and covariance matrix estimated are used to generate samples of the system's parameters. In the procedure, the Metropolis-Hastings Markov Chain Monte Carlo (MCMC) algorithm is employed, because no general method of samples generation is known when one considers only empirical marginal distributions and covariance matrix (RUBINSTEIN; KROESE, 2016). Additionally, the sampling is made considering the correlation between the random variables, through the Cholesky decomposition of the correlation matrix. The procedure is summarized as follows:

1. Calculate the correlation matrix $\boldsymbol{R}$ from the experimental samples;
2. Calculate the Cholesky decomposition of $\boldsymbol{R}$, i.e.,

$$\boldsymbol{R} = \boldsymbol{L}\boldsymbol{L}^T; \tag{11}$$

3. Generate random uncorrelated samples, for each random variable, using the Metropolis-Hastings algorithm;

4. Allocate the random uncorrelated samples into a matrix

$$\boldsymbol{S} = [\mathbb{m}_1 \ \mathbb{c}_1 \ \mathbb{k}_1 \ \mathbb{k}_2 \ \mathbb{k}_3]; \tag{12}$$

5. Normalize the matrix $\boldsymbol{S}$, i.e.,

$$\tilde{\boldsymbol{S}} = \frac{\boldsymbol{S} - \mu_{\boldsymbol{S}}}{\sigma_{\boldsymbol{S}}}; \tag{13}$$

6. Compute the normalized matrix of the correlated variables through the Cholesky decomposition of the correlation matrix, i.e.,

$$\tilde{\boldsymbol{T}} = \tilde{\boldsymbol{S}}\,\boldsymbol{L}^T; \tag{14}$$

7. Compute the unnormalized values

$$\boldsymbol{T} = \tilde{\boldsymbol{T}}\,\sigma_{\boldsymbol{S}} + \mu_{\boldsymbol{S}}. \tag{15}$$

The matrix $\boldsymbol{T}$ contains the correlated random variables generated based on the experimental marginal PDFs of the system parameters. The number of samples generated here is equal to 1024, to each random variable. This value is defined based on the convergence of the MC method, that is shown in the next section. Figures 7, 8 and 9 show the correlation between the random variables experimentally obtained in comparison with the numerically generated samples. The equivalent mass $\mathbb{m}_1$ has a clear correlation with the stiffnesses $\mathbb{k}_1, \mathbb{k}_2$ and $\mathbb{k}_3$, through the natural frequency. The correlations between the stiffnesses are a consequence of their dependence through the restoring force. It is important to take into account the correlation between the variables in the MC method, to study the uncertainties propagation, obtaining trustworthy results.

Figure 7 – Correlation between the equivalent mass and the other random variables. ○ represents the experimental values and □ the generated samples.

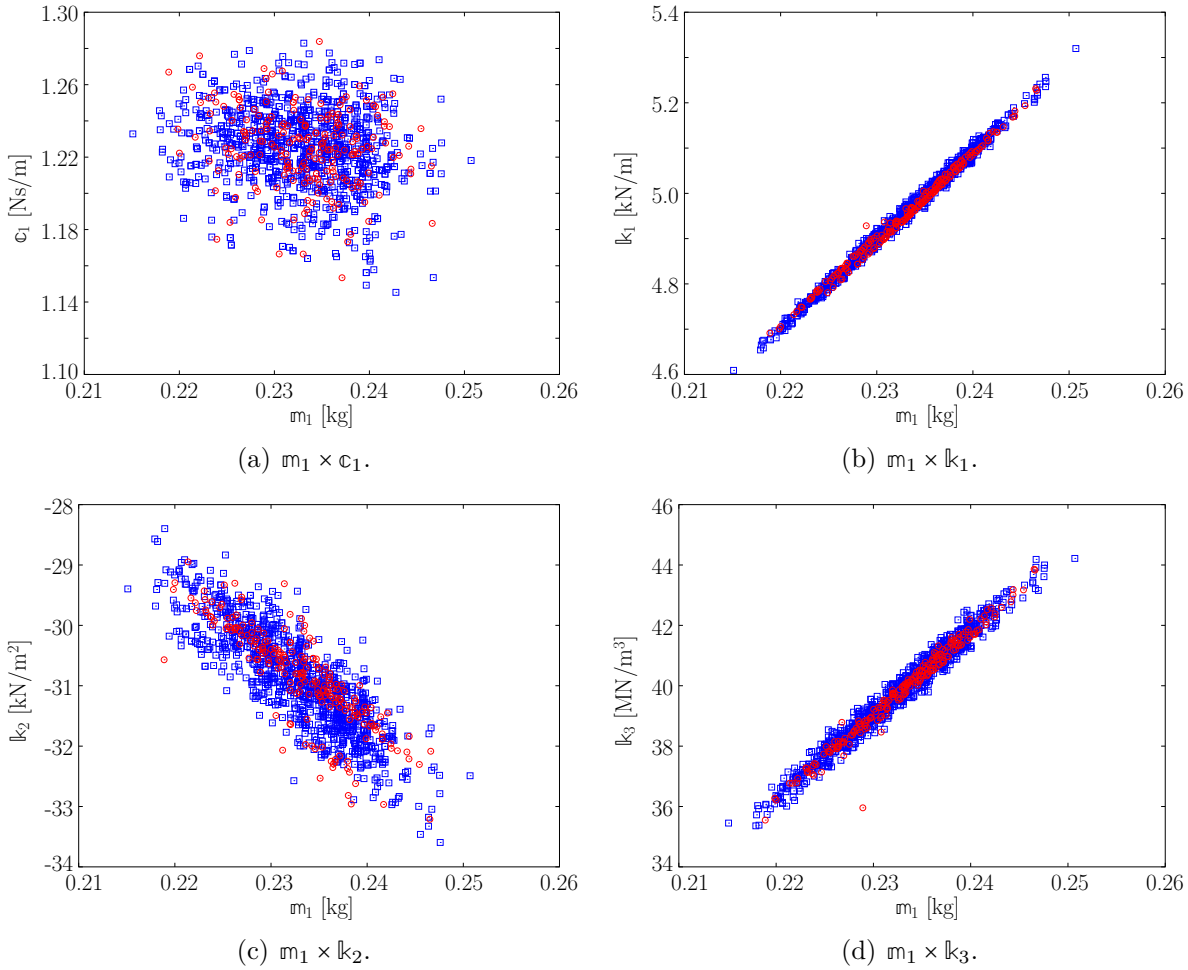

(a) $\mathbb{m}_1 \times \mathbb{c}_1$.

(b) $\mathbb{m}_1 \times \mathbb{k}_1$.

(c) $\mathbb{m}_1 \times \mathbb{k}_2$.

(d) $\mathbb{m}_1 \times \mathbb{k}_3$.

Source: Prepared by the author.

Figure 8 – Correlation between the damping and the stiffnesses random variables. ○ represents the experimental values and □ the generated samples.

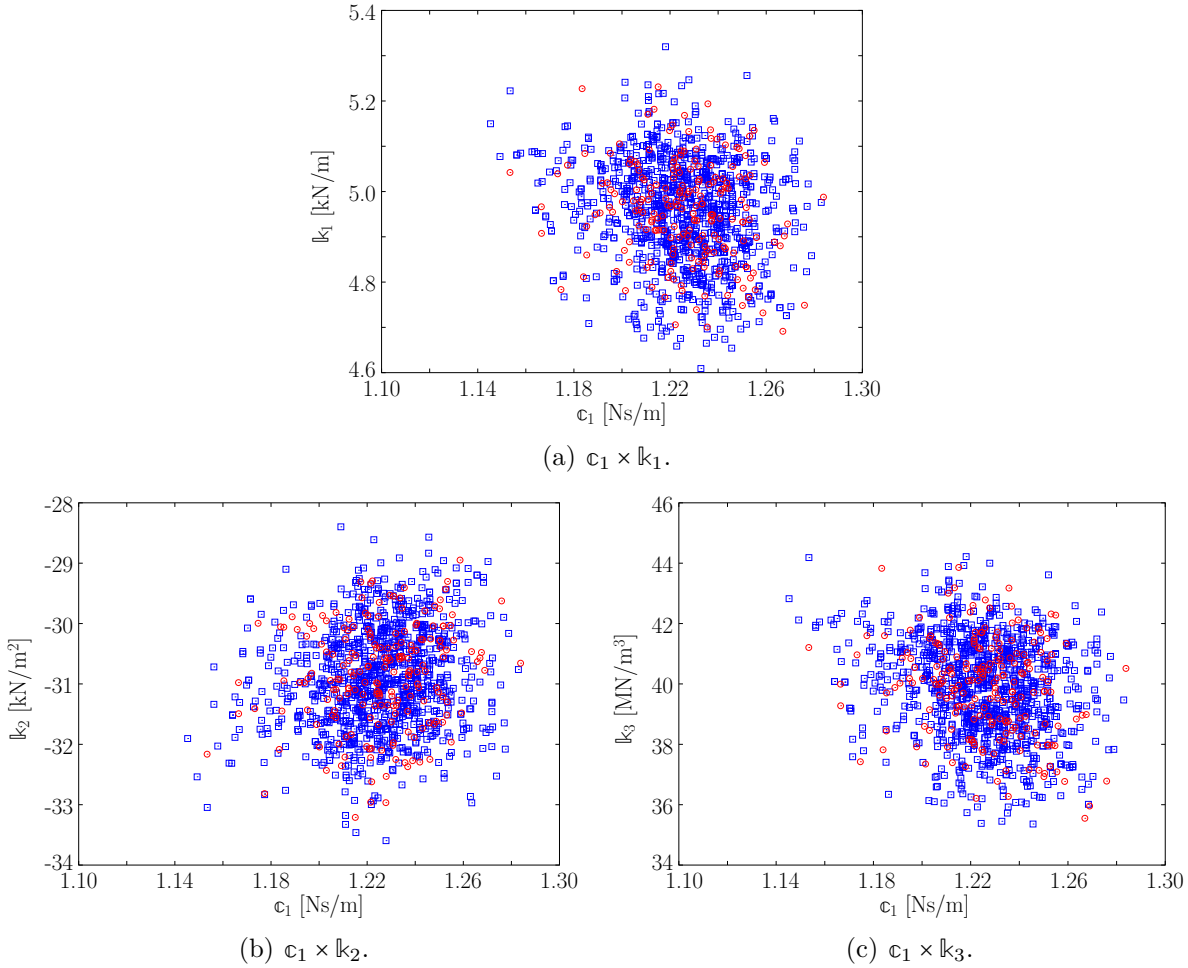

(a) $\mathbb{c}_1 \times \mathbb{k}_1$.

(b) $\mathbb{c}_1 \times \mathbb{k}_2$.

(c) $\mathbb{c}_1 \times \mathbb{k}_3$.

Source: Prepared by the author.

Figure 9 – Correlation between stiffnesses random variables. ○ represents the experimental values and □ the generated samples.

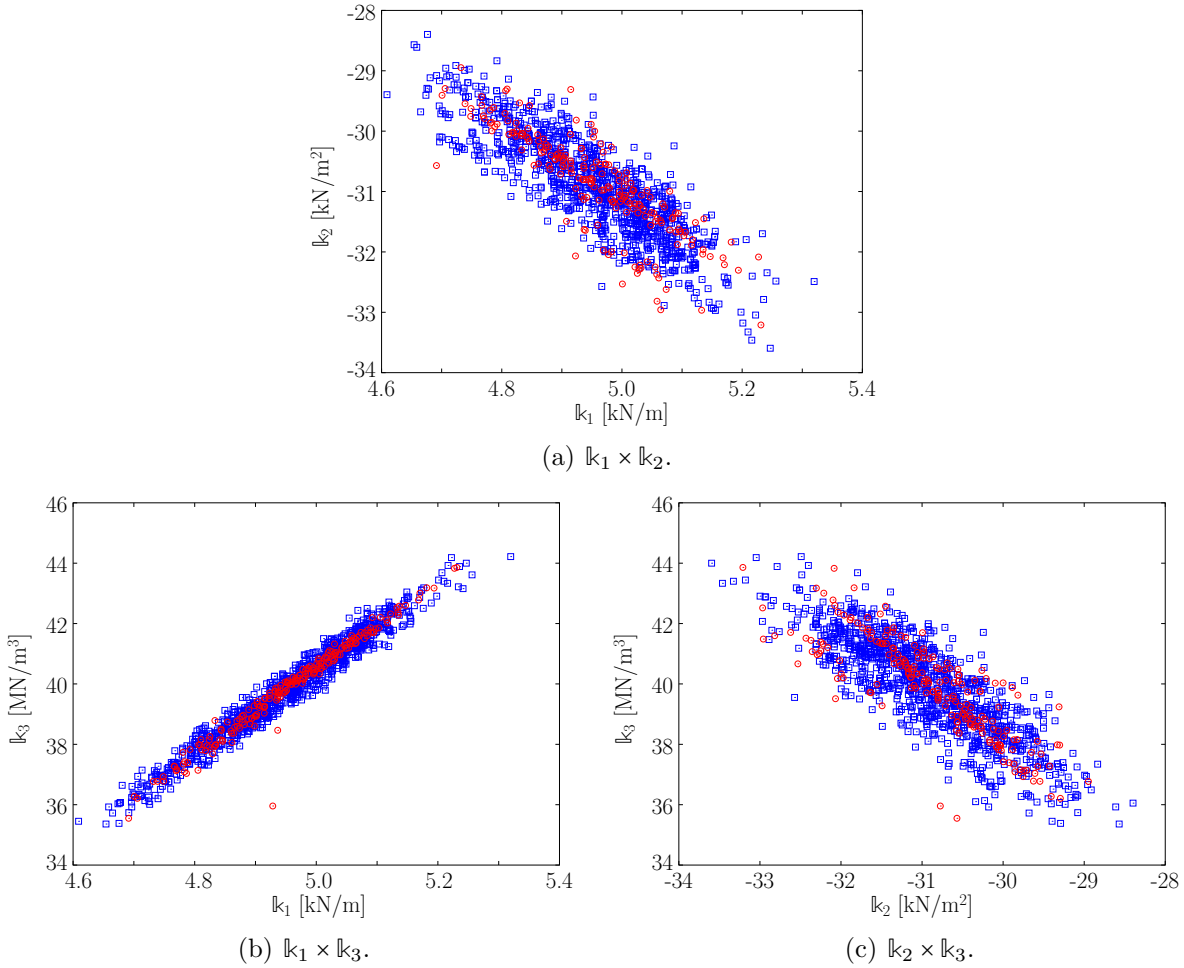

(a) $\mathbb{k}_1 \times \mathbb{k}_2$.

(b) $\mathbb{k}_1 \times \mathbb{k}_3$.

(c) $\mathbb{k}_2 \times \mathbb{k}_3$.

Source: Prepared by the author.

2.5.4 Study of MC convergence

It is important to define the number of MC simulations required to reliably compute the uncertainties propagation (SOIZE, 2005). In this sense, the convergence of the MC method is investigated by means of the Euclidean norm of the response vector, through the metric

$$conv(N_s) = \sqrt{\frac{1}{N_s}\sum_{n=1}^{N_s}\int_{t=t_0}^{t_f} \|\dot{x}(\theta_n, t)\|^2 dt} \tag{16}$$

where N_s is the number of MC simulations, $[t_0, t_f]$ is the time interval of analysis, $\|.\|$ denotes the standard Euclidean norm and $\dot{x}(\theta_n, t)$ is the n-th realization of the system's velocity. The value of this metric as a function of the number of MC realizations can be seen in Fig. 10 for two different levels of excitation, the low level (linear behavior) and the high level (nonlinear behavior). It can be seen that the convergence is obtained with the number of simulations used (N_s = 1024).

Figure 10 – Investigation of MC simulation convergence.

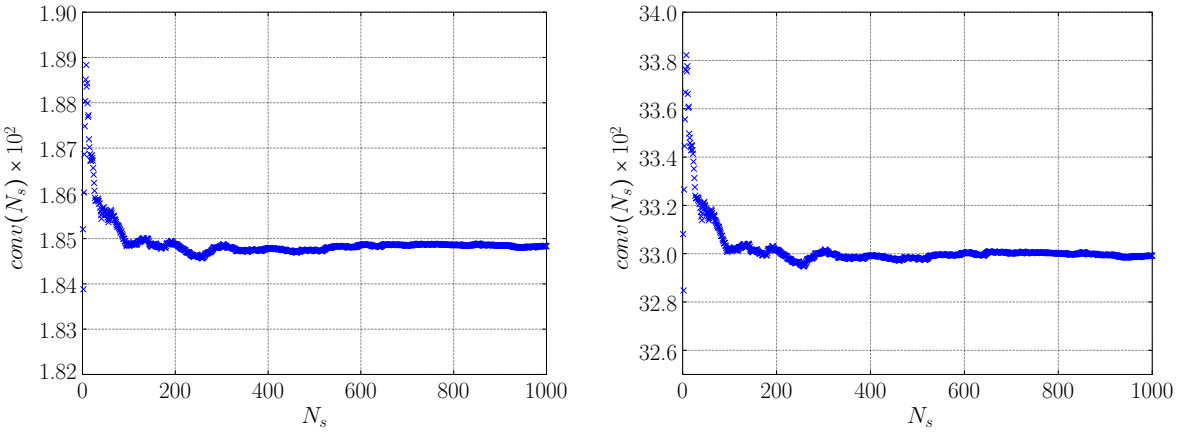

(a) Low level of input (linear behavior).

(b) High level of input (nonlinear behavior).

Source: Prepared by the author.

2.5.5 Model validation

The stochastic model's output obtained through MC simulations can be compared with new experimental signals measured. Comparisons between experimental and theoretical beam velocity, in the time domain, can be seen in Fig. 11, considering the same chirp signal used in the model identification process. It is observed that the experimental response is inside the limits with 99% of confidence, what indicates that the stochastic

model can describe adequately the system behavior in the time domain, for both linear and nonlinear regimes of motion.

Figure 11 – Comparison between experimental and theoretical responses in the time domain, considering a chirp input signal. – represents the mean value, the gray area represents the 99% confidence bands and – ∘ – the experimental realizations.

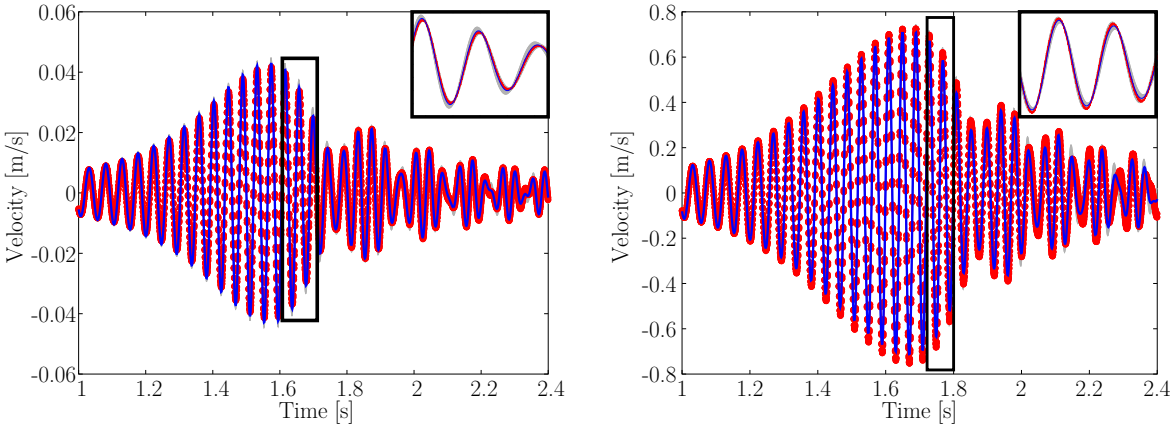

(a) Low level of input (linear behavior). (b) High level of input (nonlinear behavior).

Source: Prepared by the author.

In order to ensure the robustness of the identification process, a validation test in the frequency domain with an excitation signal of a different nature is also performed, where the stochastic model is compared with new experimental data from the stepped sine test. This test is performed with a low and a high level of amplitude in the system input, and the results are shown in Fig. 12. It is possible to see that the stochastic model describes well the system behavior in both situations. The difference between the curves saw in the linear case is related to the difficulty of conducting the stepped sine test with a very low excitation amplitude and the possible influence of the second vibration mode shape, this can be confirmed observing Fig. 2(a) where the result for excitation of 0.01 V is a little different from the other two, outside the resonance region. Discrepancies in the nonlinear regime of motion, before the jump frequency, can be related to the interaction between the shaker and structure that can not be well predicted by the simple model proposed. In the nonlinear case, the dispersion is large and the observed mean value is representative. The stochastic model is able to describe the experimental behavior. The large dispersion in the nonlinear regime of motion is a consequence of the nonlinear restoring force variation that makes with the nonlinear stiffness vary too much, as seen in Figs. 6(b) and 6(c).

Finally, the distribution of the model values close to the jump frequency can be obtained by two cuts in the results shown in Fig. 12(b). Fig. 13(a) shows the distribution of the maximum velocity values just before the occurrence of the jump phenomenon. It

can be seen a unimodal behavior with the experimental data very close to the mean value. Fig. 13(b) shows the distribution exactly in the experimental jump frequency (26 Hz considering 0.5 Hz of resolution). It is observed a bimodal behavior in the model values, but the experimental data is close to the region with greater probability of occurrence. This means that the model did not present the jump phenomenon in 26 Hz for all MC simulations, but the probability of occurrence in this frequency is bigger, showing that the stochastic model can predict the system behavior with statistic confidence.

Figure 12 – Comparison between experimental and theoretical responses obtained during the stepped sine test. – represents the mean value, the **gray area** represents the 99% confidence band and – ∘ – the experimental realizations.

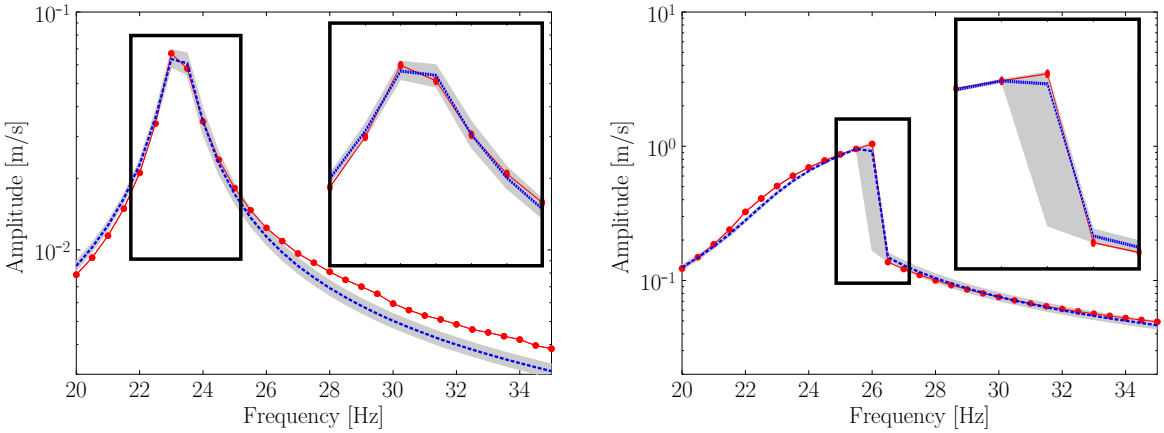

(a) Low level of input (linear behavior).

(b) High level of input (nonlinear behavior).

Source: Prepared by the author.

Figure 13 – Stepped sine test, considering a high level of input. Distributions obtained considering 2 cuts close to the jump frequency. The red line refers to the experimental data.

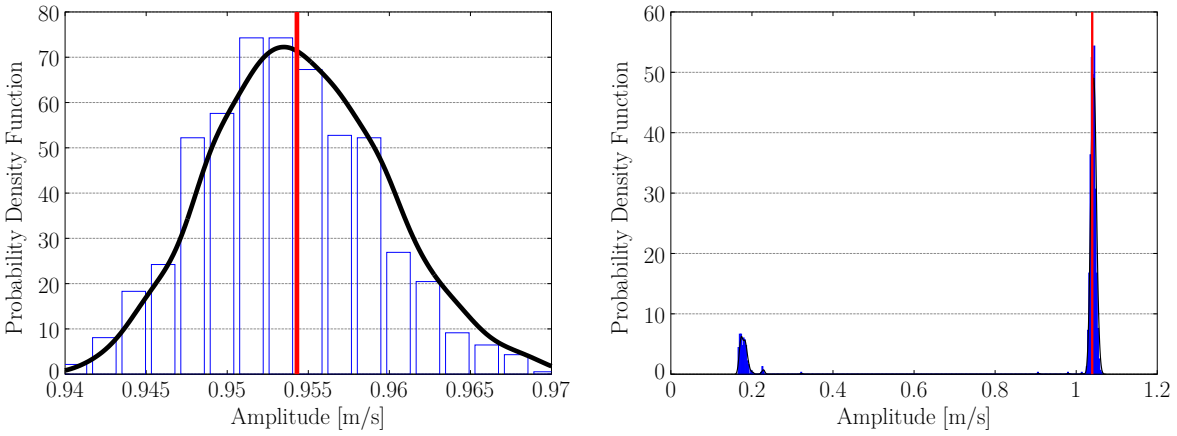

(a) Excitation frequency = 25.5 Hz.

(b) Excitation frequency = 26 Hz (Jump frequency).

Source: Prepared by the author.

2.6 CONCLUSIONS

In this chapter, a stochastic version of the restoring force surface method was proposed, to identify the parameters of a SDoF system. The formulation of this method was developed in terms of a stochastic process able to take into account the intrinsic variability of the system's parameters. In the analysis of a non-complex nonlinear system, the proposed method can be applied without the use of sophisticated mathematical tools. The effectiveness of this methodology was tested and verified in the estimation of the parameters of a clamped-free beam, with nonlinear effects induced by the presence of a magnet near to the free end. Although the variations in the system's parameters are considerable, especially in the nonlinear regime, experimental and theoretical results show that the identified stochastic model is robust, once it describes very well the structure behavior and specifies a reliability envelope. Finally, from results, we can conclude that even in experiments conducted in controlled conditions (in a laboratory), it is important to take into account the uncertainties in the parameters estimation procedures, once they are very sensitive to system's output variations. Furthermore, the construction of stochastic models allows the mathematical model to describe the system behavior with statistic confidence. The results obtained in this chapter will be considered in the simulations performed in chapter 4, with the application of a damage detection procedure in a random Duffing oscillator.

3 FROM THE DETERMINISTIC TO THE STOCHASTIC VERSION OF VOLTERRA SERIES

This chapter describes the proposed methodology for modeling nonlinear systems assuming data variation based on a stochastic version of the Volterra series, expanded using random Kautz functions. The idea of Monte Carlo simulations is used in the process of Multiple Models (MM) identification, aiming the description of the intrinsical variation of the system's behavior. The stochastic version of the Volterra series formulation presented here will be used in the next chapters in the identification of reference models to be used in the process of damage detection.

The chapter is organized as follows: section 3.1 shows the classical deterministic version of the Volterra series approach represented in discrete-time; section 3.2 shows the deterministic version of the Kautz filters formulation; section 3.3 presents an explanation of the uncertainties that will be considered using this formulation; section 3.4 presents the explanation of the stochastic version of the Volterra series based on Monte Carlo simulations; section 3.5 shows the random version of the Kautz functions formulation and the procedure used to determine the random Kautz poles; and finally, section 3.6 brings the final remarks of the chapter. All the formulation described in this chapter can be found in the following works: Shiki, Silva and Todd (2017), Villani, Silva and Cunha Junior (2017a), Villani, Silva and Cunha Junior (2019b), Villani *et al.* (2019a) and Villani *et al.* (2019b).

3.1 DETERMINISTIC VOLTERRA SERIES

Consider a discrete-time causal nonlinear system with a single output $k \in \mathbb{Z}_+ \mapsto y(k)$ caused by a single input $k \in \mathbb{Z}_+ \mapsto u(k)$, with $\mathbb{Z}_+$ representing the set of nonnegative integers. Through the discrete-time Volterra series, nonlinear system's output can be written in the form

$$y(k) = \sum_{\eta=1}^{\infty} \sum_{n_1=1}^{N_1} \dots \sum_{n_\eta=1}^{N_\eta} \mathcal{H}_\eta(n_1, \dots, n_\eta) \prod_{i=1}^{\eta} u(k - n_i), \tag{17}$$

where $(n_1, .., n_\eta) \in \mathbb{Z}_+^\eta \mapsto \mathcal{H}_\eta(n_1, \dots, n_\eta)$ represents the η-order Volterra kernel, N_1 the number of input lags considered in the first order kernel and N_η the number of input

lags considered in the η-order kernel. In this thesis, the maximum kernel order used is $\eta = 3$, since the behavior of all nonlinear systems studied can be well approximated by the first three kernels. This formalism is very versatile, in way that it allows one to represent different kinds of nonlinearities using the convolution concept (SCHETZEN, 1980). Additionally, the main benefit of the Volterra series model is the capability to reproduce the system's output as a sum of linear and nonlinear contributions

$$y(k) = \underbrace{y_1(k)}_{linear} + \underbrace{y_2(k) + y_3(k) + \cdots + y_\eta(k)}_{nonlinear}, \tag{18}$$

where $k \in \mathbb{Z}_+ \mapsto \{y_1(k), y_2(k), y_3(k), \ldots, y_\eta(k)\}$ represent, respectively, the first kernel (linear) contribution, the second kernel (quadratic) contribution, the third kernel (cubic) contribution and the η-order kernel contribution.

On the other hand, as broadly addressed in previous works, the main disadvantage of the approach is the challenge in achieving the convergence when a high number of terms is used (SHIKI; SILVA; TODD, 2017; VILLANI; SILVA; CUNHA JUNIOR, 2017a; VILLANI; SILVA; CUNHA JUNIOR, 2019b). In order to reduce the number of terms necessary to obtain a good approximation, the Volterra kernels $\mathcal{H}_\eta$ can be expanded into an orthonormal basis, such as the Kautz functions - that is employed in this thesis (KAUTZ, 1954; HEUBERGER; HOF; WAHLBERG, 2005). In this way, the Volterra kernels can be rewritten according to the approximation

$$\mathcal{H}_\eta(n_1, \ldots, n_\eta) \approx \sum_{i_1=1}^{J_1} \ldots \sum_{i_\eta=1}^{J_\eta} \mathcal{B}_\eta(i_1, \ldots, i_\eta) \prod_{j=1}^{\eta} \psi_{\eta,i_j}(n_j), \tag{19}$$

where $J_1, \ldots, J_\eta$ are the number of Kautz functions used in each orthonormal projections of the Volterra kernels, $(i_1, \ldots, i_\eta) \in \mathbb{Z}_+^\eta \mapsto \mathcal{B}_\eta(i_1, \ldots, i_\eta)$ represents the η-order Volterra kernel expanded in the orthonormal basis and $n_j \in \mathbb{Z}_+ \mapsto \psi_{i_j}(n_j)$ represents the i_j-th Kautz filter.

Thus, using the discrete Volterra series representation of Eq. (17) and the Kautz approximation (19), the system's output can be described by the multidimensional convolution between the orthonormal kernels $\mathcal{B}_\eta$ and the input signal filtered by the Kautz functions, i.e.,

$$y(k) \approx \sum_{\eta=1}^{\infty} \sum_{i_1=1}^{J_1} \ldots \sum_{i_\eta=1}^{J_\eta} \mathcal{B}_\eta(i_1, \ldots, i_\eta) \prod_{j=1}^{\eta} l_{\eta,i_j}(k), \tag{20}$$

where $k \in \mathbb{Z}_+ \mapsto l_{\eta,i_j}(k)$ is a simple filtering of the input signal $u(k)$ by the Kautz function

ψ_{η,i_j} related to each kernel

$$l_{\eta,i_j}(k) = \sum_{n_i=1}^{J_\eta} \psi_{\eta,i_j}(n_i)u(k-n_i). \tag{21}$$

Then, the coefficients of the kernels can be estimated through the least squares method. The matrix $\mathbf{\Gamma}$ can be completed with the regressors of the input signal filtered $l_{i_j}(k)$ and the vector $\mathbf{y}$ with the experimental output signal $y(k)$

$$\mathbf{\Phi} = (\mathbf{\Gamma}^{\mathrm{T}}\mathbf{\Gamma})^{-1}\mathbf{\Gamma}^{\mathrm{T}}\mathbf{y}\,, \tag{22}$$

where $\mathbf{\Phi}$ is composed by the terms of the orthonormal kernels. More information on the identification approach based on Volterra series can be found in Silva (2011b), Silva (2011a). Details about Kautz functions are given in the next section. The reader is also encouraged to see Wahlberg and Makila (1996), Oliveira *et al.* (2012), Silva, Cogan and Foltête (2010), Silva (2011a), Silva (2011b), and Shiki, Silva and Todd (2017).

3.2 DETERMINISTIC KAUTZ FUNCTIONS

The Kautz functions are used in this thesis as orthonormal bases because of their properties to describe the oscillatory dynamic models (KAUTZ, 1954). The Kautz functions are always represented in pairs and their generalized form in z-domain is written as (WAHLBERG, 1994)

$$\Psi_{\eta,2j-1}(z) = \frac{z\sqrt{(1-a_\eta^2)(1-b_\eta^2)}}{z^2 + a_\eta(b_\eta-1)z - b_\eta}\left[\frac{-b_\eta z^2 + a_\eta(b_\eta-1)z + 1}{z^2 + a_\eta(b_\eta-1)z - b_\eta}\right]^{j-1}, \tag{23}$$

and

$$\Psi_{\eta,2j}(z) = \Psi_{\eta,2j-1}(z)\frac{z-a_\eta}{\sqrt{1-a_\eta^2}}\,, \tag{24}$$

being the values of a_η and b_η defined by

$$a_\eta = \frac{(\mathcal{Z}_\eta + \bar{\mathcal{Z}}_\eta)}{1 + \mathcal{Z}_\eta\bar{\mathcal{Z}}_\eta} \tag{25}$$

and

$$b_\eta = -\mathcal{Z}_\eta\bar{\mathcal{Z}}_\eta\,, \tag{26}$$

where $\mathcal{Z}$ and $\bar{\mathcal{Z}}$ are, respectively, the Kautz pole and its complex conjugate in discrete domain. The discrete poles $\mathcal{Z}_\eta$ can be related to the continuous poles $\mathcal{S}_\eta$ through the

equation

$$\mathcal{Z}_\eta = \exp\left(\frac{\mathcal{S}_\eta}{F_s}\right), \tag{27}$$

where F_s represents the sampling frequency. Finally, the Kautz poles for each kernel, represented in the continuous domain, are defined as

$$\mathcal{S}_\eta = -\xi_\eta\omega_\eta - j\omega_\eta\sqrt{1-\xi_\eta^2}, \tag{28}$$

where ω_η and ξ_η are the Kautz parameters of the η-order kernel. Remembering that, for the first kernel the Kautz parameters are the natural frequency and damping ratio of the equivalent linear system. Generally, it is common to use an optimization process to find the values that better fits the system behavior (ROSA; CAMPELLO; AMARAL, 2007).

3.3 SYSTEM UNCERTAINTIES

In the literature, uncertainties can be classified into two main groups: *data uncertainties*[1] and *model uncertainties*[2] (SOIZE, 2012; SOIZE, 2013; SOIZE, 2017). The *data uncertainties* are intrinsic to scenarios with variabilities, such as noise in the measured data (experimental data) and variations with respect to the nominal configuration of the structures, due to geometric imperfections, manufacturing irregularities, environmental conditions, etc. These uncertainties can not be eliminated, only better characterized. On the other hand, the *model uncertainties* are a consequence of the limited knowledge about the model structure to be used, i.e., ignorance about the system's physics. By increasing knowledge about a certain system these uncertainties can be mitigated (SOIZE, 2012; SOIZE, 2013; SOIZE, 2017).

For the sake of simplicity, only the *data uncertainties* will be taken into account. In the context of system identification, such uncertainties are materialized in the form of variations in the model parameters. Implicit in this approach is the hypothesis that the Volterra series is capable of producing a reliable representation of the system's nonlinear behavior. Therefore, the nonlinearities considered in this work are smooth, polynomial and containing only quadratic and cubic terms. In this way, a parametric probabilistic approach is employed (SOIZE, 2012; SOIZE, 2013; SOIZE, 2017). Thus, the model parameters subjected to uncertainties are described as random variables or random processes, defined on the probability space $(\Theta, \mathbb{\Sigma}, \mathbb{P})$, where Θ is sample space, $\mathbb{\Sigma}$

[1] also known as *aleatory*
[2] also known as *epistemic*

is a σ-algebra over Θ, and $\mathbb{P}$ is a probability measure. It is assumed that any random variable $\theta \in \Theta \mapsto \mathbb{V}(\theta) \in \mathbb{R}$ in this probabilistic setting, with probability distribution $P_{\mathbb{V}}(dv)$ on $\mathbb{R}$, admits a probability density function (PDF) $v \mapsto p_{\mathbb{V}}(v)$ with respect to dv.

3.4 THE STOCHASTIC VERSION OF THE VOLTERRA SERIES

In the discrete-time domain, assuming the presence of uncertainties, a single system's output can be interpreted as a random process realization that is a consequence of a single deterministic input. Considering the idea of convolution showed in Eq. (17), a random version of the discrete-time Volterra series can describe the stochastic nonlinear system's output as follows

$$\mathbb{y}(\theta,k) = \sum_{\eta=1}^{\infty} \sum_{n_1=1}^{N_1} \cdots \sum_{n_\eta=1}^{N_\eta} \mathbb{H}_\eta(\theta, n_1, \ldots, n_\eta) \prod_{i=1}^{\eta} u(k-n_i)\,, \tag{29}$$

where $u(k)$ is the same deterministic input signal considered in Eq. (17), the random process $(\theta,k) \in \Theta \times \mathbb{Z}_+ \mapsto \mathbb{y}(\theta,k)$ represents the stochastic nonlinear system's output and $(\theta, n_1, .., n_\eta) \in \Theta \times \mathbb{Z}_+^\eta \mapsto \mathbb{H}_\eta(\theta, n_1, \ldots, n_\eta)$ represents the random version of the η-order Volterra kernel.

The benefit of using the Volterra series, i.e., the capability to separate the linear and nonlinear contributions through the kernels is kept, but now, the contributions are accounted as random processes

$$\mathbb{y}(\theta,k) = \underbrace{\mathbb{y}_1(\theta,k)}_{linear} + \underbrace{\mathbb{y}_2(\theta,k) + \mathbb{y}_3(\theta,k) + \cdots + \mathbb{y}_\eta(\theta,k)}_{nonlinear}, \tag{30}$$

where $(\theta,k) \in \Theta \times \mathbb{Z}_+ \mapsto \mathbb{y}_1(\theta,k)$ is the random output obtained using the first random kernel, $(\theta,k) \in \Theta \times \mathbb{Z}_+ \mapsto \mathbb{y}_2(\theta,k)$ is the random output obtained using the second random kernel, and so on.

In the same sense described previously, aiming to solve the convergence problem, the Volterra kernels can be expanded in terms of Kautz functions

$$\mathbb{H}_\eta(\theta, n_1, \ldots, n_\eta) \approx \sum_{i_1=1}^{J_1} \ldots \sum_{i_\eta=1}^{J_\eta} \mathbb{B}_\eta(\theta, i_1, \ldots, i_\eta) \prod_{j=1}^{\eta} \Psi_{\eta,i_j}(\theta, n_j)\,, \tag{31}$$

where $J_1, \ldots, J_\eta$ represents the number of Kautz functions used in the kernels projections, the η-order random Volterra kernel expanded in the orthonormal basis is represented by the random process $(\theta, i_1, \ldots, i_\eta) \in \Theta \times \mathbb{Z}_+^\eta \mapsto \mathbb{B}_\eta(\theta, i_1, \ldots, i_\eta)$ and the random process

$(\theta, k) \in \Theta \times \mathbb{Z}_+ \mapsto \mathbb{I}_{i_j}(\theta, k)$ is a filtering of the deterministic input signal using the random Kautz functions. The Kautz functions are supposed to be random because their definition depends on the dynamics of the system and, as the system's output is considered as a random process, it is presumed that the Kautz functions will randomly change too.

The stochastic equivalent equation of the approximation shown in (20) is written

$$\mathbb{y}(\theta, k) \approx \sum_{\eta=1}^{\infty} \sum_{i_1=1}^{J_1} \dots \sum_{i_\eta=1}^{J_\eta} \mathbb{B}_\eta(\theta, i_1, \dots, i_\eta) \prod_{j=1}^{\eta} \mathbb{I}_{\eta, i_j}(\theta, k), \tag{32}$$

where the random process $(\theta, k) \in \Theta \times \mathbb{Z}_+ \mapsto \mathbb{I}_{i_j}(\theta, k)$ is a simple filtering of the deterministic input signal $u(k)$ by the random Kautz function Ψ_{i_j}, i.e.,

$$\mathbb{I}_{\eta, i_j}(\theta, k) = \sum_{n_i=0}^{J_\eta} \Psi_{\eta, i_j}(\theta, n_i) u(k - n_i). \tag{33}$$

Finally, the coefficients of the kernels can be calculated using the least-squares approximation in a deterministic way (SHIKI; SILVA; TODD, 2017), as shown before, and then, using the idea of Monte Carlo simulations and assuming the stochastic output as the random variable of the problem, the random kernels can be estimated. The Monte Carlo method was chosen because it is easier to perform when the deterministic algorithm is known(RUBINSTEIN; KROESE, 2016; SOIZE, 2017). Figure 14 shows a flowchart of the Volterra kernels estimation considering the random Kautz functions and the idea of Monte Carlo simulations. Once the random kernels are estimated, considering a new input signal and using Monte Carlo simulations (at this time the random kernels are the random variables of the process) the random output can be calculated.

Figure 14 – Description of the Volterra kernels identification approach used.

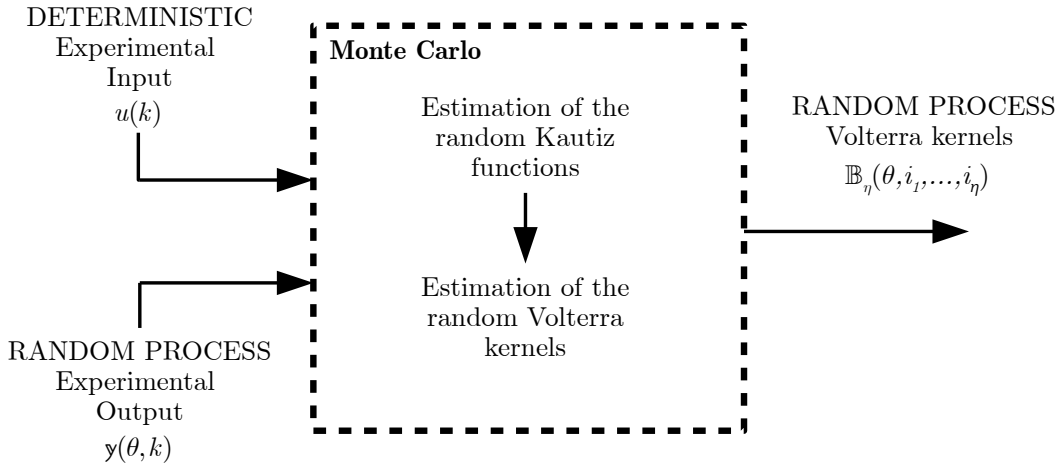

Source: Prepared by the author.

3.5 THE STOCHASTIC KAUTZ PARAMETERS

In order to create a robust identification, it is necessary to provide some type of certification, i.e., an envelope of reliability for the nominal values of the model parameters. Such certification can be obtained by a stochastic model, where probability distributions, instead of scalar values, are identified for the model parameters. In this case, the system's output also becomes random, a stochastic process to be precise, allowing the model to predict the variations in response related to uncertainties. As a consequence of the system response variation, the natural frequencies and the damping ratios of the equivalent linear system can also vary, becoming random variables $\theta \in \Theta \mapsto \zeta_n(\theta) \in \mathbb{R}$, $\theta \in \Theta \mapsto \omega_n(\theta) \in \mathbb{R}$. As mentioned before, the Kautz parameters for each kernel are related to the system's natural frequencies and damping ratios, so they are also considered as random variables $\theta \in \Theta \mapsto \xi_\eta(\theta) \in \mathbb{R}$, $\theta \in \Theta \mapsto \omega_\eta(\theta) \in \mathbb{R}$.

The random system's output is used to define the Kautz poles values. Thus, for the first kernel, the Kautz parameters can be approximated as the natural frequency and the damping ratio of the equivalent linear system. These values can be obtained through modal analysis techniques and using the system's output when a low level of energy is applied since usually in this regime of motion the behavior is approximately linear. The definition of Kautz parameters related to the high order Volterra kernels is more complicated since they are not exactly natural frequencies and damping ratios, they may be complex combinations and modulations between these values. However, a parameterization of the higher-order Kautz poles with respect to the modal parameters allows that the optimization process does not need to be repeated every time, reducing the computational costs. Remembering that the series was truncated in the third-order kernel, it was considered possible to define linear relations between modal parameters and higher-order Kautz parameters

$$\begin{aligned} \omega_2(\theta) &= p_1\,\omega_n(\theta)\,, \quad \xi_2(\theta) = p_2\,\zeta_n(\theta)\,, \\ \omega_3(\theta) &= p_3\,\omega_n(\theta)\,, \quad \xi_3(\theta) = p_4\,\zeta_n(\theta)\,, \end{aligned} \tag{34}$$

where the relationships p_1, p_2, p_3 and p_4 can be allocated at the vector $\Delta = [p_1, p_2, p_3, p_4]$ and estimated minimizing the error function

$$\mathbf{J} = \frac{||y_{exp}(k) - y(k)||}{||y_{exp}(k)||}\,, \tag{35}$$

with

$$\Delta = \text{argmin } \mathbf{J}\,, \tag{36}$$

subject to

$$p_1^{low} \leq p_1 \leq p_1^{up} \tag{37}$$

$$p_2^{low} \leq p_2 \leq p_2^{up} \tag{38}$$

$$p_3^{low} \leq p_3 \leq p_3^{up} \tag{39}$$

$$p_4^{low} \leq p_4 \leq p_4^{up} \tag{40}$$

where $y_{exp}(k)$ is the deterministic discrete-time experimental output, $y(k)$ is the deterministic model response, the vector Δ contains the coefficients of the relationship between modal and Kautz parameters, *up* and *low* represent the upper and lower bounds, respectively. Once the coefficients were defined, the Kautz parameters variation can be obtained based on the model parameters variation. The optimization procedure does not need to be repeated every time, but only for one representative data. In the simulations performed in this work, only the response correspondent to the deterministic values of the system's parameters, or the mean value of the experimental response, was used to optimize the Kautz poles. And, the variation of Kautz poles was considered through the estimation of the modal parameters in each Monte Carlo realization.

3.6 CONCLUSIONS

This chapter presented the formulation proposed to create a stochastic version of the classical Volterra series model, using random Kautz filters, to identify systems that present nonlinear behavior, taken into account the data variation related to the presence of uncertainties. This same model will be applied in different situations as reference model in the damage detection process, aiming to explore the capability of the approach to be used in this kind of problem. Thereby, depending on the application, the final methodology adopted to detect the presence of damage can change but the main idea of estimating a stochastic reference model based on the Volterra series is always the same.

4 SIMULATED DAMAGE DETECTION BASED ON STOCHASTIC VOLTERRA SERIES: A NONLINEAR DAMAGE

This chapter deals with the construction of a systematic methodology to detect damage in uncertain nonlinear systems based on the stochastic Volterra model described in the chapter 3. The methodology is applied in a simulated example, a Duffing oscillator subject to the presence of a simulated breathing crack, modeled as a bilinear oscillator. Different damage indices are proposed based on multivariate data outliers detection and a hypothesis test is proposed to define if the system is healthy or damaged. The main goal is to study the capability of the methodology to detect the breathing crack without confusions with the intrinsically nonlinear behavior of the Duffing oscillator and the data variation caused by the presence of random variables in the Duffing equation. These results can be found in Villani, Silva and Cunha Junior (2019b).

The rest of this chapter is organized as follows: section 4.1 presents the simulated system that will be considered in the application of the damage detection methodology; section 4.2 describes the damage detection methodology based on stochastic Volterra series; section 4.3 shows the identification of the set of reference models to be used in the damage detection process; section 4.4 presents the results obtained with the application of the proposed approaches based on random Volterra kernels to detect damage; finally, section 4.5 presents the main conclusions about the results presented in this chapter.

4.1 MODELING A BREATHING CRACK IN AN UNCERTAIN NONLINEAR BEAM

This section describes the studied nonlinear system that can be approximated by a nonlinear single-degree-of-freedom (SDoF) model, a Duffing oscillator (KOVACIC; BRENNAN, 2011). The deterministic reference system is presented, then, the simulated damage used, a breathing cracked model, is shown. Finally, the upgrade to the stochastic version is done with the necessary information about the uncertainties considered.

4.1.1 Deterministic system in reference condition

As it was observed in chapter 2, the nonlinear behavior of a clamped-free aluminum beam with a steel mass positioned in its free extremity interacting with a magnet can be approximated by a Duffing oscillator equation, in a limited range of frequencies (Fig. 1). Thus, the deterministic model considered in this chapter is the same Duffing oscillator represented in Eq. (1). The deterministic values of the Duffing oscillator parameters were estimated and are shown in Tab. (1). The estimation of the parameters was performed considering modal analysis and the restoring force surface method, considering experimental data measured. The description of the procedure used to approximate the real system considered by the Duffing oscillator model was the same described in chapter 2. The more attentive reader will see that the deterministic values presented here are not the same as estimated before, that is because the experimental data used to estimate these parameters were measured in a different period of time and after many changes in the setup. From now on, this configuration will be assumed as the reference condition of the system and the system's output considered will be the velocity obtained through the integration of the Duffing motion equation Eq. (1).

Table 1 – Duffing oscillator parameters.

Parameter	**Deterministic value**
m_1 [kg]	0.26
c_1 [Ns/m]	1.36
k_1 [N/m]	5.49×10^3
k_2 [N/m^2]	3.24×10^4
k_3 [N/m^3]	4.68×10^7

Source: Villani, Silva and Cunha Junior (2019b).

In order to illustrate the nonlinear behavior of the system in the reference condition (Healthy), some tests were carried out. In all the tests, it was used a sampling frequency of 512 Hz, 2048 samples and two levels of the input signal (0.1 N - Low level and 1 N - High level) were considered, in order to study the linear and nonlinear behavior of the system. The system was excited by a chirp signal varying the excitation frequency from 15 to 30 Hz in 4 seconds. Figure 15 shows the time-frequency diagram of the system's output signals, considering the low and high level of the input amplitude. The nonlinear effect can be observed with the appearance of multiple harmonics (2 and 3 times the fundamental harmonic) when a high level of input is applied. These results confirm that the system has linear behavior to the low level of the input signal and nonlinear to

the high level of input, in the reference condition. The presence of multiple harmonics is related to the nonlinear stiffnesses of the Duffing oscillator motion equation. These results show, clearly, the nonlinear behavior of the system due to large displacements (condition reached considering 1 N as excitation amplitude).

Figure 15 – Time-frequency diagram of the response for different levels of input amplitude, considering the reference condition.

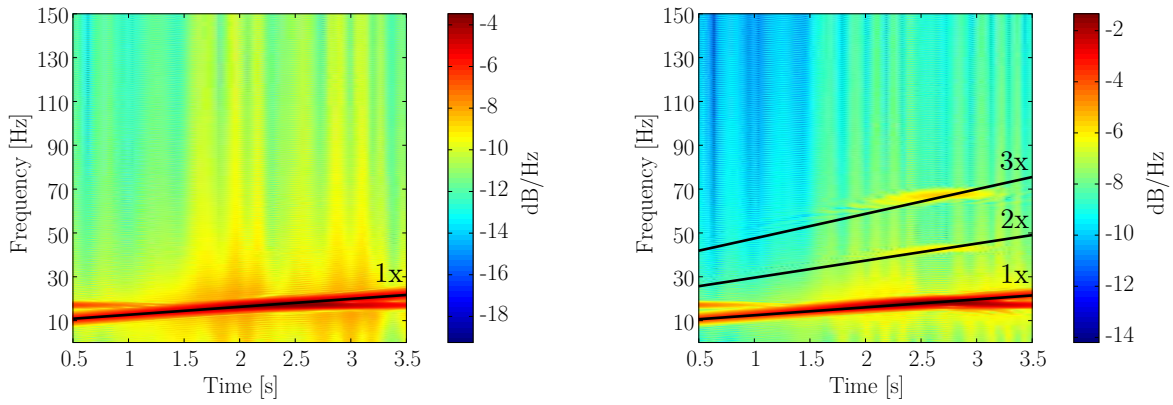

(a) Low input (0.1 N). (b) High input (1 N).

Source: Adapted from Villani, Silva and Cunha Junior (2019b).

4.1.2 Damage simulated - A breathing crack model

A breathing crack model is used to emulate the presence of a damage in the reference studied system. Figure 16 shows the presence of a crack in the system of interesting.

Figure 16 – Nonlinear system simulated in the damaged condition.

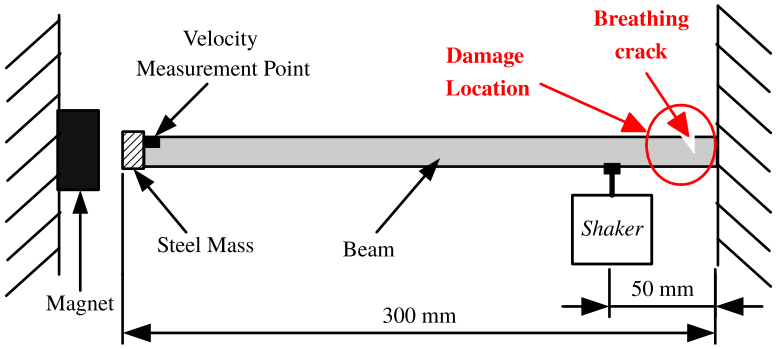

Source: Villani, Silva and Cunha Junior (2019b).

The objective is to detect the presence of the crack in the beam, considering that the system has nonlinear behavior before (Duffing oscillator) and after (breathing crack)

the damage occurrence, taking into account the data variation. In other words, the nonlinear characteristic of the damage has a different nature of the nonlinear behavior of the system in the reference condition. Many manuscripts, over the years, have shown the approximation of the breathing crack phenomenon by a single-degree-of-freedom (SDoF) model, as a bilinear oscillator (CHATI; RAND; MUKHERJEE, 1997; ANDREAUS; CASINI; VESTRONI, 2007; CHATTERJEE, 2010b; PRAWIN; RAO, 2018). Combining the reference model (Duffing oscillator) with the cracked beam model, the system behavior can be approximated by

$$m_1\,\ddot{x}(t) + c_1\,\dot{x}(t) + \mathcal{G}(x(t),t) + k_2\,x(t)^2 + k_3\,x(t)^3 = U(t), \tag{41}$$

where $\mathcal{G}(x(t),t)$ is the bilinear force

$$\mathcal{G}(x(t),t) = \begin{cases} k_1\,x(t), & \text{if } x(t) \geq 0 \\ \alpha\,k_1\,x(t), & \text{if } x(t) < 0 \end{cases}$$

where $0 < \alpha < 1$ represents the crack severity. If $\alpha = 1$ the system is in the reference condition (without crack). The breathing crack phenomenon generates a nonlinear behavior with different nature of the cubic effect of the reference model but similar to the quadratic effect of k_2. This situation makes the application of damage detection procedures difficult. The applied approach has to be able to detect the nonlinear damage without confusions with the nonlinear behavior of the reference condition. This is a great improvement compared with other authors like Peng, Lang and Billings (2007), Surace, Ruotolo and Storer (2011), and Prawin and Rao (2018), for example, that have used the Volterra series to detect damage, considering the linear behavior in reference condition and the nonlinear effects as a consequence of the crack occurrence.

In the presence of the breathing crack, the nonlinear behavior does not depend on the amplitude of the output signal and can be observed for all excitation amplitudes. Figure 17 shows the time-frequency diagram of the system response signals to the low and high level of amplitude excitation, considering the presence of a crack with $\alpha = 0.9$. The appearance of quadratic harmonics can be observed for both excitation amplitude. This behavior brings closer the breathing crack phenomenon by a SDoF model and it is a consequence of the bilinear characteristic of the response.

Figure 17 – Time-frequency diagram of the response for different levels of input amplitude, considering the crack severity $\alpha = 0.9$.

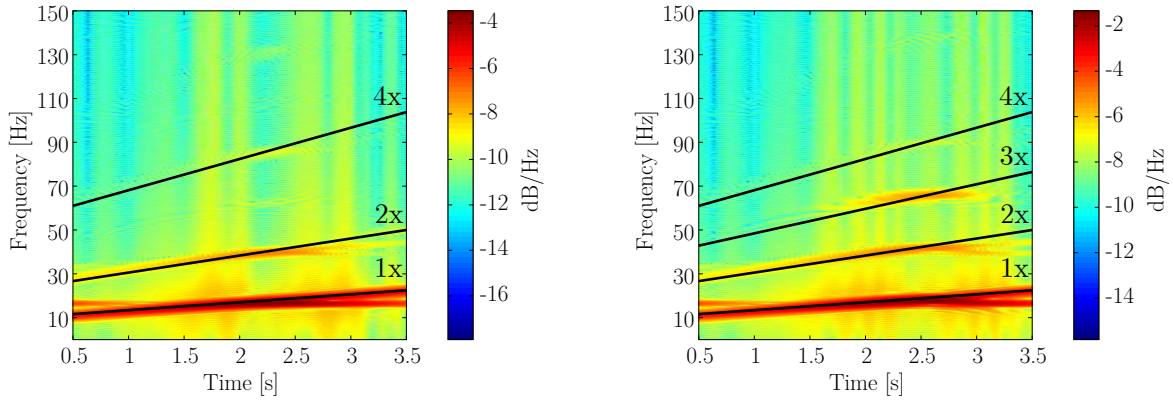

(a) Low input (0.1 N). (b) High input (1 N).

Source: Adapted from Villani, Silva and Cunha Junior (2019b).

4.1.3 Random version of the nonlinear system

As it is known, is essential to take the uncertainties into account to make robust predictions (CUNHA JUNIOR; FELIX; BALTHAZAR, 2017). The data uncertainties are related to environmental or operating conditions, temperature and humidity changes, sensor bonding conditions, that can generate variations in the fundamental frequencies and damping ratios of the structures and systems, making difficult the application of damage detection procedures (SOHN, 2007). Therefore, the main idea is to simulate these variabilities in order to reproduce, in a more realistic way, the difficulties involved in the damage detection process. In this context, it is not considered the simple noise addition in the measurements, but the variations in the system's dynamic behavior. Thus, the linear stiffness k_1 and damping coefficient c_1 of Eq. (41) are considered as random variables $\theta \in \Theta \mapsto \Bbbk_1(\theta) \in \mathbb{R}$, $\theta \in \Theta \mapsto \mathbb{c}_1(\theta) \in \mathbb{R}$. The variation of k_1 and c_1 reflects directly in the system dynamics since these parameters have influence in the fundamental frequency of oscillation and the damping ratio of the system. Then, Eq. (41) can be rewritten as

$$m_1\,\ddot{\aleph}(\theta,t) + \mathbb{c}_1(\theta)\,\dot{\aleph}(\theta,t) + \mathbb{G}(\aleph(\theta,t),t) + k_2\,\aleph(\theta,t)^2 + k_3\,\aleph(\theta,t)^3 = U(t), \tag{42}$$

where the bilinear random force $\mathbb{G}(\aleph(\theta,t),t)$ can be described as

$$\mathbb{G}(\aleph(\theta,t),t) = \begin{cases} \Bbbk_1(\theta)\,\aleph(\theta,t), & \text{if } \aleph(\theta,t) \geq 0 \\ \alpha\,\Bbbk_1(\theta)\,\aleph(\theta,t), & \text{if } \aleph(\theta,t) < 0 \end{cases}$$

and the random processes $(\theta,t) \in \Theta \times \mathbb{R} \mapsto \mathbb{x}(\theta,t)$, $(\theta,t) \in \Theta \times \mathbb{R} \mapsto \dot{\mathbb{x}}(\theta,t)$, and $(\theta,t) \in \Theta \times \mathbb{R} \mapsto \ddot{\mathbb{x}}(\theta,t)$, represent, respectively, the displacement, velocity and acceleration.

To construct the probabilistic model, the PDFs of the random parameters were determined through the maximum entropy principle (JAYNES, 1957; CUNHA JUNIOR, 2017). Considering that the linear stiffness and the damping coefficient can not be negative, we assumed the interval $(0,\infty)$ as the support of these random variables. Also, it was considered that the expected value of $\mathbb{k}_1$ and $\mathbb{c}_1$ are known real numbers $\mu_{\mathbb{k}_1}$ and $\mu_{\mathbb{c}_1}$. For technical reasons, see Soize (2017) for details, we also supposed that the expected value of $\ln \mathbb{k}_1$ and $\ln \mathbb{c}_1$ are finite. Using these conditions as known information, such as done in Cunha Junior and Sampaio (2015), the principle of maximum entropy says that the probability density function (PDF) of these random variables is given by

$$p_{\mathbb{q}}(q) = \mathbb{1}_{(0,\infty)} \frac{1}{\mu_{\mathbb{q}}} \left(\frac{1}{\delta_{\mathbb{q}}^2}\right)^{\left(\frac{1}{\delta_{\mathbb{q}}^2}\right)} \frac{1}{\Gamma(1/\delta_{\mathbb{q}}^2)} \left(\frac{q}{\mu_{\mathbb{q}}}\right)^{\left(\frac{1}{\delta_{\mathbb{q}}^2}-1\right)} \exp\left(-\frac{q}{\delta_{\mathbb{q}}^2\,\mu_{\mathbb{q}}}\right) \tag{43}$$

where $\mathbb{q}$ represents the random parameter ($\mathbb{k}_1$ or $\mathbb{c}_1$), $\mu_{\mathbb{q}}$ is the mean value, $\delta_{\mathbb{q}} = \frac{\sigma_{\mathbb{q}}}{\mu_{\mathbb{q}}}$ is the dispersion coefficient, $\sigma_{\mathbb{q}}$ is the standard deviation, Γ indicates the gamma function, and $\mathbb{1}_{(0,\infty)}$ denotes the indicator function of the interval $(0,\infty)$. This PDF corresponds to a gamma distribution. The stochastic formulation was made assuming that $\mathbb{k}_1$ and $\mathbb{c}_1$ are independent random variables. The dispersion obtained in the system's output signal is bigger in this situation, representing a better test to the proposed approach. To compute the propagation of the uncertainties of the random parameters $\mathbb{k}_1$ and $\mathbb{c}_1$ through the model, the Monte Carlo (MC) method was employed using a total of 2048 MC realizations of the deterministic system's output signal. The simulations were performed considering $\mu_{\mathbb{k}_1} = 5.49 \times 10^3$ [N/m], $\delta_{\mathbb{k}_1} = 0.01$, $\mu_{\mathbb{c}_1} = 1.36$ [Ns/m], $\delta_{\mathbb{c}_1} = 0.01$. These values of dispersion were chosen to generate satisfactory variation in the system response. Figure 18 shows the probability densities of the random parameters used in the MC simulations.

To exemplify the difficulty of detecting damage in this situation, Fig. 19 shows the 99% confidence bands of the system's Frequency Response Function (FRF), considering 3 different system conditions. It is not possible to distinguish the damaged conditions from the reference state, considering the variation of the response since it can be observed an overlap of the envelopes. Therefore, the use of modal parameters or the direct system response to detecting damage in this situation is not recommended, because only conditions of high damage severity can be detected with probabilistic confidence. The idea is the use of the damage's nonlinear behavior as an indicator of its occurrence. However, the nonlinear behavior in the reference condition has to be considered to avoid false alarms.

Next section shows how to use the information given by the stochastic Volterra model to detect damage in this situation.

Figure 18 – Distribution of the random parameters $\Bbbk_1$ and $\Bbbc_1$.

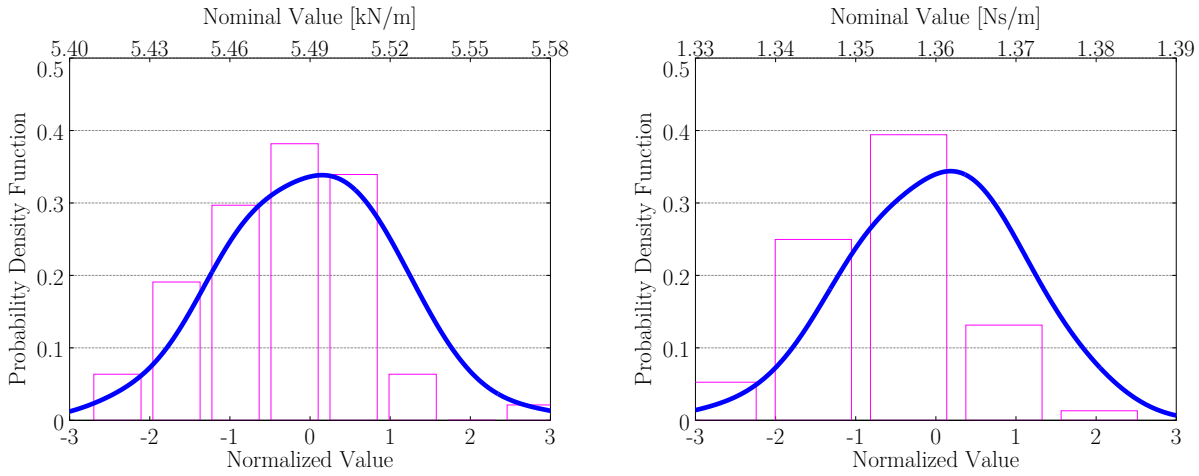

(a) Linear Stiffness. (b) Damping coefficient.

Source: Villani, Silva and Cunha Junior (2019b).

Figure 19 – FRFs considering different system conditions and 2 levels of the input amplitude. ■ represents $\alpha = 1$ (reference condition), ■ $\alpha = 0.98$ (damaged condition) and ■ $\alpha = 0.96$ (damaged condition).

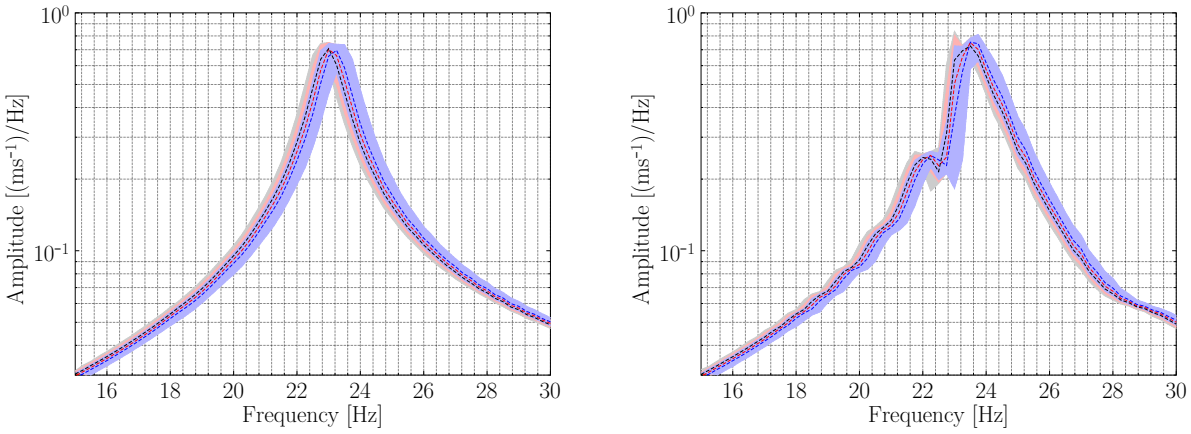

(a) Low level of input (0.1 N). (b) High level of input (1 N).

Source: Villani, Silva and Cunha Junior (2019b).

4.2 DAMAGE DETECTION METHODOLOGY

The stochastic Volterra series described in chapter 3 can be used as a mathematical model to approximate the nonlinear systems' output signal. This stochastic model is the

root of all damage detection procedures presented in this work. However, the way to establish a better manner to apply the series' advantages will change from one example to others. The differences between the approaches show the evolution of the methodology during the period of research. The first ideas and results obtained are presented in this chapter. From the estimation of the stochastic Volterra model in the reference condition, through the identification o multiple Volterra models, the kernels' coefficients and contributions can be used as damage sensitive features to be used in the detection algorithm as described below.

4.2.1 Volterra kernels' coefficients as damage sensitive feature

The first approach is based on the coefficients of the Volterra kernels identified. This methodology does not consider the direct influence of the Kautz functions in the procedure, because only the coefficients expanded in the orthonormal basis are considered. The influence of the random Kautz functions is taken into account only in the process of model identification. Considering Eq. (22) and the Volterra series truncated in the third-order term, the reduced-order kernels coefficients, for each Monte Carlo realization, are allocated as

$$\begin{aligned}
\boldsymbol{\Phi} &= \left[\boldsymbol{\Phi_1}, \boldsymbol{\Phi_2}, \boldsymbol{\Phi_3}\right]^{\mathrm{T}}, \\
\boldsymbol{\Phi_1} &= \{\mathcal{B}_1(1), \mathcal{B}_1(2), \ldots, \mathcal{B}_1(J_1)\}^{\mathrm{T}}, \\
\boldsymbol{\Phi_2} &= \{\mathcal{B}_2(1,1), \mathcal{B}_2(1,2), \ldots, \mathcal{B}_2(1,J_2), \mathcal{B}_2(J_2,1), \ldots, \mathcal{B}_2(J_2,J_2)\}^{\mathrm{T}}, \\
\boldsymbol{\Phi_3} &= \{\mathcal{B}_3(1,1,1), \mathcal{B}_3(1,2,1), \ldots, \mathcal{B}_3(1,J_3,1), \mathcal{B}_3(1,1,2), \ldots \\
&\quad \ldots, \mathcal{B}_3(1,J_3,J_3), \ldots, \mathcal{B}_3(J_3,J_3,J_3)\}^{\mathrm{T}},
\end{aligned} \tag{44}$$

remembering that J_1, J_2 and J_3 are the number of Kautz functions used, considering the first, second and third kernels, respectively. It is expected that the main information about the high order kernels is allocated in the main diagonal, so it is considered as monitoring parameters only the coefficients positioned in this region. Thus, considering the stochastic version of the Volterra series and the Monte Carlo simulations, the coefficients with higher

contribution can be used to represent the model identified in the reference condition

$$\begin{aligned}
\mathbb{\lambda}_{lin}(\theta, i_1) &= \{\mathbb{B}_1(\theta, 1), \mathbb{B}_1(\theta, 2), \ldots, \mathbb{B}_1(\theta, J_1)\}^{\mathrm{T}}, \\
\mathbb{\lambda}_{quad}(\theta, i_1 = i_2) &= \{\mathbb{B}_2(\theta, 1, 1), \mathbb{B}_2(\theta, 2, 2), \ldots, \mathbb{B}_2(\theta, J_2, J_2)\}^{\mathrm{T}}, \\
\mathbb{\lambda}_{cub}(\theta, i_1 = i_2 = i_3) &= \{\mathbb{B}_3(\theta, 1, 1, 1), \mathbb{B}_3(\theta, 2, 2, 2), \ldots, \mathbb{B}_3(\theta, J_3, J_3, J_3)\}^{\mathrm{T}}, \\
\mathbb{\lambda}_{nl}(\theta, i_{nl}) &= \{\mathbb{\lambda}_{quad}(\theta, i_1 = i_2), \mathbb{\lambda}_{cub}(\theta, i_1 = i_2 = i_3)\}^{\mathrm{T}},
\end{aligned} \tag{45}$$

where $(\theta, i_1) \in \Theta \times \mathbb{Z}_+ \mapsto \mathbb{\lambda}_{lin}(\theta, i_1)$ represents the coefficients of the first kernel, $(\theta, i_1 = i_2) \in \Theta \times \mathbb{Z}_+ \mapsto \mathbb{\lambda}_{quad}(\theta, i_1 = i_2)$ represents the coefficients of the diagonal of the second kernel, $(\theta, i_1 = i_2 = i_3) \in \Theta \times \mathbb{Z}_+ \mapsto \mathbb{\lambda}_{cub}(\theta, i_1 = i_2 = i_3)$ represents the coefficients of the main diagonal of the third kernel, all of them estimated in the reference condition. Additionally, $(\theta, i_{nl}) \in \Theta \times \mathbb{Z}_+ \mapsto \mathbb{\lambda}_{nl}(\theta, i_{nl})$ represents the nonlinear feature that takes into account $\mathbb{\lambda}_{quad}$ and $\mathbb{\lambda}_{cub}$ together. Now, considering the system in an unknown condition a new Volterra model can be estimated and the same features can be allocated in different vectors to be used in the damage detection procedure

$$\begin{aligned}
\lambda_{lin}(\theta, i_1) &= \{\mathcal{B}_1(1), \mathcal{B}_1(2), \ldots, \mathcal{B}_1(J_1)\}^{\mathrm{T}}, \\
\lambda_{quad}(i_1 = i_2) &= \{\mathcal{B}_2(1, 1), \mathcal{B}_2(2, 2), \ldots, \mathcal{B}_2(J_2, J_2)\}^{\mathrm{T}}, \\
\lambda_{cub}(i_1 = i_2 = i_3) &= \{\mathcal{B}_3(1, 1, 1), \mathcal{B}_3(2, 2, 2), \ldots, \mathcal{B}_3(J_3, J_3, J_3)\}^{\mathrm{T}}, \\
\lambda_{nl}(i_{nl}) &= \{\lambda_{quad}(i_1 = i_2), \lambda_{cub}(i_1 = i_2 = i_3)\}^{\mathrm{T}}.
\end{aligned} \tag{46}$$

Additionally, from now on the index $(.)_m$ will be used to represent the four different indicators calculated. Then, the general notation $\mathbb{\lambda}_m$ is used, with $m \in \{lin, quad, cub, nl\}$, depending on the number of the kernel considered in the analysis. The damage detection can be summarized as follow:

1. Identification of the multiple Volterra models in the reference condition, through the stochastic version of the Volterra series;
2. Construction of the indices based on kernels' coefficients, in the reference condition $(\mathbb{\lambda}_m)$;
3. Identification of a new Volterra model in an unknown condition;
4. Construction of the indexes based on kernels coefficients, in an unknown condition (λ_m);

5. Comparison between the coefficients estimated in unknown and reference conditions, if the new model belongs to the set of reference models, the structure is classified as healthy.

The comparison between the new indices and ones estimated in the reference condition will be done based on the novelty detection or outliers analysis in multivariate data, described further on.

4.2.2 Volterra kernels' contributions as damage sensitive feature

With the aim of exploring different possibilities, a different approach is proposed, based on the contribution of the Volterra kernels identified, to the total response. In this situation, the convolution between the input signal filtered by the Kautz functions and the kernels expanded in the orthonormal basis is considered, giving higher importance to the random Kautz functions. The main advantage of the Volterra series approach is the capability of separating the model response in linear and nonlinear contributions, through the kernels estimated. Considering the stochastic model identified in the reference condition, we can define the damage sensitive features based on the kernels' contributions

$$\mathbb{y}_{lin}(\theta,k) \approx \sum_{i_1=1}^{J_1} \mathbb{B}_1(\theta,i_1)\, \mathbb{l}_{i_1}(\theta,k)\,, \tag{47}$$

$$\mathbb{y}_{quad}(\theta,k) \approx \sum_{i_1=1}^{J_2}\sum_{i_2=1}^{J_2} \mathbb{B}_2(\theta,i_1,i_2)\, \mathbb{l}_{i_1}(\theta,k)\, \mathbb{l}_{i_2}(\theta,k)\,, \tag{48}$$

$$\mathbb{y}_{cub}(\theta,k) \approx \sum_{i_1=1}^{J_3}\sum_{i_2=1}^{J_3}\sum_{i_3=1}^{J_3} \mathbb{B}_3(\theta,i_1,i_2,i_3)\, \mathbb{l}_{i_1}(\theta,k)\, \mathbb{l}_{i_2}(\theta,k)\, \mathbb{l}_{i_3}(\theta,k)\,, \tag{49}$$

$$\mathbb{y}_{nl}(\theta,k) = \mathbb{y}_{quad}(\theta,k) + \mathbb{y}_{cub}(\theta,k)\,, \tag{50}$$

where $(\theta,k) \in \Theta \times \mathbb{Z}_+ \mapsto \mathbb{y}_{lin}(\theta,k)$, $(\theta,k) \in \Theta \times \mathbb{Z}_+ \mapsto \mathbb{y}_{quad}(\theta,k)$, $(\theta,k) \in \Theta \times \mathbb{Z}_+ \mapsto \mathbb{y}_{cub}(\theta,k)$ and $(\theta,k) \in \Theta \times \mathbb{Z}_+ \mapsto \mathbb{y}_{nl}(\theta,k)$ are the linear, quadratic, cubic and nonlinear contributions, respectively. Again, considering the system in an unknown condition a new Volterra

model can be estimated and the same features can be calculated

$$y_{lin}(k) \approx \sum_{i_1=1}^{J_1} \mathcal{B}_1(i_1)\, l_{i_1}(k)\,, \tag{51}$$

$$y_{quad}(k) \approx \sum_{i_1=1}^{J_2} \sum_{i_2=1}^{J_2} \mathcal{B}_2(i_1, i_2)\, l_{i_1}(k)\, l_{i_2}(k)\,, \tag{52}$$

$$y_{cub}(k) \approx \sum_{i_1=1}^{J_3} \sum_{i_2=1}^{J_3} \sum_{i_3=1}^{J_3} \mathcal{B}_3(i_1, i_2, i_3)\, l_{i_1}(k)\, l_{i_2}(k)\, l_{i_3}(k)\,, \tag{53}$$

$$y_{nl}(k) = y_{quad}(k) + y_{cub}(k)\,. \tag{54}$$

As mentioned before, the index $(.)_m$ is used to represent the five different indexes calculated. So, the general notation $\mathbb{y}_m$ is used from here, with $m \in \{lin, quad, cub, nl\}$. The damage detection is very similar to the methodology proposed using kernels coefficients and can be summarized as follow:

1. Identification of the multiple Volterra models in the reference condition, through the stochastic version of the Volterra series;
2. Calculation of the kernels contribution to the total model response, in the reference condition ($\mathbb{y}_m$);
3. Identification of the Volterra model in an unknown condition;
4. Calculation of the kernels contribution to the total model response, in an unknown condition (y_m);
5. Comparison between the contributions estimated in unknown and reference condition, if the new model belongs to the set of reference models, the structure is classified as healthy.

The difference here is that using the kernels contribution, the Kautz functions have an influence on the process, whereas using only the coefficients, they do not. Based on that, the variations in the frequency of oscillation and the damping coefficients are captured by the Kautz parameters, this version of the approach is sensitive to this variability. The damage detection is also done based on novelty detection, considering multivariate data.

4.2.3 **Novelty detection**

The indices proposed based on the Volterra models are described as random processes in the reference condition. This methodology combined with Monte Carlo simulations

allows the generation of a set of reference models that can be used as monitoring parameters, as described before. Therefore, the damage detection can be done based on novelty detection or outliers analysis, considering multivariate data. Let us consider the set of indices in the reference condition ($\mathbb{\lambda}_m$ or $\mathbb{y}_m$), the classical Mahalanobis squared distance can be calculated (WORDEN; MANSON; FIELLER, 2000)

$$\mathbb{D}_m^2(\theta) = \left[\mathbb{\lambda}_m(\theta, i) - \mu_{\mathbb{\lambda}_m}\right]^{\mathrm{T}} \mathbf{\Sigma}^{-1} \left[\mathbb{\lambda}_m(\theta, i) - \mu_{\mathbb{\lambda}_m}\right], \tag{55}$$

or

$$\mathbb{D}_m^2(\theta) = \left[\mathbb{y}_m(\theta, k) - \mu_{\mathbb{y}_m}\right]^{\mathrm{T}} \mathbf{\Sigma}^{-1} \left[\mathbb{y}_m(\theta, k) - \mu_{\mathbb{y}_m}\right], \tag{56}$$

where $\mathbb{D}_m^2(\theta)$ is the Mahalanobis squared distance in the reference condition, $\mathbf{\Sigma}$ is the covariance matrix and $\mu_{(.)}$ is the mean operator. Note that, in the reference condition, $\mathbb{D}_m^2(\theta)$ is a random variable, with a correspondent probability density function (PDF). Thus, its PDF can be empirically estimated considering the Kernel Density Estimation approach in order to establish a threshold value to the distribution (SILVERMAN, 1986; WORDEN; MANSON; ALLMAN, 2003)

$$\hat{p}_{\mathbb{D}_m^2}(d_m^2) = \frac{1}{Nh} \sum_{i=1}^{N} K\left(\frac{d_m^2 - d_{m,i}^2}{h}\right), \tag{57}$$

where $\hat{p}_{\mathbb{D}_m^2}(d_m)$ is an estimation of $p_{\mathbb{D}_m^2}(d_m^2)$ that is the true density of $\mathbb{D}_m^2(\theta)$, N is the total number of realizations of the random parameter, $d_{m,i}^2$ is the ith realization of the random variable $\mathbb{D}_m^2(\theta)$, K represents the kernel of the transformation, in this work the Gaussian kernel is used, and h is the smoothing parameter that controls the width of the Gaussian kernel chosen. The main difficulty in the use of the kernel density estimator is the choice of the optimal value to the smoothing parameter, so the cross-validation was used to set the better value of h, as suggested by Bowman and Azzalini (1997). The Kernel Density Estimation is used, because the distribution of $\mathbb{D}_m^2(\theta)$ is assumed as unknown a priori and the large number of realizations, generated using MC simulations, provides sufficient samples to estimate its density using this method.

Then, with the density estimated $\hat{p}_{\mathbb{D}_m^2}(d_m^2)$ it is possible to establish a threshold value for the distribution, which can be used in the damage detection procedure. The threshold value can be defined as (RÉBILLAT *et al.*, 2018)

$$\Lambda_m = \left\{d_m^2 \text{ such that } \int_{d_m^2}^{+\infty} p_{\mathbb{D}_m^2}(s)\, \mathrm{d}s = \beta\right\}, \tag{58}$$

where Λ_m represents the threshold value, β is the sensitivity of the approach or probability of false alarms considered and s the integration variable. The better value of β to be chosen it depends on the level of security/confidence that each operational application demands.

Now, a new model is identified in an unknown condition (healthy or damaged). The indices are computed considering the new model ($\boldsymbol{\lambda}_m$ or y_m) and compared with the stochastic model (set of reference models), through the Mahalanobis squared distance

$$\mathcal{D}_m^2 = \left[\lambda_m - \mu_{\mathbb{\lambda}_m}\right]^{\mathrm{T}} \boldsymbol{\Sigma}^{-1} \left[\lambda_m - \mu_{\mathbb{\lambda}_m}\right], \tag{59}$$

or

$$\mathcal{D}_m^2 = \left[y_m - \mu_{\mathbb{y}_m}\right]^{\mathrm{T}} \boldsymbol{\Sigma}^{-1} \left[y_m - \mu_{\mathbb{y}_m}\right], \tag{60}$$

where $\mathcal{D}_m^2$ is the Mahalanobis squared distance in the unknown condition. Finally, the hypothesis test can be applied to determine if the system is in healthy or damaged condition

$$\begin{cases} H_0 : \mathcal{D}_m^2 \leq \Lambda_m, \\ H_1 : \mathcal{D}_m^2 > \Lambda_m, \end{cases} \tag{61}$$

where the null hypothesis H_0 represents the healthy condition and H_1 the damaged. The methodology used to detect damage is summarized in the flowchart showed in Fig. 20, considering the two proposed approaches.

Figure 20 – Description of the damage detection approach based on stochastic Volterra series.

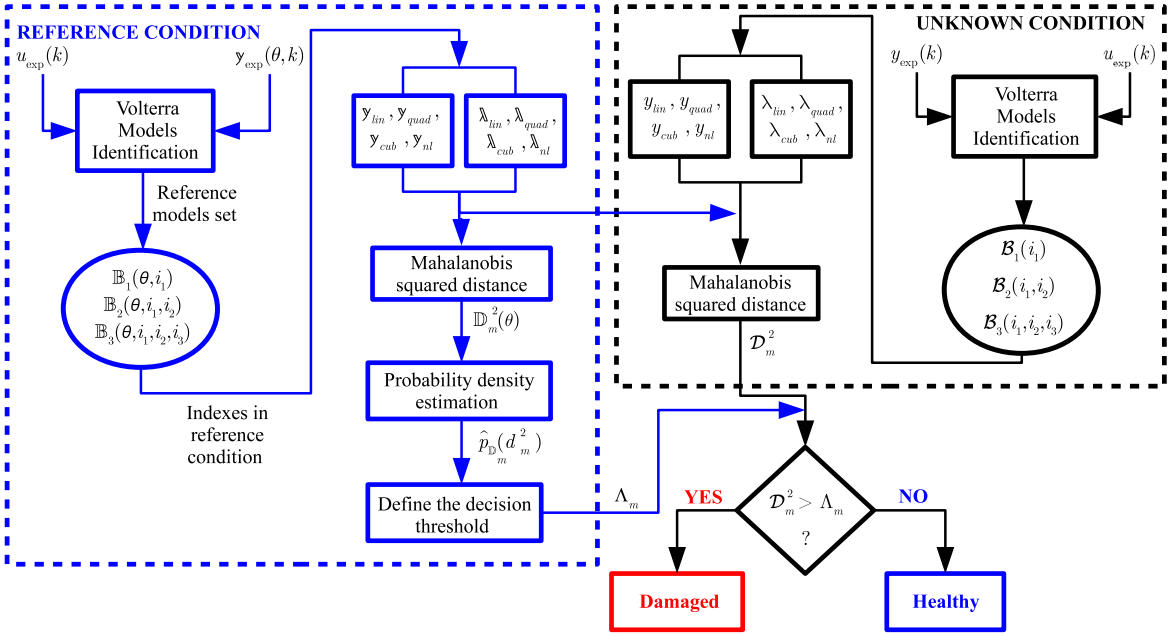

Source: Adapted from Villani, Silva and Cunha Junior (2019b).

4.3 STOCHASTIC VOLTERRA SERIES MODELING THE RANDOM DUFFING OSCILLATOR

This section describes the results obtained in the estimation of the stochastic reference model to be used in the damage detection process. In all simulations, a sampling frequency of 512 Hz was adopted with 2048 samples. The Monte Carlo simulations were performed considering 2048 realizations, to ensure the method convergence. To better emulate a real application, it was added to the system's output a Gaussian noise in order to have a signal to noise ratio (SNR) of 30 dB.

4.3.1 **Model identification**

The identification of the stochastic Volterra model was done considering 2048 realizations obtained through the simulations performed. Only the first three kernels were used to identify the system, once its nonlinear characteristic in the healthy and damaged condition can be approximated by the quadratic and cubic terms. First of all, the Kautz parameters were parametrized in terms of the natural frequency ω_n and the damping ratio ζ of the equivalent linear system. As the uncertainties have an influence on the modal parameters, they vary in each realization. Therefore, they were estimated using

each output realization and the optimization process described in section 3.5 was used to define the Kautz parameters, taking into account the relations described in (34). To exemplify the variation of the Kautz parameters with the progression of the damage, Tab. 2 shows the values of the factors p_1, p_2, p_3 and p_4 found for the higher-order kernels, considering different damage severities. Changes are observed in the position of the poles as the crack increases, mainly related to the second-order kernel, because of the quadratic effect of the crack. The number of functions were chosen as done in Shiki, Silva and Todd (2017), and defined as $J_1 = 2$, $J_2 = 4$ and $J_3 = 6$.

Table 2 – Relation factors between the Kautz and modal parameters, considering the high order Volterra kernels.

Crack severity	Second kernel		Third kernel	
(α)	p_1	p_2	p_3	p_4
1.00	1.11	2.7	1.06	1.1
0.98	1.07	2.4	1.06	1.1
0.96	1.07	2.3	1.06	1.1
0.94	1.06	2.2	1.06	1.1
0.92	1.06	2.1	1.06	1.1
0.90	1.05	2.0	1.06	1.0
0.86	1.04	1.8	1.05	1.0

Source: Villani, Silva and Cunha Junior (2019b).

With the Kautz poles defined, the random Kautz functions can be obtained and used in the models' identification process. The identification of the Volterra models was performed considering a chirp signal as the input applied to the system, varying the excitation frequency from 15 to 30 Hz (first mode region). The kernels identification was carried out in two steps, first, the linear kernel was estimated considering a low level of input (0.1 N), and then, the high order kernels were estimated considering a high level of input (1 N), as done in Shiki, Silva and Todd (2017). The models were estimated via MC simulation, in a total of 2048 realizations.

The convergence of the MC method is measured with the aid of a function that depends on the kernel vector or its main diagonal (high order kernels) represented in the time domain, defined by

$$conv(N_s) = \sqrt{\frac{1}{N_s}\sum_{n=1}^{N_s}\int_{t=t_0}^{t_f} \|\mathbb{h}(\theta_n, t)\|^2 dt}\,, \tag{62}$$

where N_s is the number of MC simulations, $\|.\|$ denotes the standard Euclidean norm

and $\mathbb{h}(\theta_n, t)$ represents the n-th realization of the random first kernel or main diagonal of higher-order kernels, in the time domain. The criterion was applied to the first, second and third kernels. Figure 21 shows the results obtained, considering the Volterra kernels identified in the reference condition. It can be seen that the MC convergence is achieved with the number of samples used.

Figure 21 – MC convergence test applied to the Volterra kernels identified.

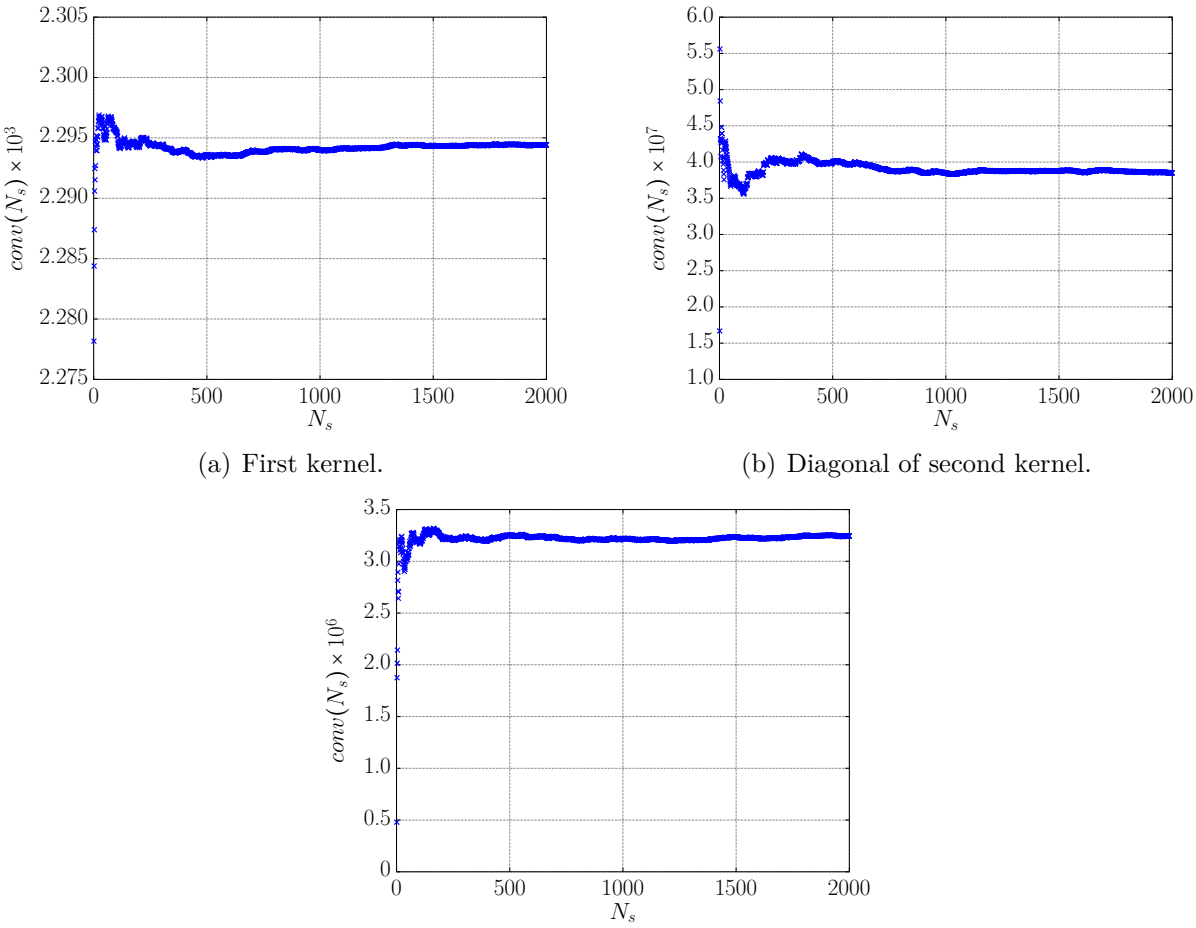

(a) First kernel.

(b) Diagonal of second kernel.

(c) Main diagonal of third kernel.

Source: Villani, Silva and Cunha Junior (2019b).

4.3.2 Model validation

Before the application of the Volterra series models in the damage detection process, it is important to verify if the Volterra kernels describe the dynamical behavior of the system with certain statistical confidence. Thus, the same input used to estimate the Volterra kernels was applied to the model. Figure 22 shows the comparison between the 99% confidence bands of the stochastic Volterra model's output and the new simulated

data, considering a high level of input (1 N). The model is able to describe the system behavior and to predict the response, even in the presence of nonlinear behavior and data variation.

Figure 22 – Stochastic Volterra model's output in comparison with new simulated data, considering a high level amplitude chirp input (1 N). The gray box represents the 99% confidence bands, – represents the mean and – ● – the simulated data.

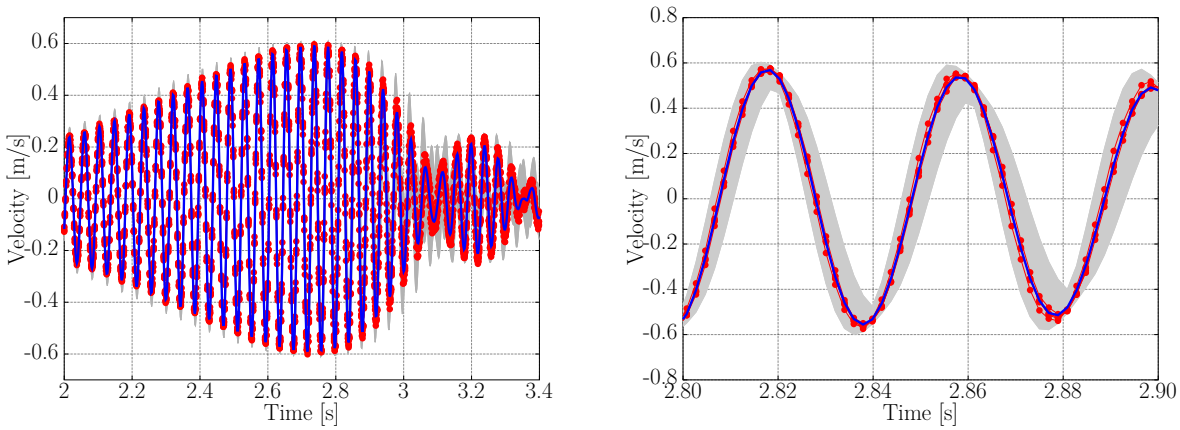

(a) Complete Signal. (b) Zoom.

Source: Adapted from Villani, Silva and Cunha Junior (2019b).

Then, a signal with a different nature was applied to the system to validate the stochastic Volterra model in the frequency domain. A single tone sine was applied with a high level of input (1 N) and frequency close to the equivalent linear system natural frequency (≈ 23 Hz), in order to amplify the nonlinear behavior. Figure 23 shows the results obtained in the frequency domain, to help the visualization of the harmonic components, with 99% of statistical confidence in comparison with new simulated data. It can be seen that the model predicts the system behavior in all frequency components. The large dispersion observed is caused by the number of Kautz functions used on the description of the third-order Volterra kernel, that amplifies the propagation of the uncertainties into the model, but a lower number of functions does not do the model able to describe the nonlinear behavior of the studied system.

The main advantage in the use of the approach based on Volterra series is the capability to separate linear and nonlinear contributions in the total response, through the Volterra kernels. The idea is to use this capability to filter and compare the nonlinear contributions to the total system response before and after the damage occurrence. In order to exemplify this information, Fig. 24 shows the contributions of the first, second and third kernels with 99% of statistical confidence, considering a high level of input signal

(1 N) and two structural conditions, healthy ($\alpha = 1.00$) and severe damage ($\alpha = 0.86$). All the contributions, linear, quadratic and cubic, change with the occurrence of the damage because the natural frequency and, consequently, the Kautz poles are influenced by the crack behavior. This result shows that the kernels' contributions and coefficients can be used in the process of damage detection. The variation of the quadratic contribution is bigger because of the quadratic effect caused by the nonlinear nature of the damage. Finally, in the situation of severe damage, the difference between the response in healthy and damaged condition can be visually observed, but at the beginning of the crack propagation, the differentiation is more difficult, mainly in the presence of uncertainties. Therefore, an index has to be used to detect structural variations. It is expected that the index related to the second kernel will be more sensitive to the presence of the crack.

Figure 23 – Stochastic Volterra model's output in comparison with new simulated data, in frequency domain, considering a single tone sine input. The gray box represents the 99% confidence bands, – represents the mean and – ● – the simulated data.

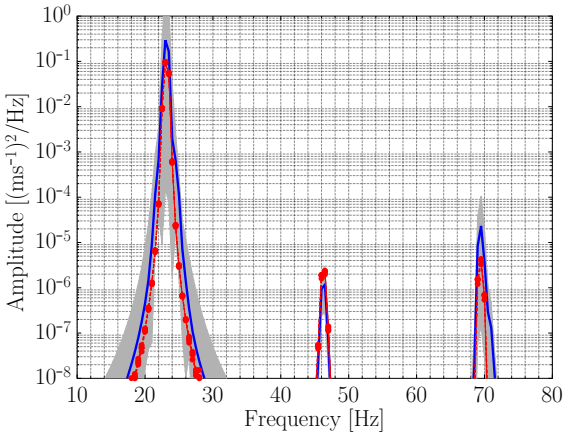

Source: Adapted from Villani, Silva and Cunha Junior (2019b).

Figure 24 – Confidence bands of the kernels' contributions to the total system's output obtained through the Volterra model with 99% of confidence, considering a high level of input (1 N). ■ represents the reference condition (α = 1.00) and ■ the damaged condition (α = 0.86).

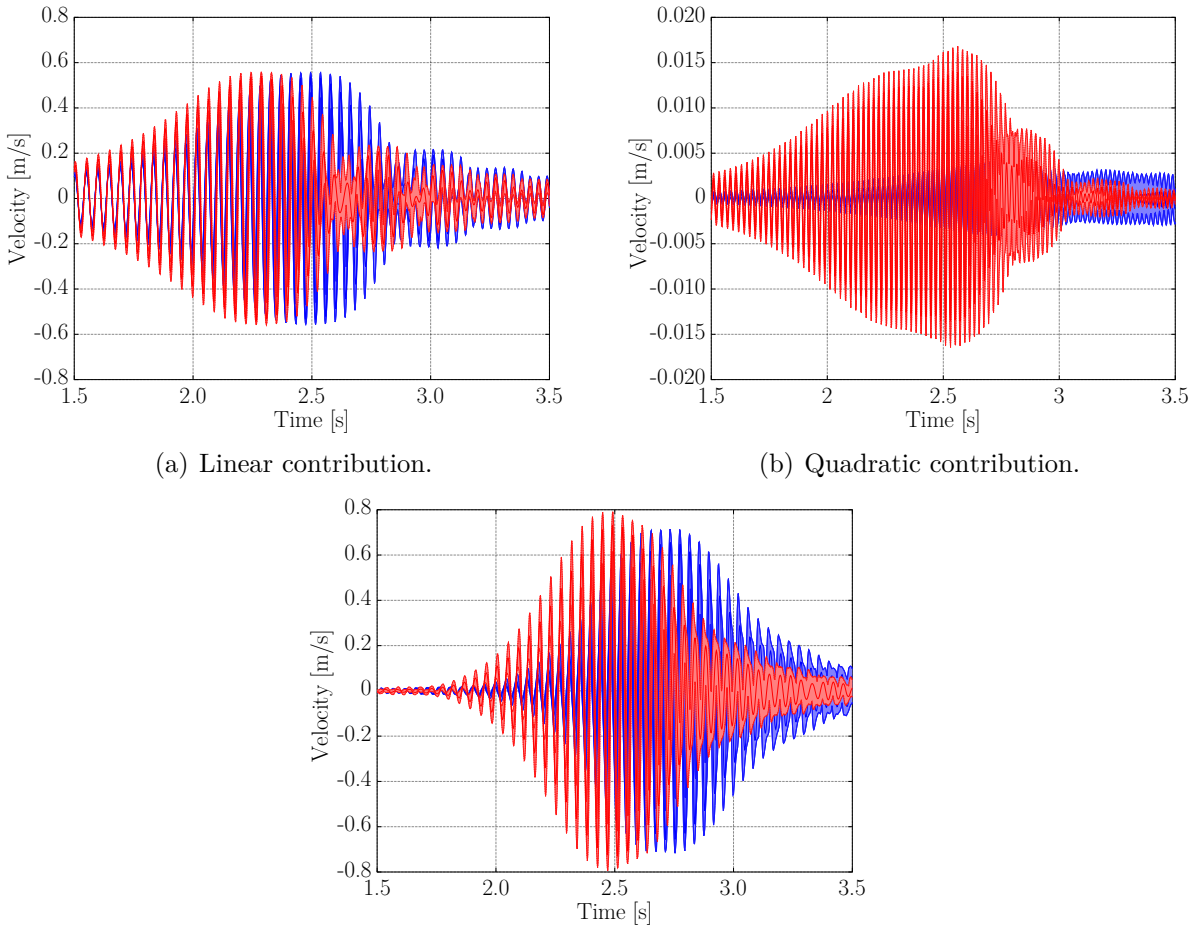

(a) Linear contribution.

(b) Quadratic contribution.

(c) Cubic contribution.

Source: Villani, Silva and Cunha Junior (2019b).

4.4 DAMAGE DETECTION

This section exemplifies the two different metrics proposed to detect damage in nonlinear systems, using the stochastic version of the Volterra series. The tests were performed considering α = 1.00, 1.00, 0.98, 0.96, 0.94, 0.92, 0.90, 0.88, 0.86 (2 reference and 7 damage conditions) and the simulated data variation, considering the uncertainties in the linear stiffness and damping coefficient. The first 2048 realizations in the reference condition were used as training data, to estimated the stochastic model described before, and the others as test data.

4.4.1 Use of kernels' coefficients

The approach proposed, based on Volterra kernels coefficients, described in section 4.2.1 was applied, combined with the novelty detection described in section 4.2.3. The stochastic reference model and the new models calculated several times in the different structural conditions were considered in the calculation of the indices. Figure 25 shows the evolution of the Mahalanobis squared distance applied to the indices, with the crack propagation. The boxplot method is used to clarify the visualization of the results. The first two boxes represent the reference condition, the data used to train the model and the data used to test the model. The linear index is not able to detect the crack evolution, considering only the kernels coefficients as an indicator. The cubic index has a small increase with the crack evolution, whereas the quadratic index has a larger increase. This occurs because of the quadratic nature of the crack behavior. How expected, the better performance is obtained through the use of the nonlinear index, considering both the coefficients of the second and third kernels. The increase of the distance with the progression the damage may be an interesting characteristic in future damage quantification applications.

With the Mahalanobis squared distance of the indices calculated in the reference condition, and considering their empirical distribution obtained, it is possible to define threshold values, taking into account a probability of false alarms β required in each application. In this work, three different values were considered, $\beta = 0.005$, 0.01 and 0.02. The results of the hypothesis test applied are shown in Fig. 26, for the three values of β used. The performance of the linear index is not satisfactory, with a low percentage of detection in the initial propagation of the crack. The cubic index can detect the crack depending on the severity of the damage, i.e., for α close to 1.00 the index fails, but for $\alpha \leq 0.86$, all damaged conditions are detected. Finally, the quadratic and nonlinear (concatenation of the quadratic and cubic coefficients) indices have similar behavior, detecting the damage even on the initial conditions of crack propagation. Remembering that it was considered the data variation, related to the presence of uncertainties, in the process of kernels identification, but, nevertheless, the nonlinear index was able to make difference between the variations related to changes in the natural frequency and damping ratio and the variations related to the crack behavior. This is an important result, showing that the approach can detect damage in uncertain nonlinear systems with probabilistic confidence.

Figure 25 – Boxplot of Mahalanobis squared distance of the kernels' coefficients calculated for different levels of crack severity.

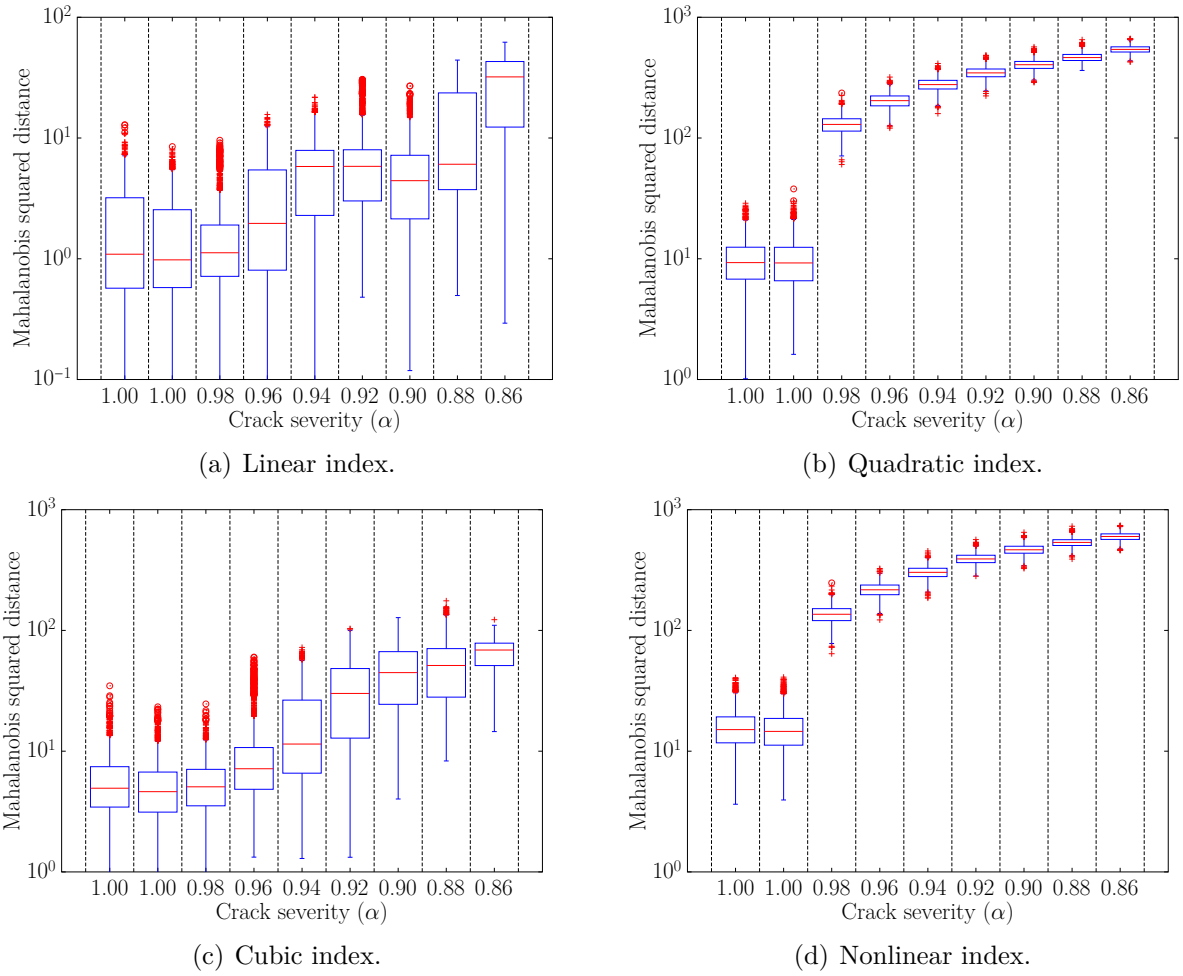

(a) Linear index.

(b) Quadratic index.

(c) Cubic index.

(d) Nonlinear index.

Source: Villani, Silva and Cunha Junior (2019b).

Aiming to study the performance of the approach proposed, the receiver operating characteristics (ROC) curve was computed (FARRAR; WORDEN, 2012). This curve presents the relation between true detections and false alarms for different β values. Figure 27 shows the results obtained when all the structural conditions are considered together. The linear index has the worst performance and the cubic index an intermediate performance. The quadratic and nonlinear indices have a similar performance, with a higher rate of detection without expressive false alarms rate. These results show that the nonlinear index proposed is able to detect the initial propagation of the crack even in the presence of uncertainties, simulated by variations in the natural frequency and damping ratio of the system. This high performance is possible because of the nonlinear nature of the damage simulated that has a large influence in the coefficients of the second kernel estimated. The use of the Volterra series in this situation improves the results in

the damage detection process, representing a real contribution when the data variation related to the uncertainties is considered.

Figure 26 – Percentage of damage detection obtained using the kernels' coefficients, considering different crack severities and probability of false alarms used. ■ represents $\beta = 0.02$, ■ represents $\beta = 0.01$ and ■ represents $\beta = 0.005$.

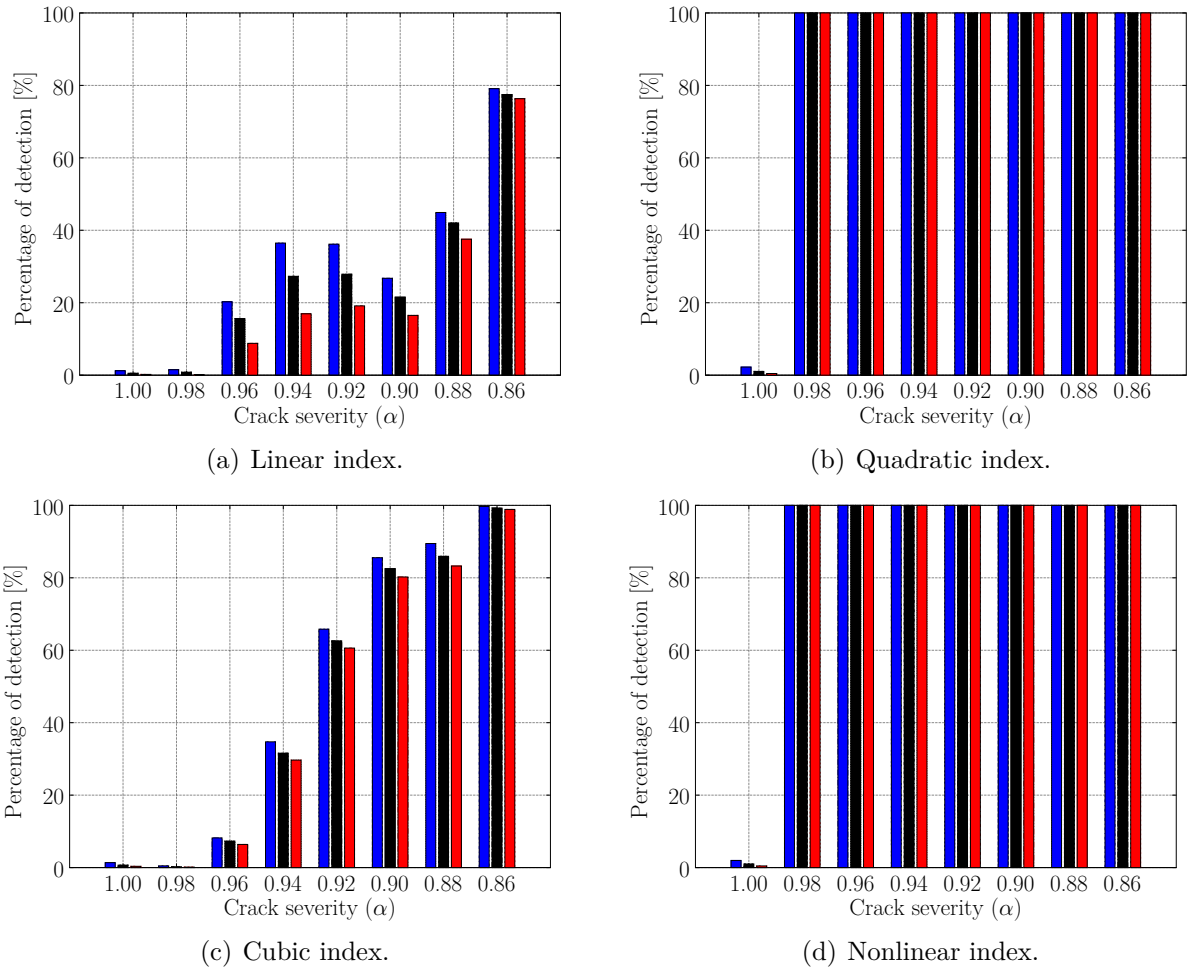

(a) Linear index.

(b) Quadratic index.

(c) Cubic index.

(d) Nonlinear index.

Source: Villani, Silva and Cunha Junior (2019b).

Figure 27 – Receiver operating characteristics (ROC) curve, obtained using the kernels' coefficients. -- ● -- represents the linear index, -- x -- the quadratic index, -- ■ -- the cubic index and -- ▲ -- the nonlinear index.

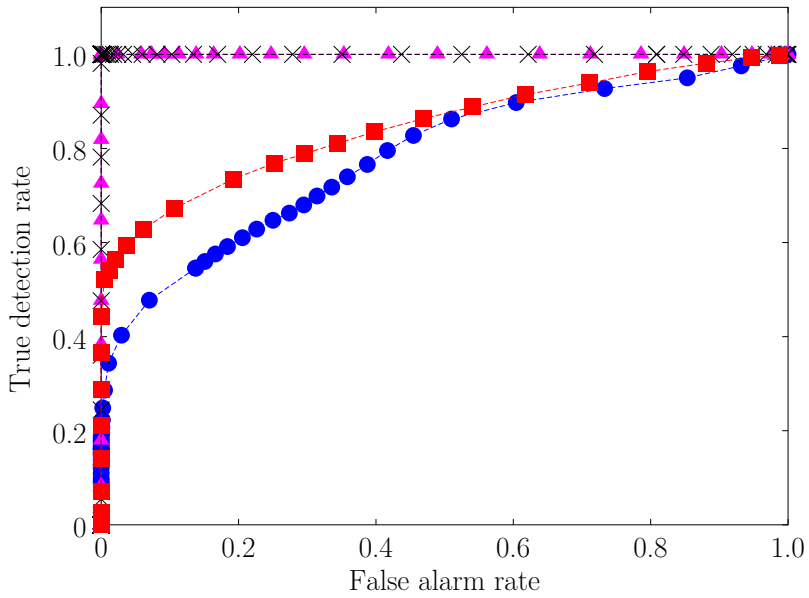

Source: Villani, Silva and Cunha Junior (2019b).

4.4.2 Use of kernels' contributions

The approach proposed based on Volterra kernels' contributions described in section 4.2.2 was applied, combined with the novelty detection described in section 4.2.3. This methodology uses the main advantage of the use of the Volterra series, that is the capability of separating the kernels' contributions to the total response. The difference compared with the approach presented in the last section is the influence of the Kautz functions in the process, that introduces the influence of the natural frequency and damping ratio in the approach, through the Kautz poles dependence. The increase of the crack makes the natural frequency of the system change, and this variation can be detected using this approach, on the other hand, it is expected that the uncertainties have more influence using this approach.

Again, new models are estimated in each structural condition to be compared with the stochastic reference model. The input used here is the same chirp signal used in the estimation of the kernels, considering a high level of amplitude (1 N), to maximizes the nonlinear influence in the response. Figure 28 shows the evolution of the Mahalanobis squared distance applied to the kernels' contributions, with the crack progression. It is clear that using this approach the linear and cubic indices have better performance to detect the presence of the crack compared with the use of kernels' coefficients. The

increase of the indices is related to the variation of the natural frequency with the progression of the damage. Again, the better results are obtained through the use of the quadratic or nonlinear indexes, because of the nature of the damage simulated.

Figure 28 – Boxplot of Mahalanobis squared distance of the kernels' contribution calculated for different levels of crack severity.

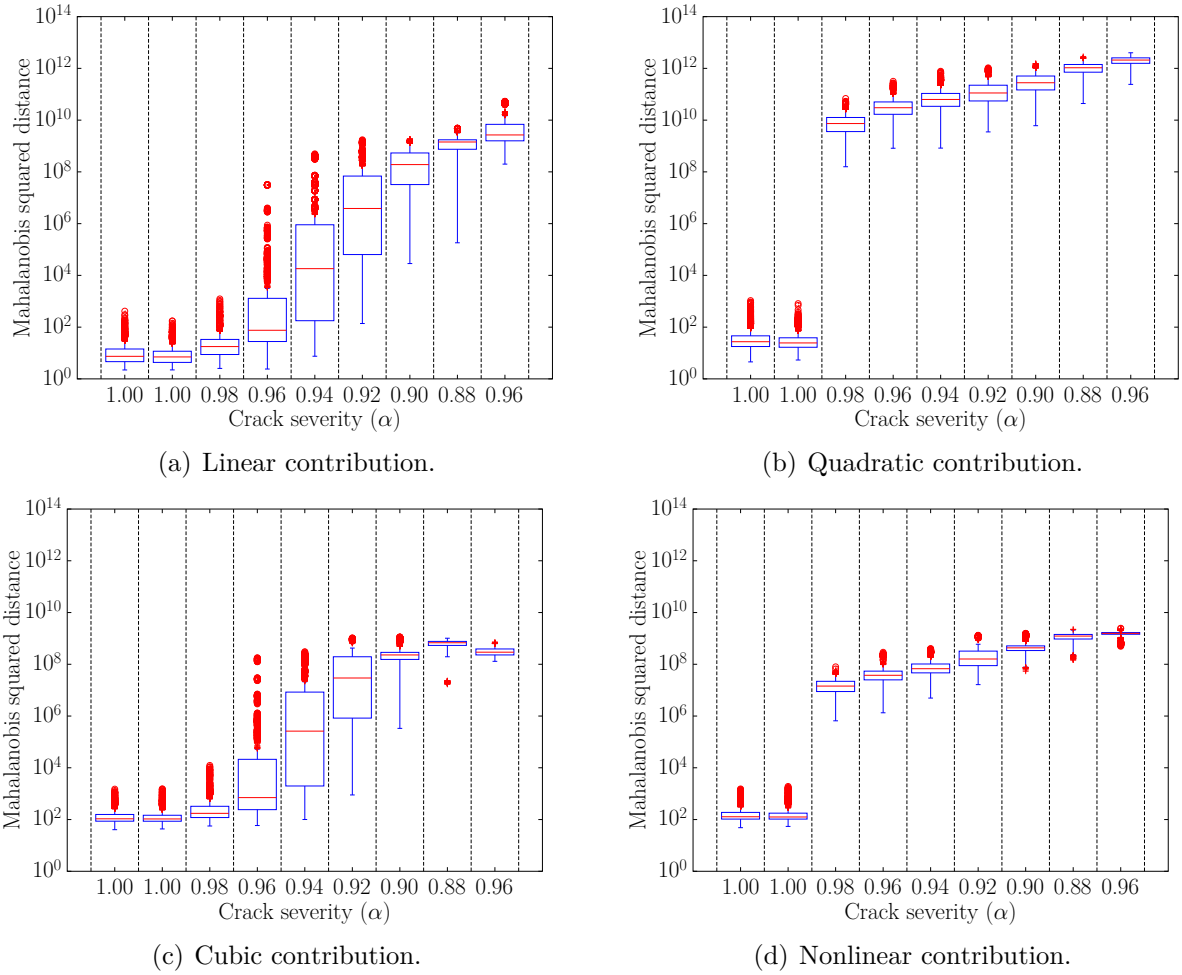

(a) Linear contribution.

(b) Quadratic contribution.

(c) Cubic contribution.

(d) Nonlinear contribution.

Source: Villani, Silva and Cunha Junior (2019b).

With the Mahalanobis squared distance of the kernels contribution calculated in the reference condition, and considering their empirical distribution obtained, it is possible to define threshold values, taking into account the probability of false alarms β required in each application. Again, three different values were considered, β = 0.005, 0.01 and 0.02. The results of the hypothesis test applied are shown in Fig. 29, for the three values of β used. The performance of the linear and cubic indices was improved with the use of kernels contribution, with a higher percentage of detection of the crack for $\alpha \leq 0.92$. The quadratic and nonlinear (sum of quadratic and cubic contributions) indices were able to detect the damage even on the initial conditions of crack propagation. The variation of

the frequency and damping is considered in the Kautz poles estimation, improving the capability of the approach to detect the frequency variation related to the crack behavior, but confusing this variation with the changes that are a consequence of the presence of uncertainties.

Figure 29 – Percentage of damage detection obtained using the kernels' contribution, considering different crack severities and probability of false alarms used. ■ represents $\beta = 0.02$, ■ represents $\beta = 0.01$ and ■ represents $\beta = 0.005$.

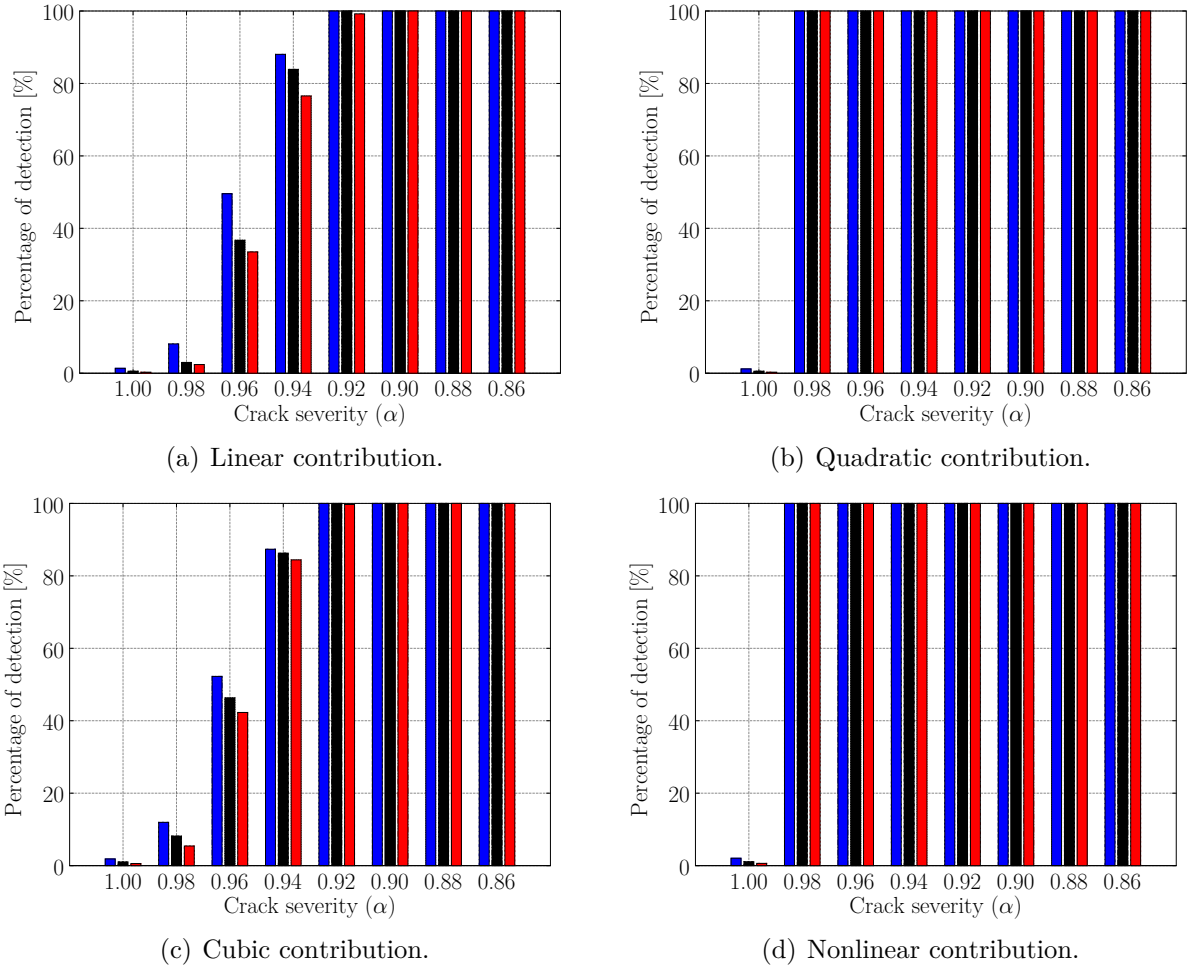

(a) Linear contribution.

(b) Quadratic contribution.

(c) Cubic contribution.

(d) Nonlinear contribution.

Source: Villani, Silva and Cunha Junior (2019b).

Finally, the ROC curve was computed again considering all structural conditions and Fig. 30 shows the results obtained. The linear and cubic contributions have the worst performance again because these components of the response have a slight variation for values of crack close to 1.00. The quadratic and nonlinear indices have similar performance, with a higher rate of detection without expressive false alarms rate. These results show that the analysis of the nonlinear contribution to the total response is able to detect the initial propagation of the crack even in the presence of the uncertainties. This

higher performance is possible because of the nonlinear nature of the damage simulated, that has a large influence on the nonlinear dynamics of the system. Again, the use of the Volterra series in this situation represents an advantage in the damage detection process, with the improvement in the results in comparison with the linear approach represented by the first kernel contribution.

Figure 30 – Receiver operating characteristics (ROC) curve, obtained using the kernels' contributions. -- ● -- represents the linear index, -- x -- the quadratic index, -- ■ -- the cubic index and -- ▲ -- the nonlinear index.

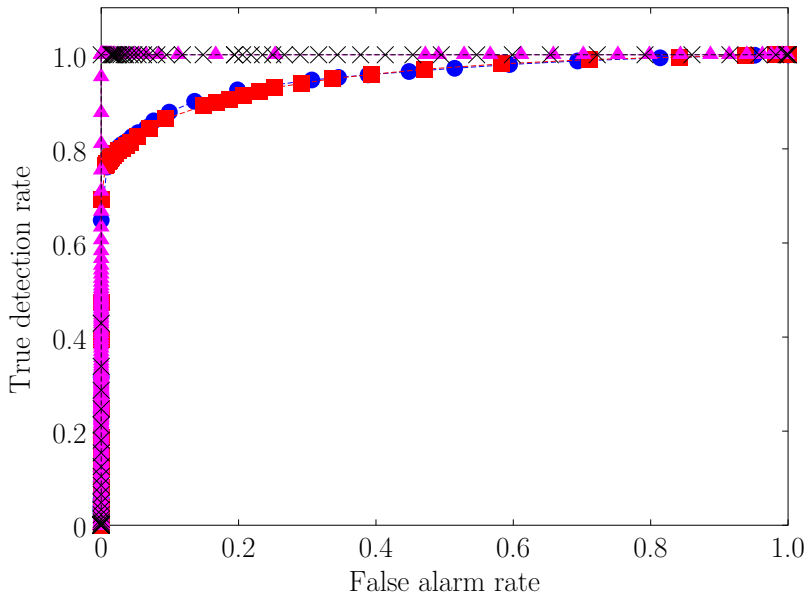

Source: Villani, Silva and Cunha Junior (2019b).

4.4.3 Comparison between the use of kernels' coefficients and kernels' contributions

This study has shown the useful characteristic of the Volterra kernels identified in the process of damage detection. Two methods to use the information provided by the kernels estimated were proposed becoming interesting to compare the main properties of each one. Thus, some comments may be pointed out:

- **Sensitivity to the uncertainties:** The use of the kernels' coefficients shown to be more sensitivity to the effect caused by the noise, mainly when the level of the noise's energy is at the same order of the energy of the nonlinear behavior caused by the presence of the damage. Alternatively, the kernels' contributions shown to be more sensitivity to the variations caused by the uncertainties simulated in the

modal parameters. This is a consequence of the influence of the Kautz poles in the process of contributions construction;

- **Sensitivity to the presence of damage:** The kernels' contributions are sensitive to different kinds of damage, that has influence in linear or nonlinear components of the response. This is a characteristic related to the capability of the Kautz functions to sense the variations in the modal parameters caused by the damage. This characteristic will be better explored in the next chapter. On the other hand, the kernels' coefficients are able to detect only damages that have an influence on the level of energy of the linear and nonlinear components of the response;

- **Number of features:** When we use the kernels' coefficients as damage detection feature the order of the classification problem, i.e., the number of features considered is far lesser than when we consider the kernels' contributions. In this point, it is always better to use the kernels' coefficients when possible. An alternative to overcome this problem with the use of kernels' contributions will be proposed further on;

- **Use of both together:** Whenever possible, it is suggested to use both approaches together to improve the confidence of the method. Further on, a different approach using both approaches together with the construction of a unique index will be presented.

4.5 CONCLUSIONS

This chapter has presented an approach to detect damages in initially nonlinear systems, considering data variation caused by the uncertainties. The approach is based on a stochastic version of the Volterra series expanded using random Kautz functions. Two different approaches were presented, considering the Volterra kernels' coefficients and the Volterra kernels' contributions. The final decision about the state of the system (healthy or damaged) was performed considering the Mahalanobis squared distance and a threshold value, established from the model estimated in the reference condition. Linear and nonlinear analysis were compared, using the capability of the Volterra series to separate the model's contributions. About the results, the two approaches proposed have presented similar performance. As expected, the linear analysis fails when the damage has a low severity, because of the influence of the uncertainties in the system's output. The nonlinear analysis uses the nonlinear dynamics of the damage to detect it. It is important

to highlight that the nonlinear behavior was considered even in the reference condition, which combined with the presence of uncertainties, makes difficult the damage detection process. Finally, the nonlinear indices have shown to be able to differ the initial nonlinear behavior and the data uncertainties from the breathing crack behavior. An experimental application may improve the confidence of the results and will be carefully discussed in the next two chapters.

5 EXPERIMENTAL DAMAGE DETECTION BASED ON STOCHASTIC VOLTERRA SERIES: A LINEAR DAMAGE

This chapter employs the experimental application of the approach based on the stochastic Volterra kernels' contributions considering the same setup used by Shiki, Silva and Todd (2017). The aim is to compare the results obtained through the deterministic and stochastic model and to show the benefit of the use of a stochastic model when the data variation is considered. The use of kernels' coefficients is not examined here because of the linear characteristic of the emulated damage that does not impact the amplitude of the higher-order harmonics, as occurred in Villani, Silva and Cunha Junior (2019b). All the results and theory presented in this chapter can be found by the reader in Villani *et al.* (2019a).

The rest of the chapter is organized as follows: section 5.1 shows the problem faced and the hypothesis considered in the application of the proposed method; section 5.2 presents the experimental setup used in the investigations; section 5.3 shows a review of the mathematical model and the results attained with the use of the deterministic approach proposed by Shiki, Silva and Todd (2017); section 5.4 shows a review of the mathematical model and the results achieved through the application of the stochastic procedure proposed by Villani, Silva and Cunha Junior (2019b); section 5.5 brings the comparison between the methodologies used; and finally, section 5.6 presents the discussion about the results and the main conclusion.

5.1 PROBLEM STATEMENT AND HYPOTHESIS CONSIDERED

Two different methodologies to detect damage in initially nonlinear systems, admitting the presence of data variation associated with uncertainties, are compared in this chapter. The first one based on the deterministic Volterra series, expanded using standard Kautz functions, and the second one based on the stochastic version of the Volterra series, expanded applying random Kautz functions. Some attention has to be made to understand correctly this experimental application:

- Problem explored:

  - The system exhibits nonlinear behavior both in the healthy and damaged conditions;
  - The system response displays random variation generated by the influence of the uncertainties;
  - The model has to sense the difference between uncertainties, nonlinear behavior, and damage.

- Experimental random data considered:
  - The data variation was not controlled during the experiments. Therefore, it is deemed a random variation;
  - The system response variation is considered through the restarting of the experimental setup during the different days of tests, to emulate the presence of uncertainties in the measurements. Consequently, the uncertainties are associated to sensors' and actuator's positions, bolts tightening in the clamp, natural temperature fluctuation (this parameter was not controlled), and others related to the assembly and disassembly of the experimental setup;
  - The measurements were conducted in different days in distinct structural conditions during two weeks;
  - Additional noise is used in the response realizations to generate enough data to be utilized in the Monte Carlo simulations;
  - The same response samples are analyzed in both methodologies with the goal of comparison.

- Input signal used:
  - A chirp input is held to identify the model in all conditions because of its nature to excite the structure in a range of frequencies with energy suitable to generate the nonlinear interactions in the response (SHIKI; SILVA; TODD, 2017; RÉBILLAT *et al.*, 2011; RÉBILLAT; HAJRYA; MECHBAL, 2014);
  - The same input is adopted in the identification/training of the models and in the test phase, to assure a reliable identification of the high-order components. The change of the excitation signal nature from the training to the test phase may lead to inferior performance;

- The damage studied has a linear characteristic (loss of mass). Hence only the method based on the Volterra kernels' contributions is analyzed.

5.2 EXPERIMENTAL SETUP

To contrast the results obtained using different methodologies, the same experimental setup used by Shiki, Silva and Todd (2017), Villani, Silva and Cunha Junior (2017a), and presented in the section 2.2 is taken into account. As demonstrated before, the experimental arrangement presents nonlinear behavior with hardening characteristic due to large displacements. As previously mentioned, a bolted connection is put in the center of the beam, with four nuts with 0.001 [kg] each one, to emulate the presence of damage, then the healthy state regards the four masses and the damage increases with the loss of the nuts (fig. 31). Table 3 shows the different structural conditions adopted in this work.

Figure 31 – Illustration of the damage emulated.

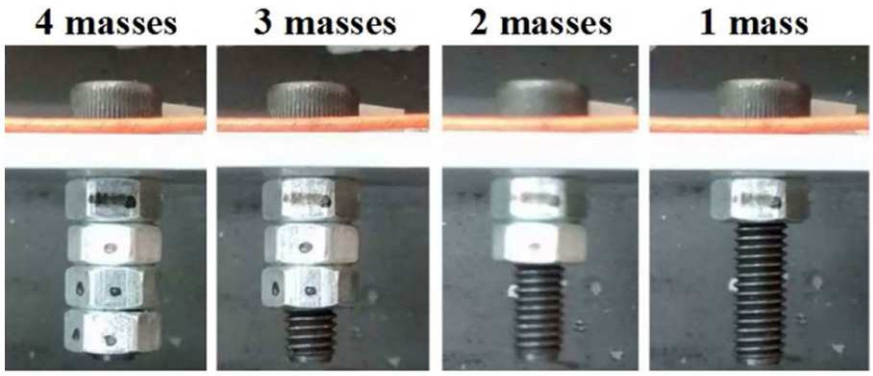

(a) Emulated damage (SHIKI; SILVA; TODD, 2017).

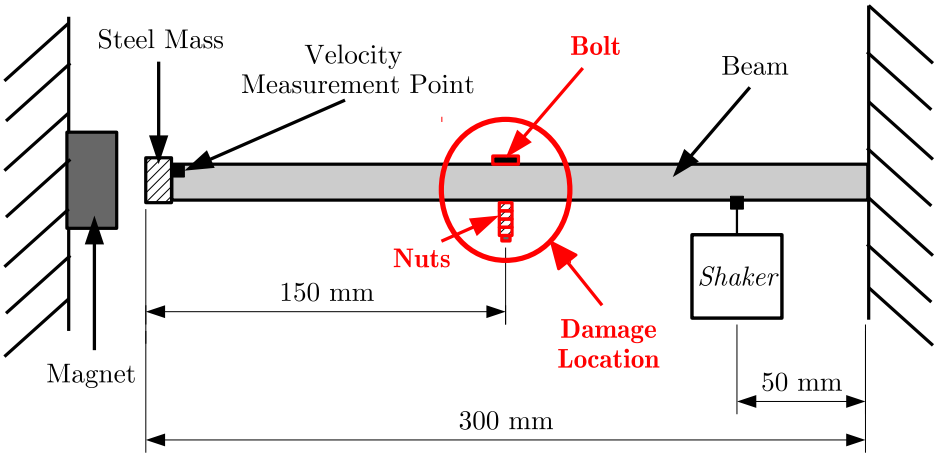

(b) Schematic representation of the damage localization.

Source: Adapted from Shiki, Silva and Todd (2017).

Furthermore, the natural variation of the data measured was considered through the repetition of the tests during two weeks in a total of 160 experimental realizations. It was assumed an aleatory variability of the experimental data by restarting the experimental

setup and data acquisition in different days, so the variability examined is related to sensors' and actuator's positions, bolts tightening in the clamp, natural temperature fluctuation, and others related to the assembly and disassembly of the experimental setup. Then, a Gaussian noise was randomly added to the data, generating a signal to noise ratio (SNR) of 25 dB and a database with 2048 synthetic realizations of the experiments to be used in the stochastic model estimation through the MC simulations (SOIZE, 2017; RUBINSTEIN; KROESE, 2016). It is expected that a deterministic model will not be able to describe the data fluctuation, confirming the use of a stochastic model to monitor structural health. This is a real issue that many SHM features have to overcome in practical applications.

Table 3 – Structure conditions.

State	H	I	II	III	R
Condition	4 masses (ref.)	3 masses	2 masses	1 mass	4 masses (repair)

Source: Villani *et al.* (2019a).

Figure 32 exemplifies the restriction in detect structural variations (damages) considering the data variation. In this figure, it can be seen the FRFs curves, considering 99% of statistical confidence bands and different structural states. The clear differentiation between the different conditions is not possible, particularly in the beginning of damage propagation (3 nuts). Therefore, using classical procedures based on deterministic models and methods without any probabilistic analysis of the models or damage indices, based on single measures, is not reasonable to execute a correct classification of the structural state with probabilistic confidence. Consequently, the method based on the stochastic Volterra series proposed by Villani, Silva and Cunha Junior (2019b) can be applied to detect the presence of the damage in these circumstances.

Figure 32 – Frequency Response Function calculated for different structural conditions with 99% of confidence bands. ■ represents reference condition (4 masses), ■ the condition I (3 masses) and ■ the condition II (2 masses).

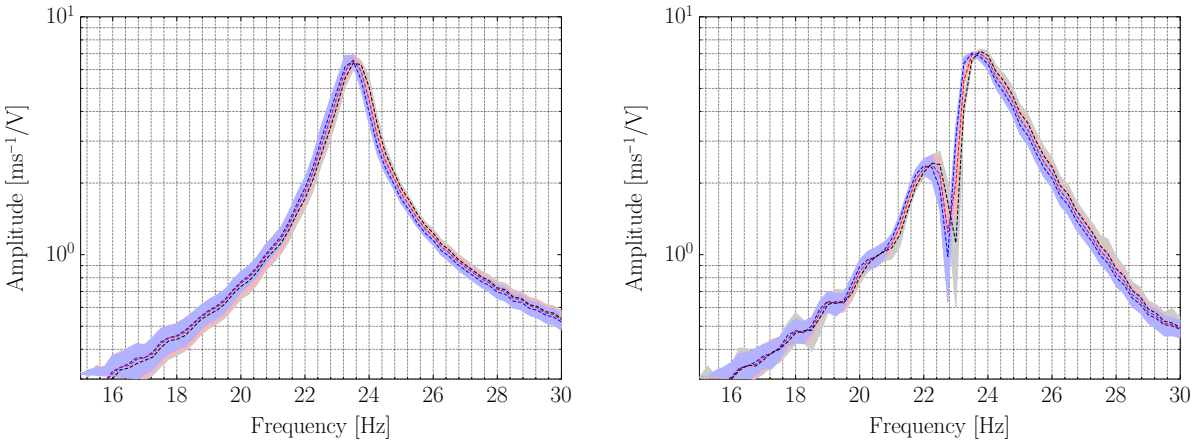

(a) Low level of input (0.01 V). (b) High level of input (0.15 V).

Source: Villani *et al.* (2019a).

5.3 DETERMINISTIC VOLTERRA SERIES FOR DAMAGE DETECTION

This section exposes the application of the damage detection procedure, based on the deterministic Volterra series, proposed by Shiki, Silva and Todd (2017), regarding the variation on the measured data caused by the appearance of uncertainties. The concepts of deterministic Volterra series can be found in section 3.1, so this section will be concentrated in the description of the damage detection approach and its application using the experimental data. The goal is to prove that the use of a methodology based on a deterministic model, without the use of probabilistic tools and metrics, is not indicated in SHM problems admitting the presence of uncertainties.

5.3.1 **Deterministic damage index**

With the deterministic Volterra model evaluated considering the healthy condition, the system response can be predicted using the approximation (20). Then, considering the response predicted by the reference model and the new experimental data measured with the structure in an unknown state, an index can be proposed (SHIKI; SILVA; TODD, 2017)

$$\gamma_\eta = \frac{\sigma_{e_{\eta,unk}}}{\sigma_{e_{\eta,ref}}}\,, \tag{63}$$

where γ_η is the damage index, $\sigma_{(.)}$ represents the standard deviation and the prediction errors can be defined as

$$e_{\eta,ref} = y_{exp}^{ref} - \sum_{n=1}^{\eta} y_n \,, \tag{64}$$

$$e_{\eta,unk} = y_{exp}^{unk} - \sum_{n=1}^{\eta} y_n \,, \tag{65}$$

where y_{exp}^{ref} is the measured response with the structure in the reference condition, y_{exp}^{unk} is the measured response with the system in an unknown state and y_n is the model response contribution of the $n-$order Volterra kernel. Only the first three Volterra kernels were considered, because of the cubic polynomial characteristic of the nonlinear structure behavior. The statistical analysis of the index has been widely discussed in Shiki, Silva and Todd (2017), so the reader is encouraged to have an attention to that manuscript for more information.

5.3.2 **Deterministic model identification**

The first step to detect damage, considering the proposed method, is to identify a reference model to be applied to the system output prediction. The deterministic Volterra model was identified considering a single sample of response, as the proposed model is deterministic. A chirp signal varying the excitation frequency from 10 to 50 Hz was used to excite the structure in the model identification process. As discussed in Shiki, Silva and Todd (2017), two levels of input amplitude were used to estimate the Volterra kernels in two steps. A low-level input (0.01 V) was used to estimate the first kernel, and then, a high-level input (0.15 V) was employed to evaluate the higher-order kernels (second and third). The number of Kautz functions were determined as performed in Shiki, Silva and Todd (2017), and defined as $J_1 = 2$, $J_2 = 2$ and $J_3 = 6$. Figure 33 presents the comparison among the system's output obtained experimentally and using the Volterra model identified, considering the two levels of input amplitude and the same chirp signal used in the model identification process. The signals are very similar, revealing that the model can predict the system response in these conditions.

Then, it is expected to use a different input signal to test the efficiency of the model. Therefore, a single tone sine wave, with a frequency of 23 Hz that is around the resonance frequency of the system, is applied to the structure to test the model performance. Figure 34(a) shows the comparison between the model's and the experimental's responses obtained in the frequency domain. It can be seen that the model can represent all

frequency components. Additionally, Fig. 34(b) shows the Volterra kernels' contributions. It is remarked that the cubic kernel has a contribution in the first and third harmonics of the response. This characteristic allows the cubic kernel to be susceptible to damages with a linear characteristic.

Figure 33 – Comparison between the system's output obtained experimentally and using the deterministic Volterra model. – represents the output obtained through the Volterra model identified and the –– represents the experimental data.

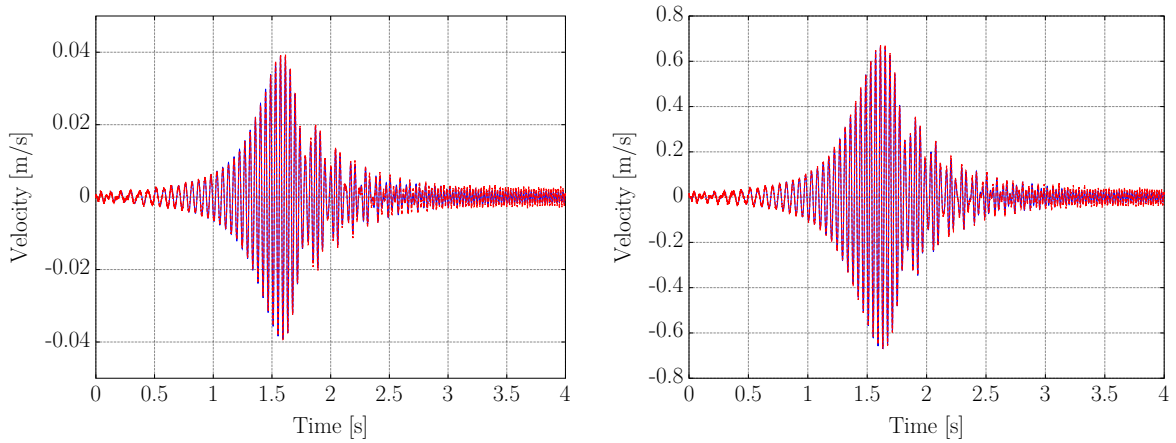

(a) Low level of input signal (0.01 V).

(b) High level of input signal (0.15 V).

Source: Villani *et al.* (2019a).

Figure 34 – Response obtained considering a sine input with a high amplitude.

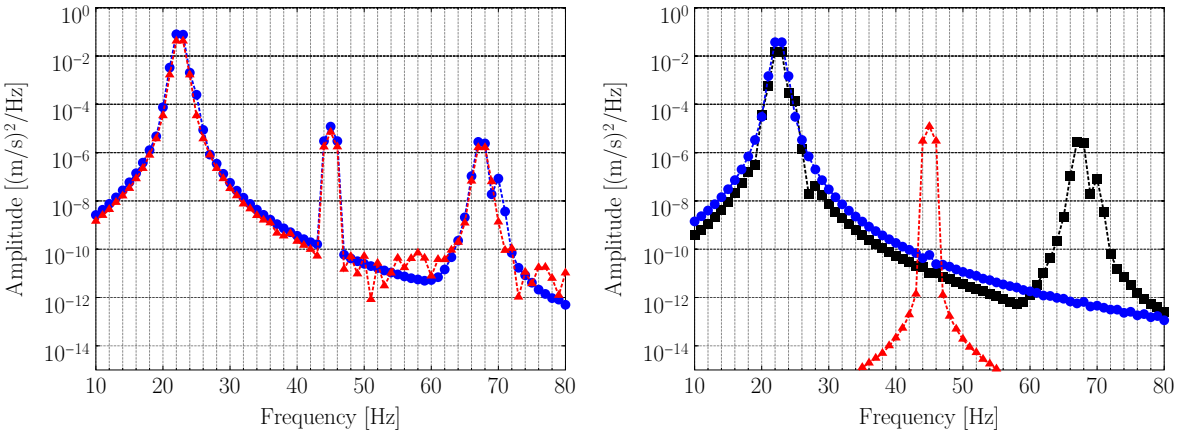

(a) Comparison between the Volterra model and experimental data. – ● – represents the output obtained through the Volterra model identified and – ▲ – represents the experimental signal.

(b) Volterra kernels contributions. – ● – represents the first kernel contribution, – ▲ – the second kernel contribution and – ■ – the thrid kernel contribution.

Source: Villani *et al.* (2019a).

5.3.3 Deterministic damage detection

Now the reference model identified is used in the damage detection procedure. Two damage indices were calculated, the linear γ_1 considering the first kernel and the nonlinear γ_3 considering the first three kernels. The procedure was applied using a high level of input amplitude, i.e., with the structure operating in a nonlinear regime of motion before the damage occurrence. First of all, Fig. 35 displays the evolution of the indices with the increase of the damage. The nonlinear index presented a higher sensitivity to the presence of damage. For both indices, it is complicate to make difference between the initial propagation of damage (Condition I) and the reference/repair states as a superposition between the upper quartile of the indices computed in the reference state and the lower quartile (even the mean value) of the indices calculated in the damage I condition can be observed.

Figure 35 – Damage index considering the deterministic model.

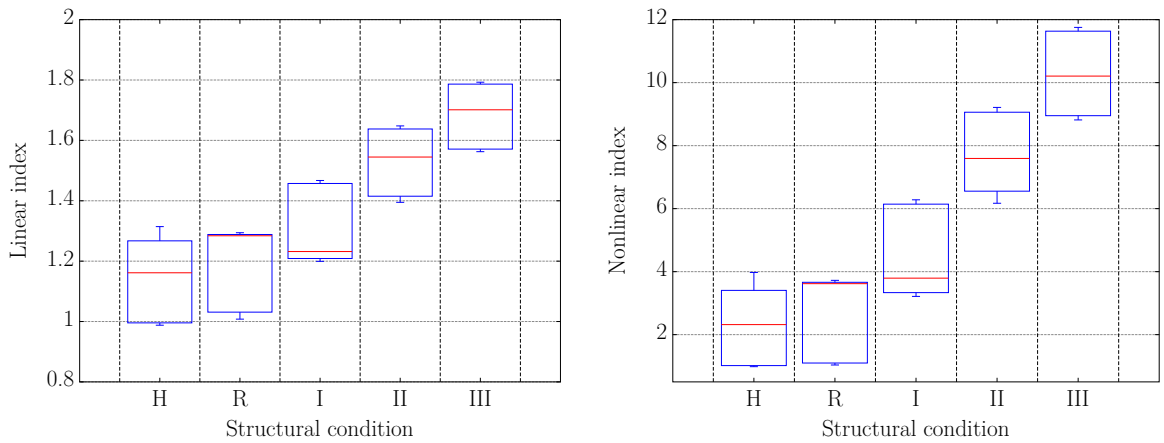

(a) Linear index. (b) Nonlinear index.

Source: Villani *et al.* (2019a).

Finally, to analyze the performance of the indices to detect damage, the ROC curve was computed, considering the two different indices computed and all structural conditions. Figure 36 shows the results achieved. The nonlinear index has a higher performance than the linear one but is evident that both indices fail to detect the damage in the initial propagation. The indices are not able to distinguish the actual data variation, related to the uncertainties, from the presence of the damage. The results shown here are unsatisfactory when we contrast with that one shown in Shiki, Silva and Todd (2017) because the samples used in the present study include more substantial data variation, not only associated with the presence of noise in the measurements but also other variations

mentioned before. Therefore, it is suggested to apply random Volterra series joined with the novelty detection concept. Next section shows the proposed approach and the main results obtained.

Figure 36 – ROC curve considering the deterministic model.

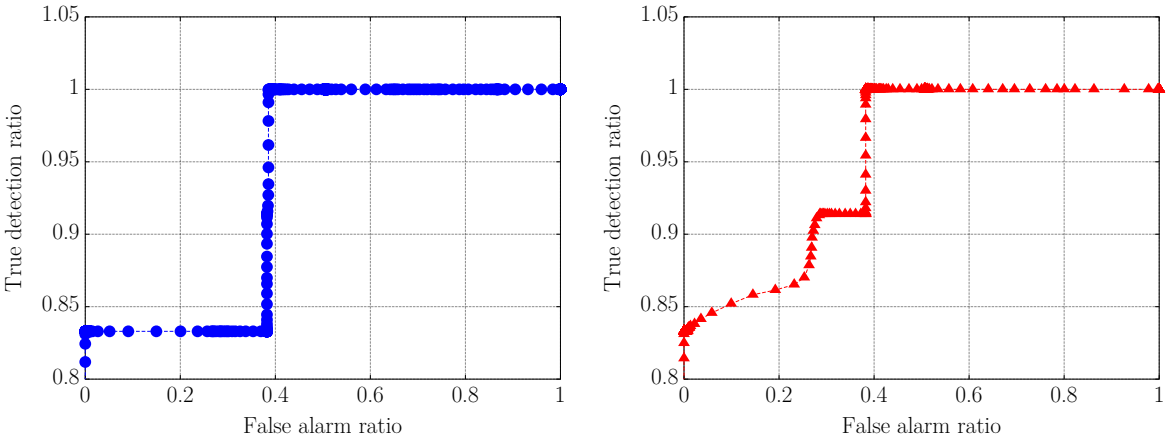

(a) Linear index. (b) Nonlinear index.

Source: Villani *et al.* (2019a).

5.4 STOCHASTIC VOLTERRA SERIES FOR DAMAGE DETECTION

The real implementation of SHM approaches, considering the uncertainties, denotes a challenging task, because of the confounding effects which can involve the indices (MAO; TODD, 2013). Some effects like measurement noise, changes in boundary conditions, humidity, temperature, and others, can mask the damages' effects or generate a higher number of false positives (WORDEN; CROSS, 2018). As a consequence, the measured response, that can vary greatly, have to be considered as a random process to ensure that the prediction model can describe the system's behavior with reliability.

Therefore, this section presents the expansion of the deterministic Volterra series theory to a stochastic model and the application on the SHM problem described before, warranting the damage detection even in the presence of data variation and nonlinear behavior. The reference stochastic model considered is the same described in chapter 3 and will not be reviewed. This experimental application holds some differences in the approach used to detect the damage from the one described before, that will be pointed out hereinafter.

5.4.1 Damage detection based on standardized Euclidean distance

On the last chapter, two different approaches were applied, using the stochastic Volterra series to detect the presence of a breathing crack in a nonlinear beam, the first one using the random Volterra kernels' coefficients and the second one applying the random Volterra kernels' contributions. As the simulated damage induced the increase of the second harmonic on the system response, i.e., produced the nonlinear system to present a nonlinear behavior with different nature, the presence of the damage had more influence on the second-order Volterra kernels' coefficients. However, the use of one or other approach depends on the characteristic of the damage that the structure can be exposed, being the better choice the use of both simultaneously. Additionally, the emulated damage admitted in this chapter does not have an influence on the amplitude of the harmonic components, only the frequency, causing the kernels coefficients to be unfeeling to the presence of the damage. Therefore, the first approach is not adopted here because of this characteristic of the emulated damage.

Thereby, the Volterra kernels' contributions in the total system response can be used as a damage sensitive index. As cited before, the use of the Volterra series method is supported by its success of separate the nonlinear model response in linear and nonlinear components, considering the kernels identified. Viewing this and the individualists of this experimental application, only two indices will be considered: $\mathbb{y}_{lin}$ and $\mathbb{y}_{nl}$ Eq. (50). Moreover, in order to obtain better results a new distance measure is proposed

$$\mathbb{D}_m(\theta) = \sum_{n=1}^{N_s} \sqrt{\left[\mathbb{y}_m(\theta,k) - \mathbb{y}_m(n,k)\right] V^{-1} \left[\mathbb{y}_m(\theta,k) - \mathbb{y}_m(n,k)\right]^{\mathrm{T}}}\,, \tag{66}$$

where $\mathbb{D}_m(\theta)$ is the standardized Euclidian distance calculated in the reference condition, V is a diagonal matrix in which the diagonal elements are the standard deviations of the columns of $\mathbb{y}_m(\theta,k)$. The difference between the use of the standardized Euclidean distance and the Mahalanobis squared distance is related to the consideration of only the terms of the main diagonal of the covariance matrix estimated. The estimation of the threshold value Λ_m is performed based on the same methodology described before, based on the density estimation of the empirical distance calculated in the reference condition. The reader can find useful information about the process in section 4.2. The same distance can be calculated in an unknown condition

$$\mathcal{D}_m = \sum_{n=1}^{N_s} \sqrt{[y_m(k) - \mathbb{y}_m(n,k)]\, V^{-1}\, [y_m(k) - \mathbb{y}_m(n,k)]^{\mathrm{T}}}\,, \tag{67}$$

where $\mathcal{D}_m$ is the standardized Euclidean distance in an unknown condition. Finally, the hypothesis test can be applied to determine if the system is in healthy or damaged condition

$$\begin{cases} H_0 : \mathcal{D}_m \leq \Lambda_m\,, \\ H_1 : \mathcal{D}_m > \Lambda_m\,, \end{cases} \tag{68}$$

where the null hypothesis H_0 represents the healthy condition and the alternative hypothesis H_1 the damaged. The procedure proposed to detect damages can be summarized in 6 main steps, organized into two phases (training and test) summarized as follows.

TRAINING PHASE:

– Step 1: The stochastic Volterra model is identified in the reference condition to construct a set of reference models;

– Step 2: The standardized Euclidean distance $\mathbb{D}_m$ is calculated considering the indices estimated in the reference condition $\mathbb{y}_m$;

– Step 3: The threshold value Λ_m is established based on the estimated density of the distances calculated in the reference condition and the probability of false alarms chosen β.

TEST PHASE:

– Step 4: A new Volterra model is estimated in an unknown structural condition;

– Step 5: The standardized Euclidean distance $\mathcal{D}_m$ is calculated considering the indices estimated in an unknown condition y_m;

– Step 6: The hypothesis test (Eqs. 68) is applied to compare the distances obtained in the unknown and reference condition.

In the two next sections, the reader can find the main results obtained through the experimental application of the method to detect damage.

5.4.2 **Stochastic model identification**

The Volterra kernels estimation was done in the same form as using the deterministic model, i.e., in two steps considering the same input signal and a low (0.01 V - linear behavior) and a high (0.15 V - nonlinear behavior) level of input. However, in this stochastic application, MC simulations were employed to determine the stochastic baseline model, analyzing 2048 realizations to guarantee the method convergence. To compare the results of this section with those shown previously, the same number of Volterra kernels and Kautz functions were used. Initially, the convergence of MC simulations has to be studied, ensuring the statistical reliability of the obtained results. Figure 37 shows the results obtained with the convergence criterion (section 4.3) applied to the first three kernels identified. It can be noted that the convergence was achieved with 2048 samples used.

Figure 37 – MC convergence test applied in the Volterra kernels estimated.

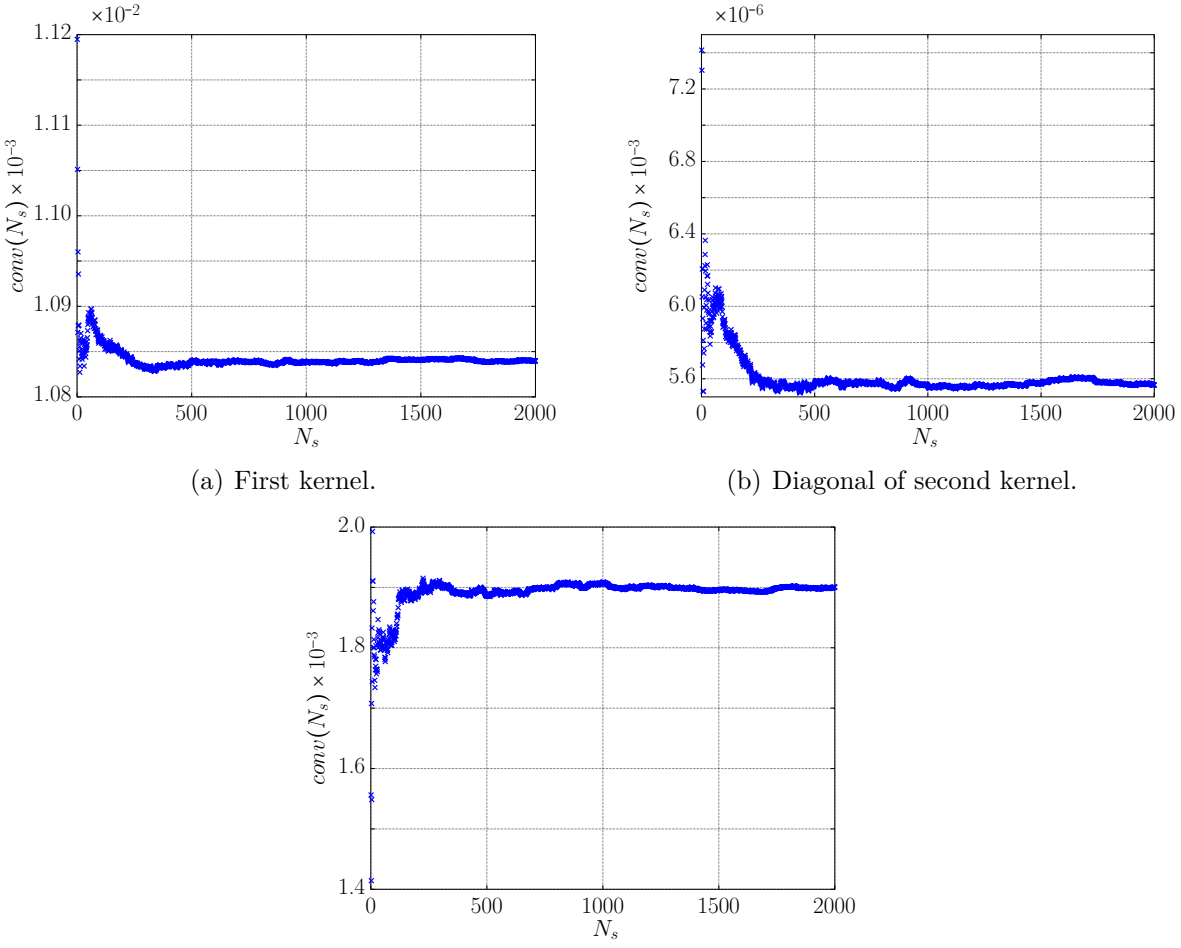

(a) First kernel.

(b) Diagonal of second kernel.

(c) Main diagonal of third kernel.

Source: Villani *et al.* (2019a).

After that, the reference model was verified using two different input signals. First, the same chirp signal examined in the model estimation was applied, and then, a sine wave with a frequency of 23 Hz (first structural fundamental frequency) was adopted. Both signals were applied with a high level of input amplitude (0.15 V) to explore the nonlinear behavior of the system. Figure 38 shows the results obtained using the chirp input signal with the 99 % confidence bands. The stochastic model can describe the system behavior with statistic confidence. Additionally, Fig. 39 shows the results reached for the sine input signal, in the frequency domain. It is observed that the 99% model's confidence bands can describe all the system's frequency components and the data variation. The third kernel has a contribution to the principal and third harmonics. This result points out that the cubic kernel is sensitive to linear variations, which allows the third kernel to detect damages with linear characteristics, as the loss of mass considered.

Finally, Fig. 40 shows the Volterra kernels contributions with 99% of statistical bands, considering a high level (0.15 V) of the input signal amplitude and two structural conditions, reference (4 masses) and severe damage (1 mass). The linear and cubic contributions manifest significant differences with the occurrence of the damage, but the second kernel contribution is not so influenced. The variation of the cubic kernel's contribution is associated with the influence of the Kautz functions variation that changes even with the linear characteristic of the damage. It is also important to recognize that the cubic kernel influences the main harmonic of the response, so if the presence of the damage alters the first harmonic's behavior, the cubic kernel will sense it. Next section presents the main results of the application of the damage detection proposition.

Figure 38 – Comparison between the response obtained through the stochastic Volterra model estimated and obtained experimentally, regarding a high-level of input amplitude (0.15 V) and the reference condition. The gray box represents 99% of confidence bands, – represents the mean and – ● – the experimental data.

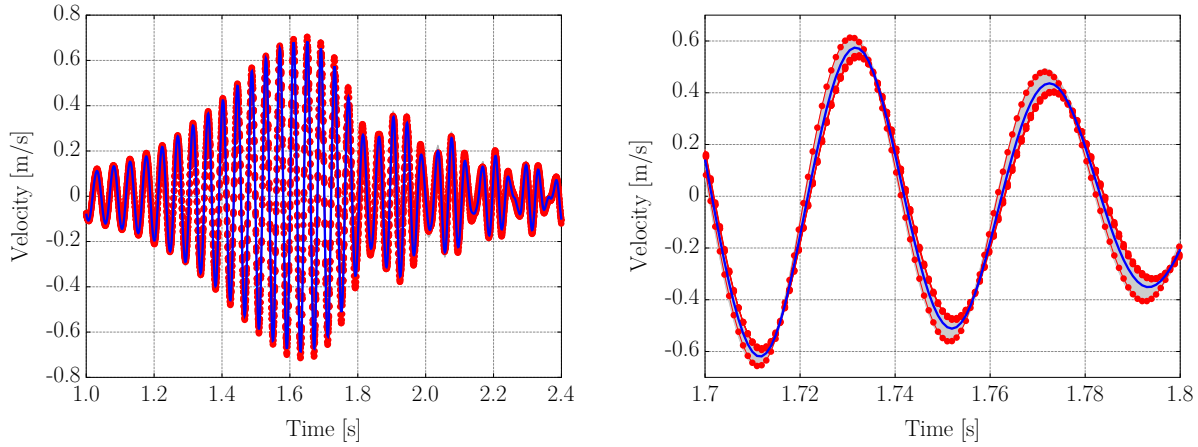

(a) Complete Signal. (b) Zoom.

Source: Villani *et al.* (2019a).

Figure 39 – Frequency components of the stochastic Volterra model's output in comparison with new experimental data, considering a sine input signal and the reference condition.

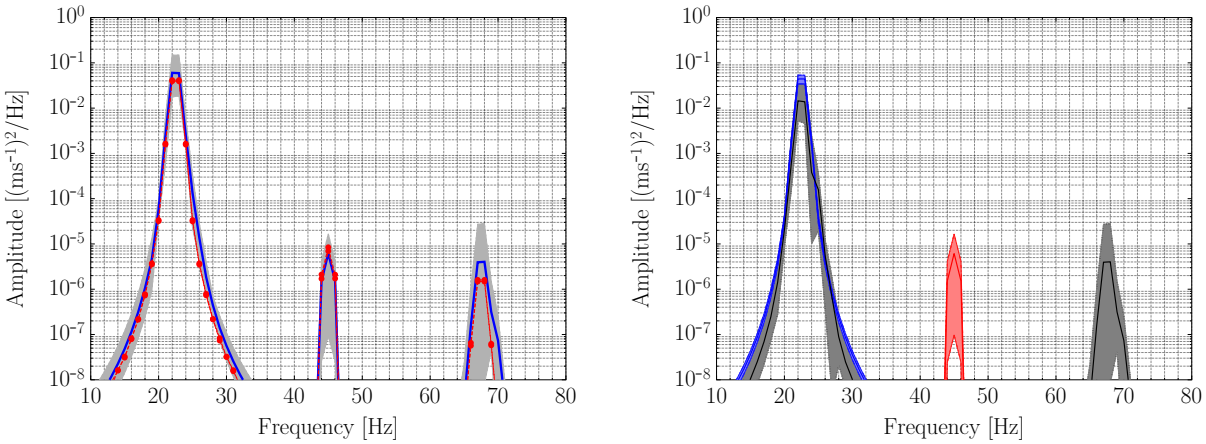

(a) Comparison between model response and new experimental data. The gray box represents 99% of confidence bands, – represents the mean and – ● – the experimental data.

(b) Kernels contributions. ■ represents the first kernel contribution, ■ the second kernel contribution and ■ the third kernel contribution.

Source: Villani *et al.* (2019a).

Figure 40 – Volterra kernels' contributions with 99% of statistical confidence bands, using a high level of input (0.15 V). ■ represents the condition H and ■ the condition III.

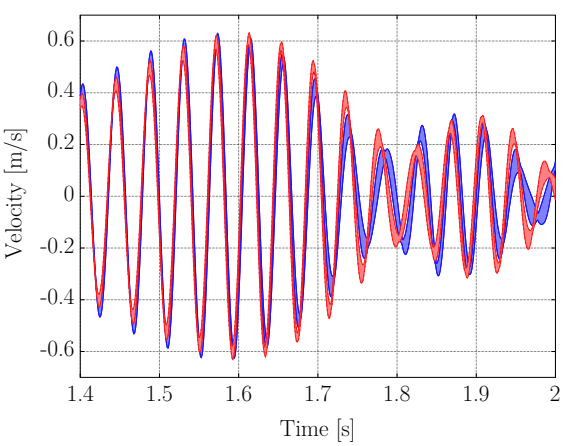

(a) Linear contribution.

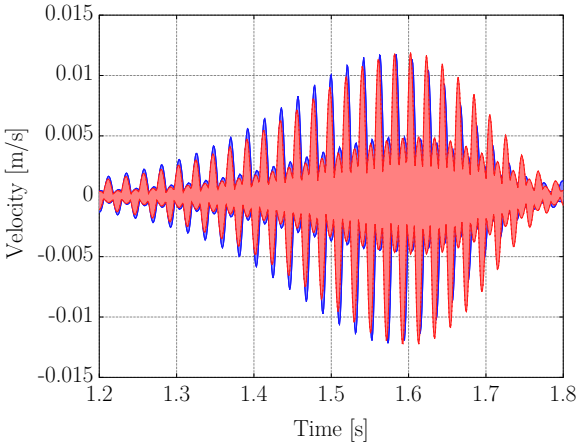

(b) Quadratic contribution.

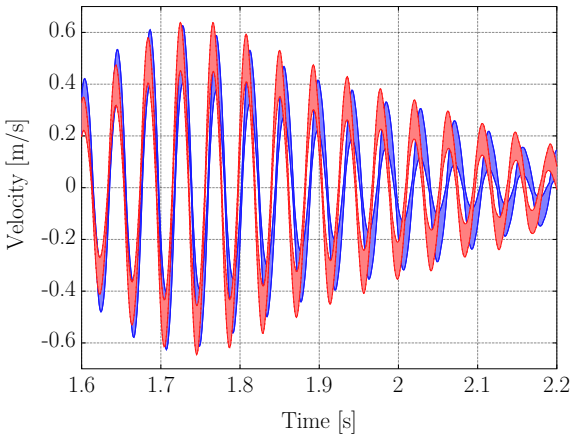

(c) Cubic contribution.

Source: Villani *et al.* (2019a).

5.4.3 Damage detection using the stochastic model

With the random model estimated and verified in the reference condition, it is feasible to apply the novelty detection approach proposed. The excitation signal assumed is the same used in the kernels identification process, using a high-level amplitude (0.15 V), aiming the analysis considering the nonlinear effects in the response. Figure 41 shows the growth of the indices, linear and nonlinear, subjected to the standardized Euclidean distance, with the progression of the damage. The linear index has large dispersion, mainly with the progress of the damage, this behavior illustrates that the presence of uncertainties has more influence in the linear contribution, thus, to detect the damage based on the linear kernel's contribution is more difficult, although the damage has a linear characteristic. The nonlinear index is more affected by the effect of the damage because the third kernel has a contribution in the fundamental frequency of system's oscillation and the presence of uncertainties does not have a high influence on it. Additionally, it can be seen some superposition between the red dots of $\mathbb{D}_{nl}$ calculated in the reference condition and the lower quartile of the damage I condition. However, these dots represent outliers with no statistical relevance in the performance of the metric as will be seen just ahead.

Figure 41 – Damage index (standardized Euclidean distance) considering the stochastic approach.

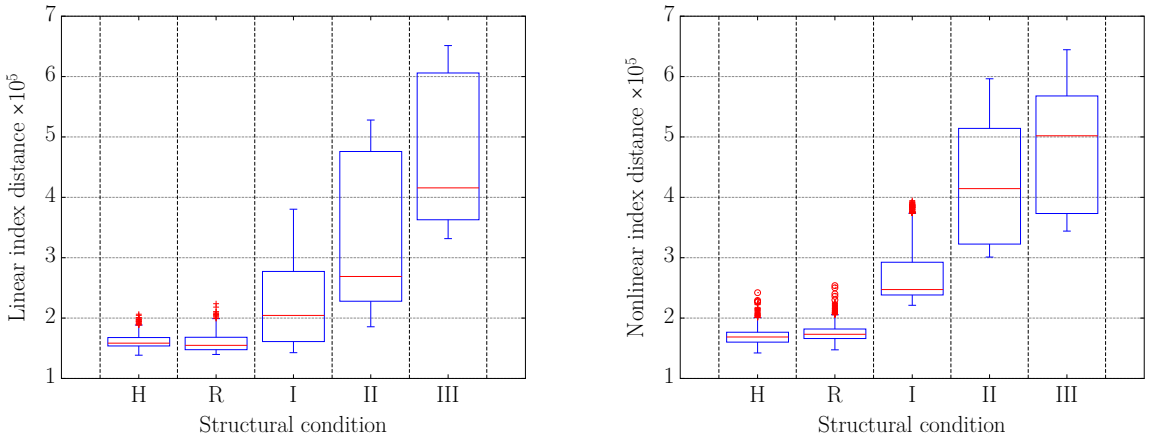

(a) Linear contribution.

(b) Nonlinear contribution.

Source: Villani *et al.* (2019a).

It is important to recognize that the estimation of the Volterra kernels was made in two steps, i.e., the linear kernel is estimated considering a low level of response amplitude, and in this condition, the influence of the uncertainties is significant. Consequently, because of this, the linear kernel is more influenced by the confounding effects contained

in the damage detection process. The fact of the cubic kernel be more sensitive to the presence of damage makes the nonlinear index capable of differing the variation related to the presence of damage to the variation related to the uncertainties. To exemplify better the capability of the indices to detect the structural variation related to the damage, the hypothesis test was applied. After the computation of the distances in the reference condition, the threshold value is determined based on the probability of false alarm β chosen, and the distribution achieved. It was considered three different values for the probability of false alarms (β = 0.005, 0.01 and 0.02) to exemplify the capability of damage detection. The hypothesis test was applied and the results obtained are pointed in Fig. 42. As supposed, the performance of the nonlinear index is better. It is pointed out that the linear index was not able to classify all the different conditions evaluated, presenting a lower level of detection.

Figure 42 – Percentage of damage detection obtained using the kernels' contributions, considering different structural conditions and probability of false alarm used. ■ represents β = 0.02, ■ represents β = 0.01 and ■ represents β = 0.005.

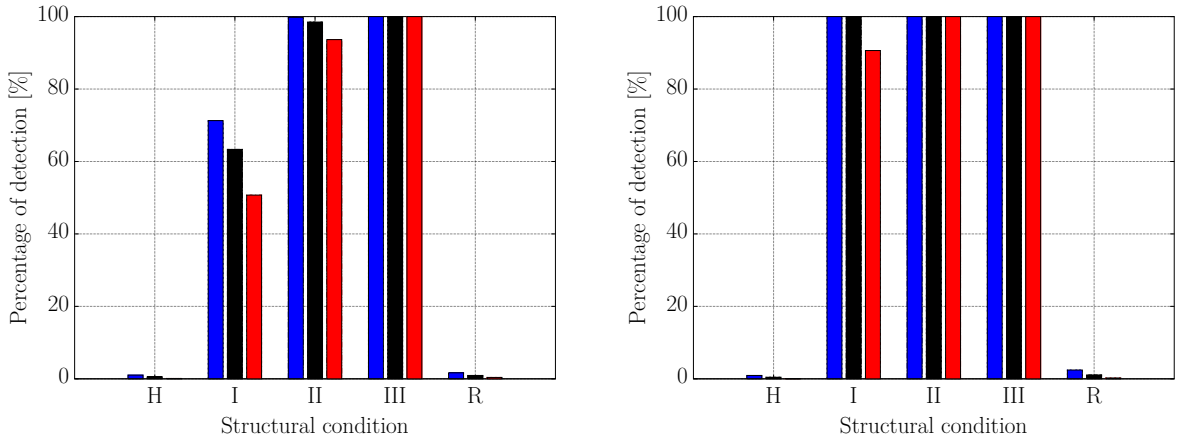

(a) Linear contribution. (b) Nonlinear contribution.

Source: Villani *et al.* (2019a).

Again, the ROC curve was calculated to analyze the performance of the approach better and to make a more direct comparison between the deterministic and stochastic method. Figure 43 brings the results for the linear and nonlinear index. The performance of the nonlinear index is better than the linear one, as it is shown with the higher level of precise detection and lower level of false alarms. Then, even though the linear feature of the damage imposed (mass variation) the nonlinear index exhibited better results because the nonlinear contributions are more sensitive to the damage, with a lower impact of the uncertainties. Additionally, when we confront these results with those obtained with the deterministic model, a large improvement in the capability of damage

detection considering the nonlinear index can be regarded, with a higher number of true detection and a lower number of false alarms. Hence, it can be observed that the use of the stochastic version of the Volterra series outlines an evolution in the field of damage detection regarding the nonlinear behavior and the uncertainties if we compare Fig. 43 and Fig. 36.

Figure 43 – ROC curve considering the stochastic model.

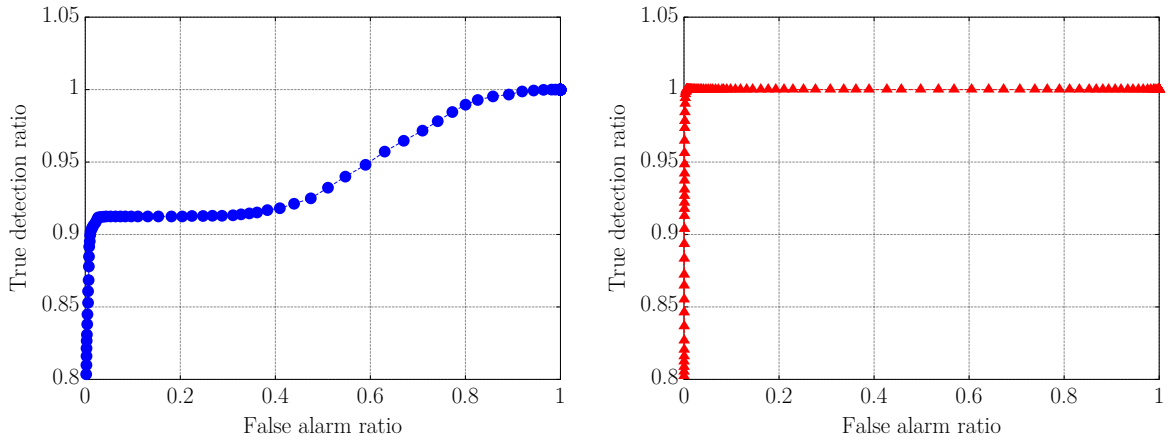

(a) Linear index. (b) Nonlinear index.

Source: Villani *et al.* (2019a).

5.5 COMPARISON BETWEEN THE USE OF DETERMINISTIC AND STOCHASTIC VOLTERRA SERIES FOR DAMAGE DETECTION

With the goal of comparison between the methodologies used, Tab. 4 shows the main characteristics of both metrics. As discussed before, the stochastic method proposed improves the capability of the model to detect damage considering the data variation in the response of the initially nonlinear system. This improvement is associated with the ability of the method to "learn" with the data variation in the training phase to predict the response with statistic confidence.

On the other hand, the stochastic methodology requires a higher number of experimental data in the training phase to assure the statistical confidence of the reference model. This characteristic leads to longer processing time. Therefore, the choice of the process to be used depends on the level of uncertainties/data variation that the system is exposed.

Table 4 – Main characteristics of both methodologies.

Methodology	Deterministic	Stochastic
Reference model	One single model	Set of reference models
Volterra kernels	Deterministic -- $\mathcal{H}$	Random -- $\mathbb{H}$
Kautz functions	Deterministic -- ψ	Random -- Ψ
Model output	A single signal -- y	Set of signals predicting the response with statistical confidence -- $\mathbb{y}$
Damage detection	The reference model response is compared with the system response in different conditions	The model is identified in each condition and the contributions are compared
Damage index	Prediction error based method	Distance-based method
Experimental data required to estimate the model	One single signal measured in reference condition	A high number of data measured in reference condition to ensure the Monte Carlo convergence
Processing time to estimate the reference model	Lower	Higher
Performance	Poor performance considering the data variation	High performance considering the data variation

Source: Villani *et al.* (2019a).

5.6 CONCLUSIONS

This chapter has compared the use of the deterministic Volterra series methodology and the new stochastic version of the series to detect damage in an initially nonlinear system, regarding the data variation occasioned by the presence of uncertainties. The methodologies were applied in an experimental test using a clamped-free beam operating in a nonlinear regime of motion because of the influence of a magnet positioned near to its free extremity. The damage was emulated through the loss of mass in a bolted connection placed in the center of the beam. Although the damage has a linear characteristic, with influence in the natural frequency of the equivalent linear system, the nonlinear indices have shown to be more sensitive to detect it when the system is operating in a nonlinear regime of vibration, as presumed by previous results (SHIKI; SILVA; TODD, 2017).

As the newest result, the use of the stochastic Volterra kernels' contributions mixed with the novelty detection metric offered a more significant capability to detect the

damage when the data deviation, related to the measurements performed in different days, was admitted. Therefore, this experimental application has shown the effectiveness of the proposed strategy to detect structural variations considering the intrinsically nonlinear effect and uncertainties in the data measured. The stochastic Volterra kernels' coefficients were not used as damage sensitive feature because of the linear characteristic of the damage examined, as stated before. Thus, the next chapter deals the application of the stochastic approach, including the use of the kernels coefficients, to detect damage with nonlinear characteristic (a breathing crack) experimentally, considering the intrinsically nonlinear behavior of the structure and the data variation.

6 ON THE DETECTION OF A NONLINEAR DAMAGE IN AN UNCERTAIN NONLINEAR BEAM USING STOCHASTIC VOLTERRA SERIES

This chapter aims to cover issues that were not yet considered previously: (a) an experimental application of the stochastic Volterra series methodology with the presence of damage that produces nonlinear behavior to the system - a breathing crack emulation; (b) the observance of variation in the intrinsic nonlinearity of the structure including the data variability, thus not only considering its influence in the linear components; (c) the generalization of the approaches studied before with the development of a new hybrid method that considers both the kernels' coefficients and contributions simultaneously in the damage index; and, finally, (d) the construction of a theoretical distribution of the damage index calculated in the reference condition to reduce the number of experimental realizations needed to estimate the threshold value based on the Kernel Density Method used before (a practical problem when we consider real-world experiments). All the results presented can be found on Villani *et al.* (2019b).

The present chapter is organized as follows: section 6.1 shows the nonlinear structure considered in this work, the damage simulated and the main characteristics of its behavior; section 6.2 the approach proposed to detect the damage considering the data variation related to uncertainties through the stochastic version of the Volterra series; section 6.3 shows the application of the methodology proposed and the main results obtained; and finally, the section 6.4 presents the conclusions obtained.

6.1 EXPERIMENTAL SETUP

The experimental setup used is presented in Fig. 44. The structure monitored is formed by a clamped-free beam, that is constructed by gluing four thin beams of Lexan together, $2.4 \times 24 \times 240$ [mm^3] each one, to emulate a damage propagation that is described further on. At the free boundary, two steel masses are affixed and interact with a magnet, generating a nonlinear behavior in the system response, even in the reference condition due to added magnetic potential. Moreover, the setup includes:

- A National Instruments acquisition system:

  - CompactDAQ Chassis(NI cDAQ-9178);
  - A C Series Sound and Vibration Input Modules (NI-9234);
  - A C Series Voltage Output Module (NI-9263).
- Electrodynamic Transducer Labworks Inc. (ET-132);
- Amplifier MB Dynamics SL500VCF);
- Load cell PCB PIEZOTRONICS (208C02);
- Accelerometer PCB PIEZOTRONICS (352C22).

Figure 44 – Experimental apparatus.

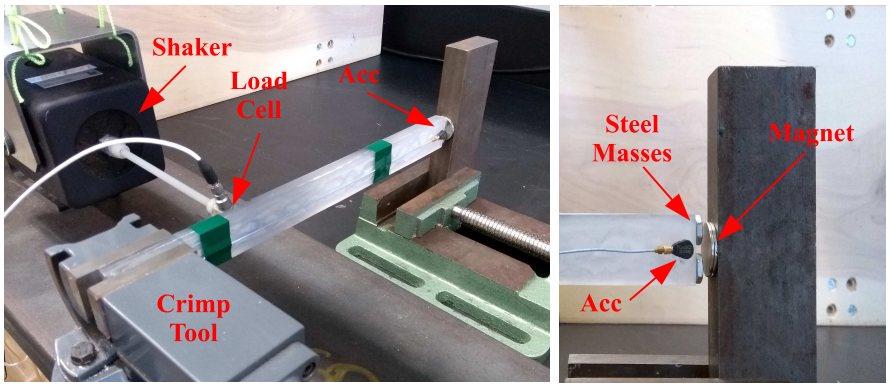

(a) Photos.

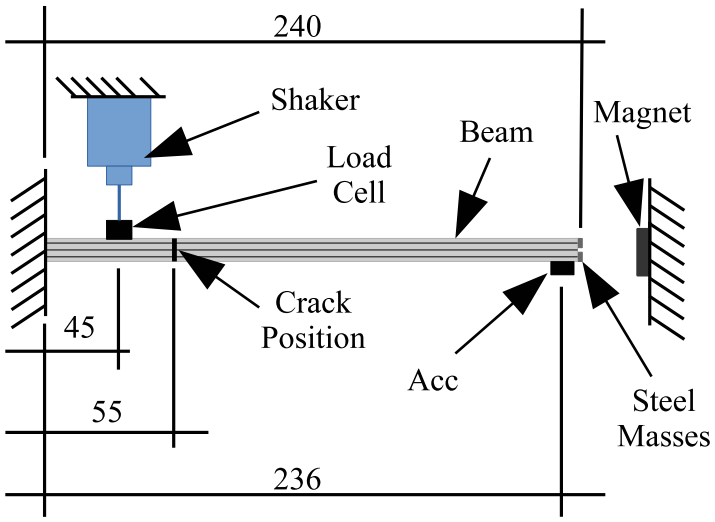

(b) Scheme - dimensions in mm.

Source: Villani *et al.* (2019b).

The electrodynamic transducer is employed to excite the structure with different signals and considering two levels of input (low - 1 V RMS and high - 6 V RMS). The

output data is measured by the accelerometer positioned close to the free extremity of the beam because the authors are only interested in the region of the first mode shape of the structure (see Fig. 44). The input signal analyzed is the voltage signal applied in the electrodynamic transducer. As a single-input/single-output (SISO) model is considered, this pair of signals is enough to identify the Volterra kernels and monitor the structural health. All the acquisition parameters, signals considered, and equipment used were the same in the experiments performed considering the different structural conditions.

6.1.1 **Intrinsically nonlinear behavior**

The mechanical system used exhibits nonlinear operation even in the reference condition, without the presence of damage. Figure 45a shows the results obtained during the stepped sine test applied considering two levels of input. When the input applied has a low level of amplitude (1 V RMS), the output signal shows linear characteristics for both up-sweep and down-sweep inputs. However, when the input signal is at a sufficiently high amplitude (6 V RMS), the nonlinear phenomena can be seen with the jump presented in the test.

Additionally, Fig. 45b shows the time-frequency diagram of the system's response considering a high level of a chirp input in the region of the first mode shape of the structure. The presence of the cubic harmonic in the response confirms the nonlinear characteristic of the response caused by the interaction between the magnet and the steel masses. Therefore, the system studied presents nonlinear behavior, subject to sufficient level of input, even when the structure is healthy. This characteristic is obtained because the magnetic force changes nonlinearly with distance from the end masses to the magnet. This intrinsically nonlinear behavior can be confused with the simulated damage that causes a distinct nonlinear characteristic to the system response.

Figure 45 – Intrinsically nonlinear behavior of the system.

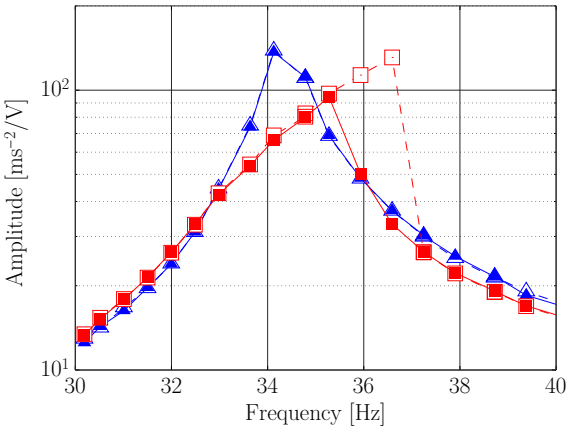

(a) Stepped sine test, where – △ –, –▲–, –□– and –■– represent, respectively, frequency up and frequency down considering low level of input, and frequency up and frequency down considering high level of input.

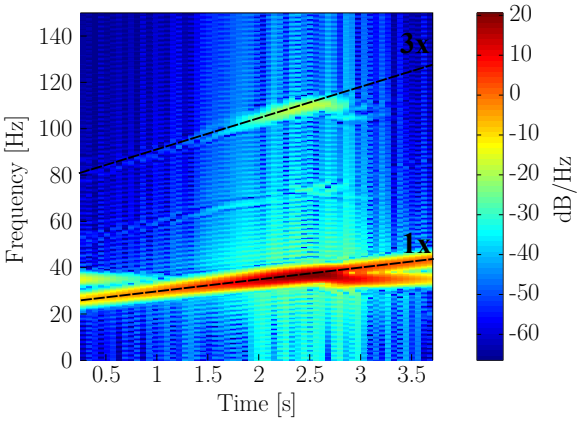

(b) Time-frequency diagram of the system response.

Source: Villani *et al.* (2019b).

6.1.2 **Damage simulated**

The damage imposed on the structure aims to simulate a breathing crack present in the system. In this sense, four different beams were built to be used in the application of the damage detection methodology:

- Training beam: beam constructed with 4 intact Lexan beams and used in the training phase of the algorithm (see Fig. 46a);
- Test beam: beam constructed with 4 intact Lexan beams and used in the test phase of the algorithm (see Fig. 46a);
- Damage I: beam constructed with 3 intact and 1 cut beam (see Fig. 46a and b);
- Damage II: beam constructed with 2 intact and 2 cut beams (see Fig. 46a and b);

The cut in the beams is positioned close to the excitation point (see in Fig. 44b). This spot was chosen to obtain the required nonlinear behavior to test the performance of the algorithm. The damage condition might be judged severely, but the position and excitation combined were defined to generate a condition that is difficult to detect -- mainly in the condition Damage I -- as will be shown further along. Figure 47 shows

Figure 46 – Structural conditions considered.

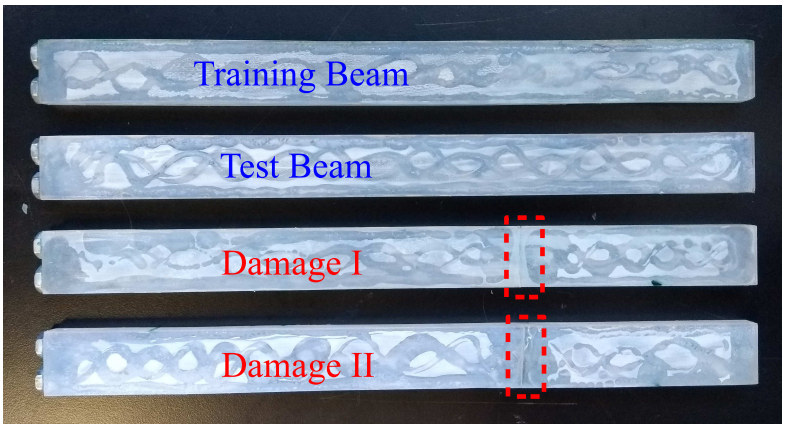

(a) All beams constructed.

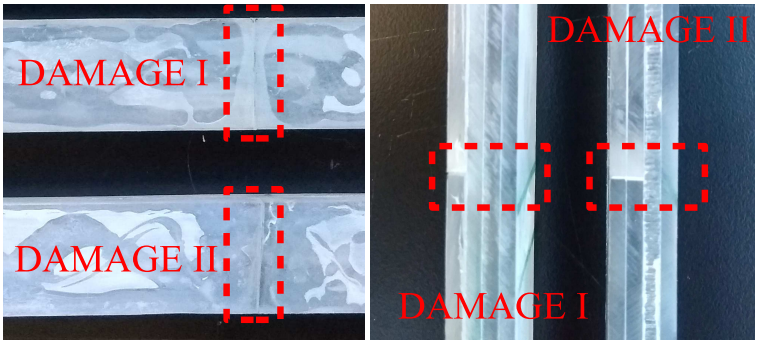

(b) Damaged beams (zoom).

Source: Villani *et al.* (2019b).

the time-frequency diagram of the system response considering a chirp input with a high level of amplitude and the structure in damaged conditions. In Fig. 47a it is observed the appearance of a quadratic harmonic when we compare with Fig. 45b, that is a consequence of the crack, without significant alterations in the behavior of other components of the response (first and third harmonics look similar to the ones observed in Fig. 45b). With the propagation of the damage (damage II) the quadratic and cubic harmonics grow up and the resonance frequency changes (see in Fig. 47b).

Thus, it is recommended that the initial propagation of the damage has influence in the quadratic harmonic of the system and when the extension of the damage is more significant, all linear and nonlinear components of the response are affected. The damage detection approach applied has to be able to detect the appearance of the nonlinear behavior caused by the damage, without confusing this evolution with the cubic nonlinear behavior caused by the presence of the magnet. Additionally, the problem becomes more complicated when the data variation is assumed in the problem, requiring a strategy to

separate these effect as shown in the next section.

Figure 47 – Time-frequency diagram of the system's output measured in damaged conditions.

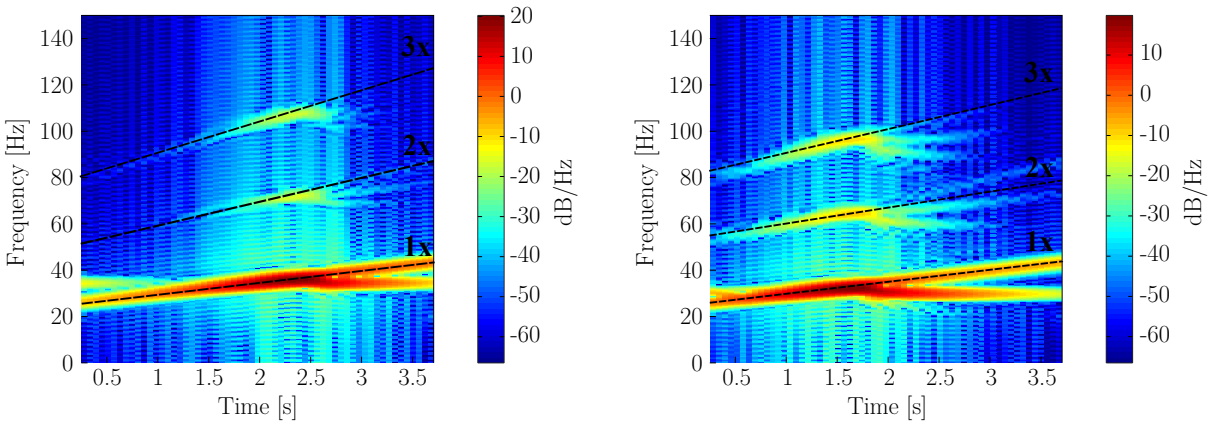

(a) Damage I.

(b) Damage II.

Source: Villani *et al.* (2019b).

6.1.3 Data variation

In order to study the performance of the strategy in the presence of data variation or other uncertainties, the distance between the magnet and the steel masses (see in Fig. 44b) was varied from 2 mm to 3.5 mm during the tests, repeated on different days to obtain a total of 200 experimental tests for each beam constructed.

Figure 48 illustrates the variation of the system response during the tests. The results consider only the first mode shape frequency range, as only this range will be examined in the damage detection process. It is clear that it is easy to classify the structural condition when the extension of the damage is even more severe (damage II), but it is not plausible to observe visually the deviation between the reference and damage I conditions when the Frequency Response Function (FRF) and the linear modal parameters are considered. These modal parameters were estimated considering a line-fit method (EWINS; SAUNDERS, 1986) and the experimental realizations of the FRF.

These results show how hard is to detect the presence of the damage when the data variation is considered in the analysis. In the scenario considered, with the experimental data measured, the model proposed has to be able to detect the presence of the damage in the uncertain ambient state without confusions between the nonlinear behavior caused by the presence of the magnet and that one caused by the presence of the damage.

Figure 48 – Variation of the data measured.

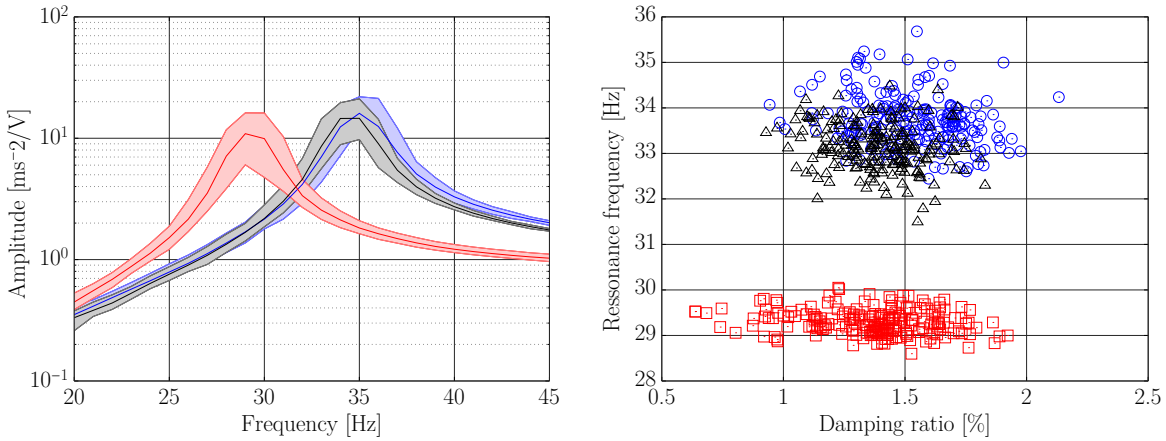

(a) Frequency Response Function, where the continuous lines represent the mean values and the color zones the curves obtained with 99% of confidence, - reference, - damage I and - damage II.

(b) Variation of linear modal parameters, where ∘ represents the reference condition, △ damage I and □ damage II.

Source: Villani *et al.* (2019b).

6.2 DAMAGE DETECTION BASED ON MAHALANOBIS SQUARED DISTANCE

Previously, two points were analyzed separately in the damage detection process: the kernels' coefficients and the kernels' contributions. Nevertheless, it is difficult for practical applications to decide which feature is better. Thus, the damage detection index used here examines both features jointly. Regarding the stochastic model identified with training data in the reference condition, the damage-sensitive index may be determined in the reference status. First of all, recognizing that the Volterra series will be truncated in the third order kernel, the kernels coefficients can be allocated together to be used as damage sensitive feature $\mathbb{k}_{lin}$, $\mathbb{k}_{quad}$ and $\mathbb{k}_{cub}$ Eq. (45).

Additionally, the contribution of the kernels can be calculated as $\mathbb{y}_{lin}$, $\mathbb{y}_{quad}$ and $\mathbb{y}_{cub}$ Eq. (50). After that, to reduce the order of the classification problem, the principal component analysis (PCA) (PARK *et al.*, 2008; PAVLOPOULOU; WORDEN; SOUTIS, 2016) can be applied to the kernels' contributions

$$\begin{aligned}
\mathbb{y}_{lin}(\theta,k) \gg \quad & \text{PCA} \gg \mathbb{C}_{lin}(\theta,1),\dots,\mathbb{C}_{lin}(\theta,n_{pca}),\\
\mathbb{y}_{qua}(\theta,k) \gg \quad & \text{PCA} \gg \mathbb{C}_{qua}(\theta,1),\dots,\mathbb{C}_{qua}(\theta,n_{pca}),\\
\mathbb{y}_{cub}(\theta,k) \gg \quad & \text{PCA} \gg \mathbb{C}_{cub}(\theta,1),\dots,\mathbb{C}_{cub}(\theta,n_{pca}),
\end{aligned} \tag{69}$$

where $(\theta, n_{pca}) \in \Theta \times \mathbb{Z}_+ \mapsto \mathbb{C}_{lin}(\theta, n_{pca})$ represents the principal components of the linear contribution, $(\theta, n_{pca}) \in \Theta \times \mathbb{Z}_+ \mapsto \mathbb{C}_{qua}(\theta, n_{pca})$ represents the principal components of the quadratic contribution, $(\theta, n_{pca}) \in \Theta \times \mathbb{Z}_+ \mapsto \mathbb{C}_{cub}(\theta, n_{pca})$ represents the principal components of the cubic contribution and n_{pca} is the number of principal components considered. The number of components was defined based on the contribution of each component in the construction of the covariance matrix, with a threshold of 95 % to the total contribution (PARK *et al.*, 2008).

After the calculation of the kernels' coefficients and the principal components of the kernels' contributions, the damage index can be defined in the reference condition

$$\begin{aligned} \mathbb{I}_{lin} &= [\mathbb{\lambda}_{lin}(\theta, i_1) \;\; \mathbb{C}_{lin}(\theta, n_{pca})]_{(N_s \times (J_1 + n_{pca}))}, \\ \mathbb{I}_{nl} &= [\mathbb{\lambda}_{qua}(\theta, i_1 = i_2) \;\; \mathbb{\lambda}_{cub}(\theta, i_1 = i_2 = i_3) \;\; \ldots \\ &\qquad \ldots \;\; \mathbb{C}_{qua}(\theta, n_{pca}) \;\; \mathbb{C}_{cub}(\theta, n_{pca})]_{(N_s \times (J_2 + J_3 + 2n_{pca}))}, \end{aligned} \tag{70}$$

where $\mathbb{I}_{lin}$ and $\mathbb{I}_{nl}$ are, respectively, the linear and nonlinear indices in the reference situation. Therefore, in the reference condition, $\mathbb{I}_{lin}$ is a $N_s \times (J_1 + n_{pca})$ matrix and $\mathbb{I}_{nl}$ is a $N_s \times (J_2 + J_3 + 2n_{pca})$ matrix, being N_s the number of observations used in the training phase of the reference stochastic model.

Now, with the structure in an unknown (test) situation, a new deterministic model can be identified, and the indices may be estimated in the unknown status

$$\begin{aligned} \mathcal{I}_{lin} &= [\lambda_{lin}(i_1) \;\; \mathcal{C}_{lin}(n_{pca})]_{(1 \times (J_1 + n_{pca}))}, \\ \mathcal{I}_{nl} &= [\lambda_{qua}(i_1 = i_2) \;\; \lambda_{cub}(i_1 = i_2 = i_3) \;\; \ldots \\ &\qquad \ldots \;\; \mathcal{C}_{qua}(n_{pca}) \;\; \mathcal{C}_{cub}(n_{pca})]_{(1 \times (J_2 + J_3 + 2n_{pca}))}, \end{aligned} \tag{71}$$

where $\mathcal{I}_{lin}$ and $\mathcal{I}_{nl}$ are the linear and nonlinear indices in an unknown condition. As the indices calculated in the reference condition are matrices composed by more than one single feature, the novelty detection has to be performed considering multivariate data. Therefore, the comparison between the indices calculated in the reference and an unknown condition can be made considering de Mahalanobis squared distance (WORDEN; MANSON; FIELLER, 2000; WORDEN; MANSON; ALLMAN, 2003)

$$\mathcal{D}_m^2 = [\mathcal{I}_m - \mu_{\mathbb{I}_m}]^{\mathrm{T}} \, \Sigma_{\mathbb{I}_m}^{-1} \, [\mathcal{I}_m - \mu_{\mathbb{I}_m}], \tag{72}$$

where $m = lin$ or $m = nl$, $\mu_{\mathbb{I}_m}$ and $\Sigma_{\mathbb{I}_m}$ are, respectively, the mean vector and the covariance

matrix of the index calculated in the reference condition. The simple machine learning method based on Mahalanobis squared distance is used here because the classification is done between two possible conditions (healthy and damaged) and the goal is to examine the performance of the Volterra kernels characteristics as damage sensitive features and not to investigate the differences between refined classification methods. Other classification methods can be used in the future to improve the methodology depending on the real application confronted.

With the Mahalanobis squared distance calculated, a hypothesis test may be proposed. The distance calculated in the reference condition is modeled with a chi-square distribution, which may be calculated based on the assumption of independence and normality in the underlying multivariate features from which the Mahalanobis squared distance is calculated (HARDIN; ROCKE, 2005; YEAGER *et al.*, 2019). Ideally, a *sampling* distribution of the Mahalanobis squared distance is desirable, but no such analytical form is known to exist, so the theoretical model is fit to the (limited) empirical data obtained. This approximation has satisfactory performance, as will be shown further along. Then, the hypothesis is proposed

$$\begin{cases} H_0 : \mathcal{D}_m^2 \sim \mathcal{X}^2 \,, \\ H_1 : \mathcal{D}_m^2 \nsim \mathcal{X}^2 \,, \end{cases} \tag{73}$$

where $\mathcal{X}^2$ is the chi-square distribution, H_0 is the null-hypothesis (healthy condition) and H_1 is the alternative hypothesis (damaged condition).

Besides, the probability of a distance value calculated to be included in the theoretical chi-square distribution can be computed integrating its probability density function (PDF)(GRIMMETT; WELSH, 2014)

$$p_m = F(\mathcal{D}_m^2|\nu) = 1 - \int_0^{\mathcal{D}_m^2} \frac{t^{(\nu-2)/2} e^{-t/2}}{2^{\nu/2}\Gamma(\nu/2)} dt \,, \tag{74}$$

where p_m is the probability of the value $\mathcal{D}_m^2$ belonging to the chi-square distribution in a right hand test, $\Gamma(.)$ is the Gamma function, and ν is the number of degrees-of-freedom. Finally, a sensitivity value can be determined depending on the application and probability of false alarms tolerated, and the hypothesis test can be rewritten

$$\begin{cases} H_0 : p_m \geq \beta \,, \\ H_1 : p_m < \beta \,, \end{cases} \tag{75}$$

where β represents the sensitivity chosen for the hypothesis test. The definition of this parameter depends on the practical application and, as an experimental laboratory setup

is utilized, several values will be examined to study the performance of the method. Figure 49 shows a flowchart of the damage detection approach. On the left, it can be observed the training phase, with the identification of the stochastic reference model and the estimation of the damage indices in the reference condition. On the right, it is represented the identification of a new model in an unknown status and the calculation of the new indices. Then, the indices are correlated using the Mahalanobis squared distance, and finally, the hypothesis test is applied to classify the condition of the structure between healthy and damaged.

Figure 49 – Flowchart of the damage detection methodology proposed.

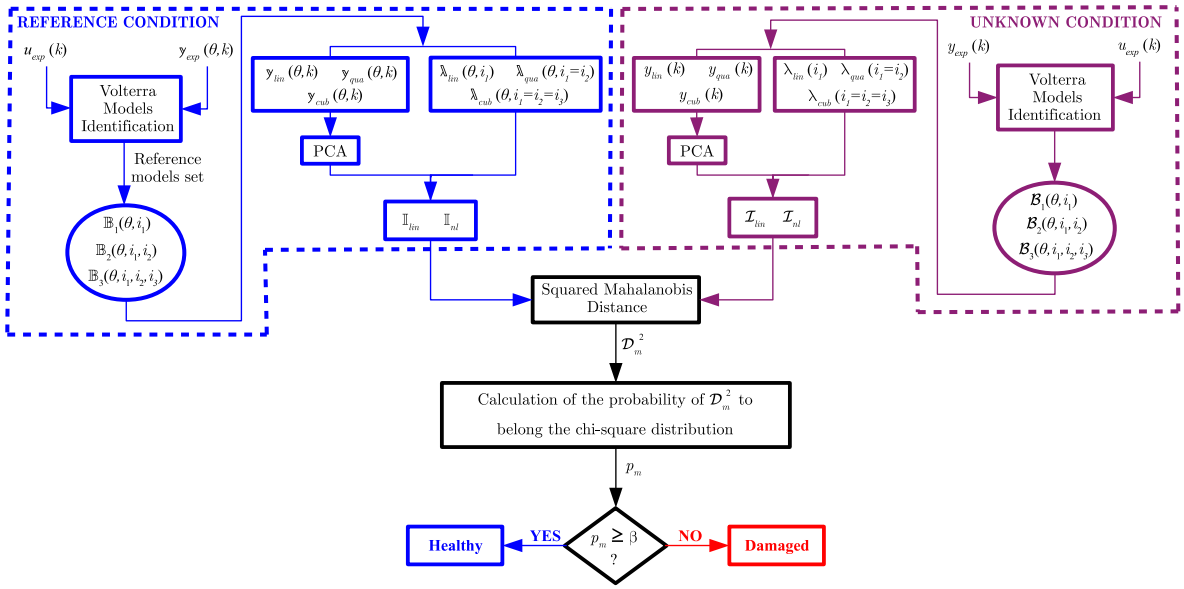

Source: Villani *et al.* (2019b).

6.3 APPLICATION OF THE PROPOSED METHODOLOGY

This section matches the application of the methodology described in the section 6.2 to detect damage admitting the experimental setup described in section 6.1. The main results obtained are shown, and the performance of the linear and nonlinear analysis are compared.

6.3.1 **Reference model identification**

The first step to the utilization of the methodology is the estimation of the stochastic reference model. The number of Kautz functions and the Kautz parameters related

to each Volterra kernel were defined as described in Villani, Silva and Cunha Junior (2019b). Thus, the number of functions used here are $J_1 = 2$, $J_2 = 4$ and $J_3 = 6$. To obtain the input/output signals used in the kernels estimation, the structure was excited admitting a chirp input signal varying the excitation frequency from 25 to 40 Hz (first mode shape region) and considering two levels of amplitude (1 V RMS - linear system behavior and 6 V RMS - nonlinear system behavior). The chirp input is attractive because it excites the linear and nonlinear components of the system response with enough energy, leading to a better estimation of the high-order kernels (RÉBILLAT *et al.*, 2011; RÉBILLAT; HAJRYA; MECHBAL, 2014; SHIKI; SILVA; TODD, 2017). The output signal considered (velocity vibration signal) is obtained through the integration of the acceleration signal measured by the accelerometer (see Fig. 44). The velocity signals are used because of the previous implementation of the model identification procedure considering this type of output. As done before, the kernel estimation is performed in two steps, i.e., the first kernel is identified considering the underline linear behavior of the system, and then, the second and third kernels are identified considering the nonlinear components of the system response.

The deterministic model is identified several times, considering the 200 experimental realizations obtained from the healthy training beam, to construct the stochastic reference model. Figure 50 presents the verification and validation of the model identified. Figures 50a and 50b shows the stochastic model output with 99% of confidence bands, in the time domain, considering the same chirp input used in the model estimation with a high level of amplitude (6 V RMS), in comparison with experimental data measured. It is observed that the stochastic model can predict the system output considering the data variation. Additionally, Fig. 50c shows the stochastic model output with 99% of confidence bands, in the frequency domain, considering a single sine input with excitation frequency close to the system resonance frequency ($\approx$ 35 Hz) and a high level of amplitude (6 V RMS), in comparison with experimental data measured. As can be seen, the stochastic model can predict the harmonic components of the response. This characteristic is unusual in the sense that as the damage considered produces variations in the nonlinear components of the response, it is expected that the model could be sensitive to these variations with adequate performance to detect the damage faster than the linear approach. With the stochastic reference model estimated, the damage detection procedure can be applied and the results obtained are shown in the next section.

Figure 50 – Verification and validation of the reference model. The gray area represents the 99% model response confidence bands, – represents the model response mean and – ● – represents five realizations of the experimental data.

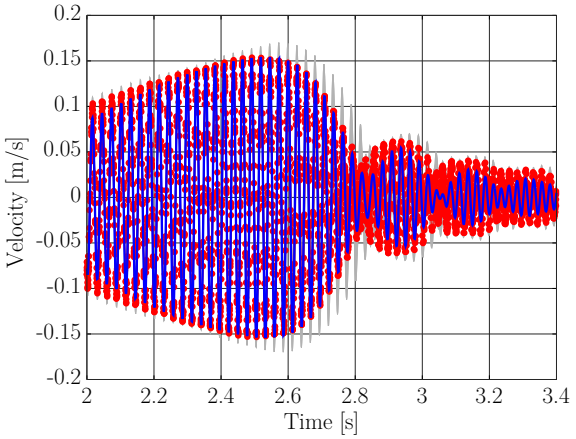

(a) Model response in the time domain considering a chirp excitation.

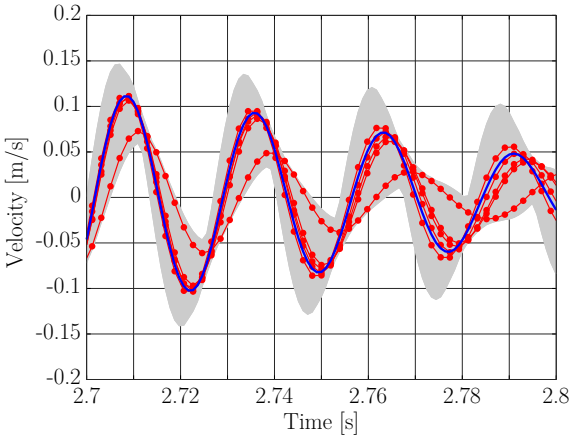

(b) Model response in the time domain considering a chirp excitation (zoom).

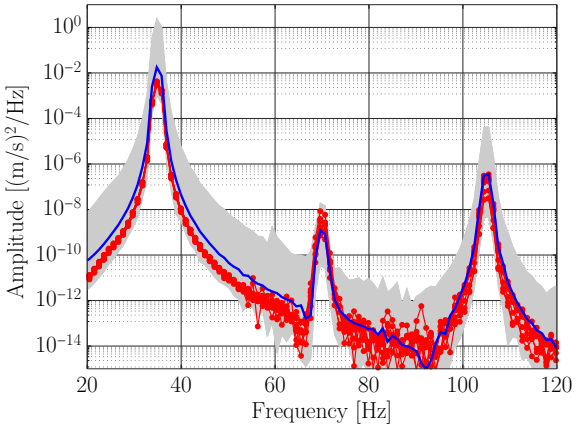

(c) Model response in the frequency domain considering a sine excitation.

Source: Villani *et al.* (2019b).

6.3.2 **Damage detection performance**

First of all, it is interesting to observe whether the Mahalanobis distance computed considering the indices obtained in the reference condition ($\mathbb{I}_{lin}$ and $\mathbb{I}_{nlin}$) belongs to the chi-square distribution, as proposed in the methodology. Figure 51 shows adjustment between the histograms obtained from the Mahalanobis squared distance, calculated with the indices in the reference condition, and the chi-square theoretical distribution. Of course, the theoretical approximation is not perfect but satisfactory, considering the limited amount of data available in the analysis. Moreover, this approximation overcomes the problems involving the empirical estimation of distributions based on experimental data, and the Kernel Density Estimator used before, related to the needed amount of experimental data and the choices of the kernel and smoothing parameter (SILVERMAN, 1986; WORDEN; MANSON; ALLMAN, 2003). This aspect of the indices distribution allows the application of the hypothesis test proposed based on the probability of the distance calculated belonging to the chi-square distribution.

Figure 51 – Comparison between the theoretical and experimental distributions. The histogram represents the experimental data and the **black line** represents the theoretical chi-square distribution.

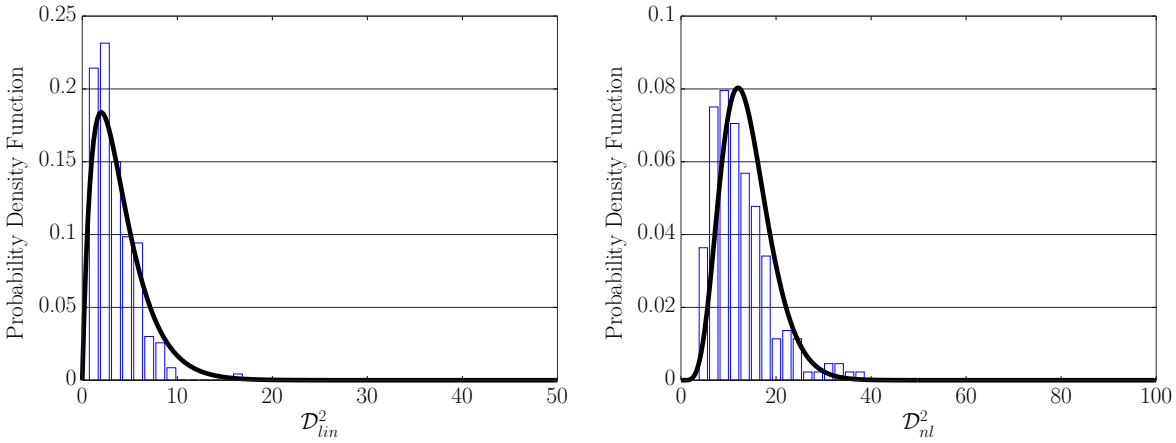

(a) Distance calculated based on the linear index in the reference condition.

(b) Distance calculated based on the nonlinear index in the reference condition.

Source: Villani *et al.* (2019b).

The evolution of the distance calculated from the indices with the propagation of the damage is presented in Fig. 52. It is observed that the linear index is not sensitive to the presence of the damage at the beginning of the propagation, i.e., the damage I condition (see Fig. 52a). The nonlinear index presented more sensitivity to the presence of damage, showing an adequate separation between the damage I condition and the

Figure 52 – Evolution of the Mahalanobis squared distance calculated with the progression of the damage. ∘ represents the reference training beam, × represents the reference test beam, △ represents the damage I condition beam and □ represents the damage II condition beam.

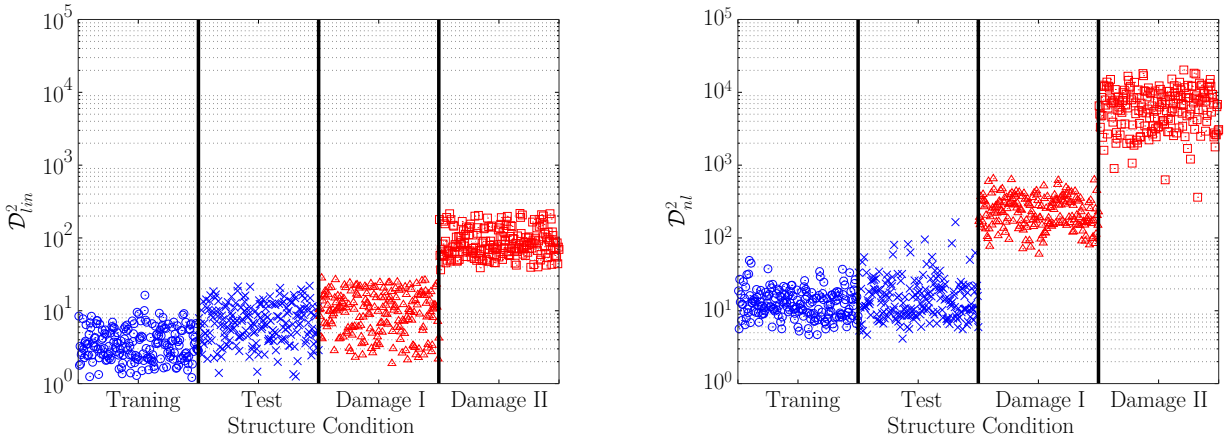

(a) Distance calculated based on the linear index.

(b) Distance calculated based on the nonlinear index.

Source: Villani *et al.* (2019b).

reference condition (see Fig. 52b). Besides, the nonlinear index calculated from the data measured considering the test beam presents some outliers that will be reflected, probably, in false positives, depending on the threshold value used. These outliers are a consequence of the high sensitivity of the nonlinear components to structural variations. These results are not unexpected since the test and training beams are nominally the same, but not identical. The use of more than one training beam could improve the methodology performance in a real application. Another interesting aspect of the index used is the increase of the distance values with the propagation of the damage that, in the future, may be well correlated to the severity of the damage.

Considering the distances determined, the hypothesis test proposed may be applied. Table 5 shows the results obtained for both linear and nonlinear indices. It is clear that the nonlinear index presented a higher capability to detect the presence of the damage. The false alarms (false detection) are also higher considering the nonlinear index. However, this value can be reduced without loss of performance to detect the damage with the decrease of the test sensitivity as performed, e.g., by Avendaño-Valencia and Fassois (2017a). The linear index presented problems to detect the damage I condition, even with the variation of the test sensitivity. In real applications, the value of the test sensitivity β has to be determined depending on the level of security/confidence required and on the previous knowledge about the monitored structure. In some applications, this value

can also be optimized to present a better performance in the damage detection process, based on measured data obtained from damaged structures (AVENDAÑO-VALENCIA; FASSOIS, 2017a).

Table 5 – Results obtained through the application of the hypothesis test.

	Hypothesis test sensitivity	**Percentage of false detection** [%]	
		Training Beam	**Test Beam**
Linear Index	10^{-2}	0.5	15.5
	10^{-4}	0	0
	10^{-6}	0	0
	10^{-12}	0	0
Nonlinear Index	10^{-2}	4.5	12.5
	10^{-4}	1	7
	10^{-6}	0	4.5
	10^{-12}	0	1.0
		Percentage of true detection [%]	
		Damage I	**Damage II**
Linear Index	10^{-2}	34.5	100
	10^{-4}	5	100
	10^{-6}	0	100
	10^{-12}	0	75
Nonlinear Index	10^{-2}	100	100
	10^{-4}	100	100
	10^{-6}	100	100
	10^{-12}	96.5	100

Source: Adapted from Villani *et al.* (2019b).

However, a better way to analyze the damage detection capability of the methodology is computing the ROC curve. This curve relates the false alarm ratio with the true detection ratio obtained applying the hypothesis test for different values of sensitivity β. As a result, the closer to the point (0,1) is the curve, better is the performance of the index because it presents a higher probability of detecting the damage with a low level of false alarms. This curve is used here to study the discrepancies between the performance of the linear and nonlinear approaches proposed. Figure 53 shows the curves obtained after the application of the hypothesis test using different threshold values, considering both indices (linear and nonlinear) and all structural conditions studied (training beam, test beam, the damage I and damage II). In the figure, it can be seen that the nonlinear index presents a better performance since the red curve is close to the point (0,1). This result was expected as the linear components of the response are not sensitive to the initial propagation of the damage (see Fig. 52 and Tab. 5).

Moreover, the performance of the nonlinear index (almost perfect, but this is admit-

tedly a consequence of a finite data set), with the curve very close to the point (0,1), was achieved in an experimental laboratory application. Even with the consideration of the data variation simulated during the experimental tests, these results do not reflect a real-structure application. It is supposed in a real-world application a higher number of confounding effects, different types of damage occurring coincidentally and other aspects that may decrease the methodology performance. However, the better capability of the features related to the nonlinear kernels to detect the presence of the damage considering the confounding effects caused by the nonlinearities and uncertainties must be preserved.

Figure 53 – Receiver operating characteristics curve. ● represents the linear index and ▲ represents the nonlinear index.

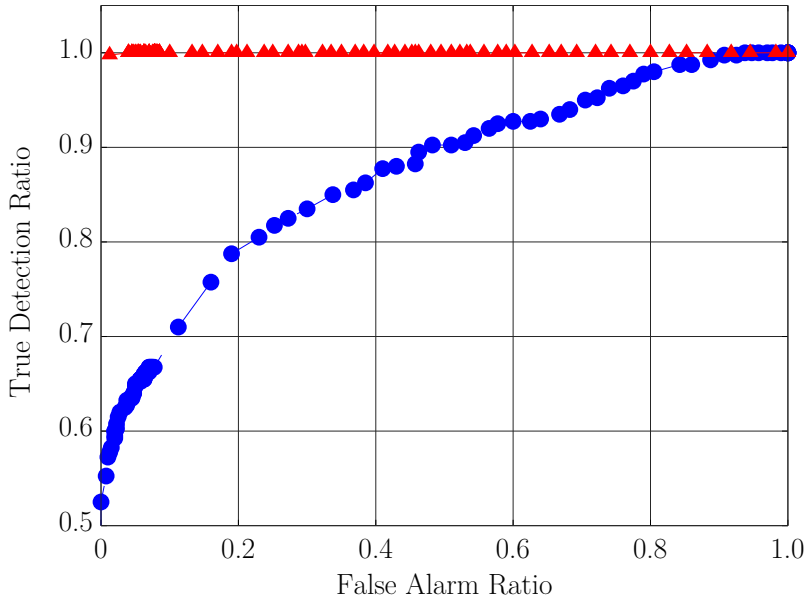

Source: Villani *et al.* (2019b).

6.4 CONCLUSIONS

The problem of damage detection in an intrinsically nonlinear system, regarding the data variation associated to uncertainties, subjected to the presence of damage that causes a nonlinear characteristic in the system's response was investigated in this chapter. In this sense, an initially nonlinear beam was analyzed, and the data variation was emulated by the random variation imposed in the experimental setup (variation of the distance between the magnet and the beam). The damage studied was a breathing crack that affects the system to exhibit a nonlinear operation with a distinct character of the initial one. In this condition, the methodology has to be adequate to distinguish the intrinsically nonlinear operation and the data variation to the presence of the damage. A method

based on a stochastic version of the Volterra series, with the use of the random kernels' coefficients and contributions as damage detection features, combined with a novelty detection technique, was applied to solve the problem.

Unlike what has been shown previously, the kernels' coefficients and the kernels' contributions approaches were applied together, considering a single index to monitor the structural condition, aiming to increase the robustness of the method. Moreover, a theoretical distribution was introduced to the Mahalanobis squared distance computed in the reference condition to reduce the possible problems related to the use of the kernel density estimator previously assumed. Additionally, for the first time, the methodology was examined through an experimental application considering an intrinsically nonlinear beam subordinated to the presence of damage that produces nonlinear aspects to the system response, all this, considering data variation that reflects changes in the linear and nonlinear components of the response.

The results obtained revealed that the monitoring of the nonlinear components of the system response, denoted by the higher-order kernels' coefficients and contributions considered as damage detection features, is a helpful method to be implemented in damage detection problems when the nonlinear system response is present. Again, the nonlinear metric confirmed to be more sensitive to the appearance of the damage and showed better performance considering the data variation compared with the monitoring of linear components. Finally, the use of the stochastic reference model, combined with the novelty detection technique and the hypothesis test, exhibited satisfactory performance to overcome the problem related to the data measured variation, providing the metric for detecting the presence of the damage with probabilistic confidence even in an uncertain ambient.

7 FINAL REMARKS

This final chapter presents in the section 7.1 the main conclusions about the approach and the results showed and in the section 7.2 the main contributions of the thesis to the literature. Additionally, section 7.3 shows the suggestions for future works and applications in the research.

7.1 CONCLUSIONS

Considering all the results obtained and presented in this thesis, about the system identification and damage detection considering uncertainty analysis, some remarks can be done:

- The uncertainty analysis in the process of system identification or models' parameters estimation demonstrated to be extremely important to improve the results of prediction, with statistic confidence. The results obtained in the identification of the random Duffing oscillator model revealed that the use of a stochastic version of the restoring force surface method can be an interesting approach to be used in low order nonlinear systems identification, considering the data variation caused by the presence of uncertainties. It is important to observe that, even in laboratory conditions, the uncertainties related to measurement noise, the position of the sensors and actuators, and others, make the system response vary and have to be taken into account in the process of parameters estimation;

- This thesis confirms the premises that the use of nonlinear models in the damage detection applications results in better performance when the intrinsically nonlinear behavior of the structures is considered. In all the results, emulating damages with influence in linear and nonlinear components of the system's output signal, the use of nonlinear indices presented an improvement in the capability to detect damage. This characteristic was discussed before by Shiki, Silva and Todd (2017) in a deterministic application and was proved here;

- The adaptation of the Volterra series formulation from the deterministic version to the stochastic one, using the idea of Multiple Models (MM) identification,

increased the capability of the methodology to deal with the presence of uncertainties expressed as variations in the experimental data measured. This new formulation, combined with the idea of novelty detection used in this thesis, brings the methodology closer to the real-world applications where the uncertainties are always present. The reader can see in chapter 5 the comparison between the performance of the deterministic and stochastic methodology to deal with the data variation in the damage detection process;

- Different applications were performed with different kinds of damages showing the capability of the proposed approach to be implemented in different conditions. Of course, several damage sensitive indices were proposed and the usability of each one depends on the previous knowledge about the structure or system to be monitored. When a low level of information is avaiable the author suggests the use of the nonlinear index that considers both kernels' coefficients and contributions together;

- The nonlinearities considered were always assumed to be well represented by polynomial functions of cubic order. It was regarded that the damages emulated caused variations in quadratic and cubic terms of the systems' output signals. In this situation, the performance of the approach was satisfactory. However, real damages can induce more complex behavior, with non-smooth nonlinearities that can complicate the application of this method. Probably, the problem can be overcome with the use of higher-order kernels, however, the computational cost of the estimation of these random kernels (4^{th} and 5^{th} order) is a limitation. Therefore, depending on the application, it is suggested the use of other nonlinear models that can deal with strong nonlinear phenomena.

7.2 CONTRIBUTIONS TO THE LITERATURE

As stated before, this thesis contributes to the literature with the proposition of a stochastic version of the input/output based Volterra series, stochastic nonlinear model, to be used in damage detection problems considering intrinsically nonlinear behavior and uncertainties at the same time. New ways to detect structural variations related to damages were proposed based on random Volterra kernels' features (contributions and coefficients) and novelty detection classifiers. These new indices were tested considering different kinds of damages that can induce variations in linear and nonlinear components of the structures' measured output signal. Furthermore, this thesis presents a comparison between the use of the classical deterministic Volterra series and the stochastic version

proposed in a problem of damage detection in a nonlinear structure considering data variation, showing the higher performance of the use of the stochastic model when one takes into account the presence of uncertainties.

A few examples and applications performed during the doctorate studies with the subject of this thesis were published in the following journal papers:

- Villani, Silva and Cunha Junior (2017a): "Damage detection in an uncertain nonlinear beam";
- Villani, Silva and Cunha Junior (2019b): "Damage detection in uncertain nonlinear systems based on stochastic Volterra series";
- Villani *et al.* (2019a): "Damage detection in an uncertain nonlinear beam based on stochastic Volterra series: An experimental application";
- Villani *et al.* (2019b): "On the detection of a nonlinear damage in an uncertain nonlinear beam using stochastic Volterra series".

And in the following conference papers:

- Teloli *et al.* (2016): "Use of Restoring Surface Method to Estimate a Stochastic Model of a Nonlinear Beam with Cubic Stiffness";
- Villani, Silva and Cunha Junior (2016): "Identification of a nonlinear beam through a stochastic model based on a Duffing oscillator";
- Villani, Silva and Cunha Junior (2017b): "Quantificação de Incertezas nos Núcleos de Volterra de um Oscilador de Duffing";
- Villani, Silva and Cunha Junior (2017c): "Uncertainty quantification in Volterra series analysis of a nonlinear beam considering the noise effect";
- Villani, Silva and Cunha Junior (2019a): "Application of a stochastic version of the restoring force surface method to identify a Duffing oscillator";
- Villani *et al.* (2019c): "Structural Health Monitoring in Uncertain Nonlinear Systems".

7.3 SUGGESTIONS FOR FUTURE WORKS

Some topics for future research works can be suggested by the author to improve the results obtained and to make the methodology even more close to real applications:

- This work was developed based on a frequentist statistical analysis that demands a high number of experimental realizations. It is suggested to apply a Bayesian methodology in the process of Volterra kernels estimation to reduce the amount of data required;
- The Monte Carlo simulations represent a high computational cost to the methodology. So, propagation of uncertainties based o Polynomial Chaos Expansions (PCE) can improve the method, reducing the time consumed in the estimation of the stochastic reference model;
- The consideration of the model uncertainties and not only data uncertainties as described in this thesis;
- The use of more powerful classification methods instead of the Mahalanobis Squared Distance (MSD) in problems where multiple damages can occur at the same time or when the localization of the damage is necessary. Applications considering more complex structures subjected to different kinds of damage at the same time can require more sophisticated classification methods;
- The implementation of another nonparametric stochastic model to compare the performance as a reference model in the process of damage detection. In this sense, the Gaussian Process - Nonlinear Autoregressive with Exogenous input (GP-NARX) models and Polynomial Chaos Expansion - kriging (PCE-kriging) models can be interesting candidates to be studied;
- The analysis of damages with a higher level of complexity, e. g., damages that have influence in the damping of structures or that can induce hysteresis behavior (TELOLI; SILVA, 2019). It is expected a requirement of an improvement in the model to describe these kinds of damages since the Volterra series suggests a weakly nonlinear behavior of the structure;
- Applications considering quantification of damages extension based on the indices estimated in different structural conditions and tendency curves based on Gaussian Process (GP) regression models (AMER; KOPSAFTOPOULOS, 2019).

REFERENCES

AMER, A.; KOPSAFTOPOULOS, F. Probabilistic damage quantification via the integration of non-parametric time-series and Gaussian Process regression models. In: INTERNATIONAL WORKSHOP ON STRUCTURAL HEALTH MONITORING - IWSHM 2019, 12., 2019, Stanford. **Proceedings** [...]. Stanford: [s.n.], 2019.

ANDREAUS, U.; BARAGATTI, P. Experimental damage detection of cracked beams by using nonlinear characteristics of forced response. **Mechanical Systems and Signal Processing**, London, v. 31, p. 382--404, 2012. ISSN 0888-3270. Available from: http://www.sciencedirect.com/science/article/pii/S0888327012001343. Access on: 17 Jan. 2018.

ANDREAUS, U.; CASINI, P.; VESTRONI, F. Non-linear dynamics of a cracked cantilever beam under harmonic excitation. **International Journal of Non-Linear Mechanics**, Kidlington, v. 42, n. 3, p. 566--575, 2007. ISSN 0020-7462. Available from: http://www.sciencedirect.com/science/article/pii/S0020746207000820. Access on: 24 Jun. 2016.

AVENDAÑO-VALENCIA, L. D.; FASSOIS, S. D. Damage/fault diagnosis in an operating wind turbine under uncertainty via a vibration response Gaussian mixture random coefficient model based framework. **Mechanical Systems and Signal Processing**, London, v. 91, p. 326--353, 2017. ISSN 0888-3270. Available from: http://www.sciencedirect.com/science/article/pii/S0888327016305040. Access on: 12 Nov. 2018.

AVENDAÑO-VALENCIA, L. D.; FASSOIS, S. D. Gaussian mixture random coefficient model based framework for SHM in structures with time--dependent dynamics under uncertainty. **Mechanical Systems and Signal Processing**, London, v. 97, p. 59--83, 2017. Available from: http://www.sciencedirect.com/science/article/pii/S0888327017302054. Access on: 14 Oct. 2019.

AVITABILE, P. Experimental modal analysis. **Sound and vibration**, Henderson, v. 35, n. 1, p. 20--31, 2001.

BARTON, D. A. W.; BURROW, S. G.; CLARE, L. R. Energy harvesting from vibrations with a nonlinear oscillator. **Journal of Vibration and Acoustics**, London, v. 132, n. 2, mar. 2010. ISSN 1048-9002. 021009. Available from: http://doi.org/10.1115/1.4000809. Access on: 23 Oct. 2017.

BATOU, A.; SOIZE, C.; AUDEBERT, S. Model identification in computational stochastic dynamics using experimental modal data. **Mechanical Systems and Signal Processing**, London, v. 50, p. 307--322, 2015. ISSN 0888-3270. Available from: http://www.sciencedirect.com/science/article/pii/S0888327014001393. Access on: 21 Aug. 2017.

BEHMANESH, I.; MOAVENI, B.; LOMBAERT, G.; PAPADIMITRIOU, C. Hierarchical Bayesian model updating for structural identification. **Mechanical Systems and Signal Processing**, London, v. 64-65, p. 360--376, 2015. ISSN 0888-3270. Available from: http://www.sciencedirect.com/science/article/pii/S0888327015001545. Access on: 18 May 2017.

BORNN, L.; FARRAR, C. R.; PARK, G. Damage detection in initially nonlinear systems. **International Journal of Engineering Science**, Amsterdam, v. 48, n. 10, p. 909--920, 2010. ISSN 0020-7225. Structural Health Monitoring in the Light of Inverse Problems of Mechanics. Available from: http://www.sciencedirect.com/science/article/pii/S0020722510001059. Access on: 10 Dec. 2015.

BOWMAN, A. W.; AZZALINI, A. **Applied smoothing techniques for data analysis:** the kernel approach with S-Plus illustrations. [S.l.]: OUP Oxford, 1997.

BUSSETTA, P.; SHIKI, S. B.; SILVA, S. da. Nonlinear updating method: a review. **Journal of the Brazilian Society of Mechanical Sciences and Engineering**, Berlin, v. 39, n. 11, p. 4757--4767, Nov 2017. ISSN 1806-3691. Available from: http://doi.org/10.1007/s40430-017-0905-7. Access on: 10 Sep. 2018.

CAKIR, F.; UYSAL, H.; ACAR, V. Experimental modal analysis of masonry arches strengthened with graphene nanoplatelets reinforced prepreg composites. **Measurement**, Amsterdam, v. 90, p. 233--241, 2016. ISSN 0263-2241. Available from: http://www.sciencedirect.com/science/article/pii/S0263224116301282. Access on: 20 Aug. 2018.

CAPIEZ-LERNOUT, E.; SOIZE, C. Robust updating of uncertain damping models in structural dynamics for low- and medium-frequency ranges. **Mechanical Systems and Signal Processing**, London, v. 22, n. 8, p. 1774--1792, 2008. ISSN 0888-3270. Available from: http://www.sciencedirect.com/science/article/pii/S0888327008000393. Access on: 20 Jul. 2017.

CHANG, J.; LIU, W.; HU, H.; NAGARAJAIAH, S. Improved independent component analysis based modal identification of higher damping structures. **Measurement**, Amsterdam, v. 88, p. 402--416, 2016. ISSN 0263-2241. Available from: http://www.sciencedirect.com/science/article/pii/S0263224116001858. Access on: 10 Oct. 2017.

CHATI, M.; RAND, R.; MUKHERJEE, S. Modal analysis of a cracked beam. **Journal of Sound and Vibration**, London, v. 207, n. 2, p. 249--270, 1997. ISSN 0022-460X. Available from: http://www.sciencedirect.com/science/article/pii/S0022460X97910993. Access on: 10 Apr. 2017.

CHATTERJEE, A. Parameter estimation of Duffing oscillator using Volterra series and multi-tone excitation. **International Journal of Mechanical Sciences**, Kidlington, v. 52, n. 12, p. 1716--1722, 2010. ISSN 0020-7403. Available from: http://www.sciencedirect.com/science/article/pii/S002074031000216X. Access on: 18 Aug. 2017.

CHATTERJEE, A. Structural damage assessment in a cantilever beam with a breathing crack using higher order frequency response functions. **Journal of Sound and**

Vibration, London, v. 329, n. 16, p. 3325--3334, 2010. ISSN 0022-460X. Available from: http://www.sciencedirect.com/science/article/pii/S0022460X10001495. Access on: 16 Aug. 2016.

CUNHA JUNIOR, A. Modeling and quantification of physical systems uncertainties in a probabilistic framework. In: EKWARO-OSIRE, S.; GONCALVES, A. C.; ALEMAYEHU, F. M. (Ed.). **Probabilistic Prognostics and Health Management of Energy Systems**. New York: Springer International Publishing, 2017. p. 127--156.

CUNHA JUNIOR, A.; FELIX, J. L. P.; BALTHAZAR, J. M. Quantification of parametric uncertainties induced by irregular soil loading in orchard tower sprayer nonlinear dynamics. **Journal of Sound and Vibration**, London, v. 408, p. 252--269, 2017. ISSN 0022-460X. Available from: http://www.sciencedirect.com/science/article/pii/S0022460X17305473. Access on: 18 Aug. 2017.

CUNHA JUNIOR, A.; NASSER, R.; SAMPAIO, R.; LOPES, H.; BREITMAN, K. Uncertainty quantification through the Monte Carlo method in a cloud computing setting. **Computer Physics Communications**, Amsterdam, v. 185, n. 5, p. 1355--1363, 2014. ISSN 0010-4655. Available from: http://www.sciencedirect.com/science/article/pii/S0010465514000198. Access on: 13 Jun. 2016.

CUNHA JUNIOR, A.; SAMPAIO, R. On the nonlinear stochastic dynamics of a continuous system with discrete attached elements. **Applied Mathematical Modelling**, New York, v. 39, n. 2, p. 809--819, 2015. ISSN 0307-904X. Available from: http://www.sciencedirect.com/science/article/pii/S0307904X14003552. Access on: 18 Aug. 2017.

EWINS, D. J.; SAUNDERS, H. **Modal testing:** theory and practice. [S.l.]: American Society of Mechanical Engineers Digital Collection, 1986.

FARRAR, C. R.; WORDEN, K. An introduction to structural health monitoring. **Philosophical Transactions of the Royal Society A: Mathematical,Physical and Engineering Sciences**, London, v. 365, n. 1851, p. 303--315, 2007. Available from: http://rsta.royalsocietypublishing.org/content/365/1851/303.abstract. Access on: 20 Jul. 2015.

FARRAR, C. R.; WORDEN, K. **Structural health monitoring:** a machine learning perspective. [S.l.]: John Wiley & Sons, 2012. 654 p.

FIGUEIREDO, E.; RADU, L.; WORDEN, K.; FARRAR, C. R. A Bayesian approach based on a Markov-Chain Monte Carlo method for damage detection under unknown sources of variability. **Engineering Structures**, Kidlington, v. 80, p. 1--10, 2014. ISSN 0141-0296. Available from: http://www.sciencedirect.com/science/article/pii/S0141029614005136. Access on: 12 Jun. 2017.

FIGUEIREDO, E.; TODD, M. D.; FARRAR, C. R.; FLYNN, E. Autoregressive modeling with state-space embedding vectors for damage detection under operational variability. **International Journal of Engineering Science**, Amsterdam, v. 48, n. 10, p. 822--834, 2010. ISSN 0020-7225. Structural Health Monitoring in the Light of Inverse Problems of Mechanics. Available from: http://www.sciencedirect.com/science/article/pii/S0020722510000996. Access on: 20 May 2016.

GHRIB, M.; RéBILLAT, M.; ROCHES, G. V. des; MECHBAL, N. Automatic damage type classification and severity quantification using signal based and nonlinear model based damage sensitive features. **Journal of Process Control**, London, 2018. ISSN 0959-1524. Available from: http://www.sciencedirect.com/science/article/pii/S0959152418301975. Access on: 10 Aug. 2019.

GRIMMETT, G.; WELSH, D. **Probability:** an introduction. [S.l.]: Oxford University, 2014.

HARDIN, J.; ROCKE, D. M. The distribution of robust distances. **Journal of Computational and Graphical Statistics**, Taylor & Francis, New York, v. 14, n. 4, p. 928--946, 2005. Available from: http://doi.org/10.1198/106186005X77685. Access on: 10 Jul. 2017.

HEIDENREICH, S.; GROSS, H.; BÄR, M.; WRIGHT, L. Uncertainty propagation in computationally expensive models: A survey of sampling methods and application to scatterometry. **Measurement**, Amsterdam, v. 97, p. 79 -- 87, 2017. ISSN 0263-2241. Available from: http://www.sciencedirect.com/science/article/pii/S0263224116302901. Access on: 20 Aug. 2018.

HEUBERGER, P. S. C.; HOF, P. M. J. Van den; WAHLBERG, B. **Modelling and identification with rational orthogonal basis functions**. [S.l.]: Springer, 2005.

JAYNES, E. T. Information theory and statistical mechanics. **Physical Review**, American Physical Society, College Park, v. 106, p. 620--630, May 1957. Available from: http://link.aps.org/doi/10.1103/PhysRev.106.620. Access on: 18 Aug. 2017.

KAUTZ, W. H. Transient synthesis in the time domain. **Transactions of the IRE Professional Group on Circuit Theory**, Piscataway, CT-1, n. 3, p. 29--39, September 1954. ISSN 0197-6389. Available from: http://ieeexplore.ieee.org/document/1083588. Access on: 10 Feb. 2015.

KERSCHEN, G.; GOLINVAL, J. C.; WORDEN, K. Theoretical and experimental identification of a non-linear beam. **Journal of Sound and Vibration**, London, v. 244, n. 4, p. 597--613, 2001. ISSN 0022-460X. Available from: http://www.sciencedirect.com/science/article/pii/S0022460X00934904. Access on: 15 Apr. 2016.

KERSCHEN, G.; LENAERTS, V.; GOLINVAL, J. C. VTT Benchmark: Application of the restoring force surface method. **Mechanical Systems and Signal Processing**, London, v. 17, n. 1, p. 189 --193, 2003. ISSN 0888-3270. Available from: http://www.sciencedirect.com/science/article/pii/S088832700291558X. Access on: 20 Sep. 2016.

KERSCHEN, G.; LENAERTS, V.; MARCHESIELLO, S.; FASANA, A. A frequency domain versus a time domain identification technique for nonlinear parameters applied to wire rope isolators. **Journal of Dynamic Systems, Measurement, and Control**, New York, v. 123, n. 4, p. 645--650, nov. 2000. ISSN 0022-0434. Available from: http://doi.org/10.1115/1.1410368. Access on: 15 Feb. 2016.

KERSCHEN, G.; WORDEN, K.; VAKAKIS, A. F.; GOLINVAL, J.-C. Past, present and future of nonlinear system identification in structural dynamics. **Mechanical Systems and Signal Processing**, London, v. 20, n. 3, p. 505--592, 2006. ISSN 0888-3270.

Available from: http://www.sciencedirect.com/science/article/pii/S0888327005000828. Access on: 21 Nov. 2016.

KERSCHEN, G.; WORDEN, K.; VAKAKIS, A. F.; GOLINVAL, J.-C. Nonlinear system identification in structural dynamics: current status and future directions. In: IMAC - XXV - CELEBRATING 25 YEARS OF IMAC, 25., 2007, Orlando. **Conference Proceedings of the Society for Experimental Mechanics Series**. Orlando: [s.n.], 2007.

KOVACIC, I.; BRENNAN, M. J. **The Duffing equation:** nonlinear oscillators and their behaviour. [S.l.]: John Wiley & Sons, 2011.

KROESE, D. P.; TAIMRE, T.; BOTEV, Z. I. **Handbook of Monte Carlo methods**. [S.l.]: John Wiley & Sons, 2013. ISBN 978-0-470-17793-8.

LEBEL, D.; SOIZE, C.; FUNFSCHILLING, C.; PERRIN, G. Bayesian calibration of mechanical parameters of high-speed train suspensions. **Procedia Engineering**, Amsterdam, v. 199, p. 1234--1239, 2017. ISSN 1877-7058. Available from: http://www.sciencedirect.com/science/article/pii/S1877705817337098. Access on: 10 Oct. 2019.

LEBEL, D.; SOIZE, C.; FUNFSCHILLING, C.; PERRIN, G. High-speed train suspension health monitoring using computational dynamics and acceleration measurements. **Vehicle System Dynamics**, Abingdon, 2019. Available from: http://www.doi.org/10.1080/00423114.2019.1601744. Access on: 15 Oct. 2019.

LESTOILLE, N.; SOIZE, C.; FUNFSCHILLING, C. Stochastic prediction of high-speed train dynamics to long-term evolution of track irregularities. **Mechanics Research Communications**, Oxford, v. 75, p. 29--39, 2016. ISSN 0093-6413. Available from: http://www.sciencedirect.com/science/article/pii/S0093641316300337. Access on: 15 Oct. 2019.

LIM, H. J.; SOHN, H.; DESIMIO, M. P.; BROWN, K. Reference-free fatigue crack detection using nonlinear ultrasonic modulation under various temperature and loading conditions. **Mechanical Systems and Signal Processing**, London, v. 45, n. 2, p. 468 -- 478, 2014. ISSN 0888-3270. Available from: http://www.sciencedirect.com/science/article/pii/S0888327013006468. Access on: 12 Jun. 2017.

MANDAL, D. D.; WADADAR, D.; BANERJEE, S. Health monitoring of stiffened metallic plates using nonlinear wave interaction and embedded PZT transducers. In: SINHA, J. (Ed.). **Vibration Engineering and Technology of Machinery**. Cham: Springer, 2015. v. 23, p. 629--638. ISBN 978-3-319-09918-7. Available from: http://doi.org/10.1007/978-3-319-09918-7_56. Access on: 05 Nov. 2019.

MAO, Z.; TODD, M. Statistical modeling of frequency response function estimation for uncertainty quantification. **Mechanical Systems and Signal Processing**, London, v. 38, n. 2, p. 333 -- 345, 2013. ISSN 0888-3270. Available from: http://www.sciencedirect.com/science/article/pii/S0888327013000757. Access on: 14 Mar. 2018.

MASRI, S. F.; CAUGHEY, T. K. A nonparametric identification technique for nonlinear dynamic problems. **Journal of Applied Mechanics**, American Society of Mechanical Engineers, New York, v. 46, n. 2, p. 433--447, 1979. Available from: http://doi.org/10.1115/1.3424568. Access on: 20 Jan. 2016.

NOËL, J.-P.; KERSCHEN, G. Nonlinear system identification in structural dynamics: 10 more years of progress. **Mechanical Systems and Signal Processing**, London, v. 83, p. 2--35, 2016. Available from: http://dx.doi.org/10.1016/j.ymssp.2016.07.020i. Access on: 14 Aug. 2017.

NOËL, J. P.; KERSCHEN, G.; NEWERLA, A. Application of the restoring force surface method to a real-life spacecraft structure. In: D. KERSCHEN G., C. A. A. (Ed.). **Topics in Nonlinear Dynamics**. New York: Springer, 2012. v. 3, p. 1--19. ISBN 978-1-4614-2416-1. Available from: http://doi.org/10.1007/978-1-4614-2416-1_1. Access on: 05 Nov. 2019.

NOËL, J. P.; RENSON, L.; KERSCHEN, G. Complex dynamics of a nonlinear aerospace structure: Experimental identification and modal interactions. **Journal of Sound and Vibration**, London, v. 333, n. 12, p. 2588--2607, 2014. ISSN 0022-460X. Available from: http://www.sciencedirect.com/science/article/pii/S0022460X14000704. Access on: 05 Dec. 2016.

OLIVEIRA, G. H. C.; ROSA, A. da; CAMPELLO, R. J. G. B.; MACHADO, J. B.; AMARAL, W. C. An introduction to models based on Laguerre, Kautz and other related orthonormal functions - Part II: non-linear models. **International Journal of Modelling, Identification and Control**, Olney, v. 16, n. 1, p. 1--14, 2012. Available from: http://www.inderscienceonline.com/doi/abs/10.1504/IJMIC.2012.046691. Access on: 18 Aug. 2017.

PARK, S.; LEE, J.-J.; YUN, C.-B.; INMAN, D. J. Electro-mechanical impedance-based wireless structural health monitoring using PCA-data compression and k-means clustering algorithms. **Journal of Intelligent Material Systems and Structures**, London, v. 19, n. 4, p. 509--520, 2008. Available from: http://doi.org/10.1177/1045389X07077400. Access on: 16 Sep. 2016.

PAVLOPOULOU, S.; WORDEN, K.; SOUTIS, C. Novelty detection and dimension reduction via guided ultrasonic waves: Damage monitoring of scarf repairs in composite laminates. **Journal of Intelligent Material Systems and Structures**, London, v. 27, n. 4, p. 549--566, 2016. Available from: http://dx.doi.org/10.1177/1045389X15574937. Access on: 14 Jan. 2019.

PENG, Z. K.; LANG, Z. Q.; BILLINGS, S. A. Crack detection using nonlinear output frequency response functions. **Journal of Sound and Vibration**, London, v. 301, n. 3, p. 777--788, 2007. ISSN 0022-460X. Available from: http://www.sciencedirect.com/science/article/pii/S0022460X06008315. Access on: 15 Jun. 2017.

POULIMENOS, A. G.; SAKELLARIOU, J. S. A transmittance-based methodology for damage detection under uncertainty: An application to a set of composite beams with manufacturing variability subject to impact damage and varying operating conditions. **Structural Health Monitoring**, New York, v. 18, n. 1, p. 318--333, 2019. Available from: http://doi.org/10.1177/1475921718779190. Access on: 15 Oct. 2019.

PRAWIN, J.; RAO, A. R. M. Nonlinear structural damage detection based on adaptive Volterra filter model. **International Journal of Structural Stability and Dynamics**, Singapore, v. 18, p. 12, 2018. Available from: http://www.worldscientific.com/doi/abs/10.1142/S0219455418710037. Access on: 10 Apr. 2019.

RÉBILLAT, M.; HAJRYA, R.; MECHBAL, N. Nonlinear structural damage detection based on cascade of Hammerstein models. **Mechanical Systems and Signal Processing**, London, v. 48, n. 1, p. 247--259, 2014. ISSN 0888-3270. Available from: http://www.sciencedirect.com/science/article/pii/S0888327014000843. Access on: 13 Nov. 2017.

RÉBILLAT, M.; HENNEQUIN, R.; CORTEEL, E.; KATZ, B. F. G. Identification of cascade of Hammerstein models for the description of nonlinearities in vibrating devices. **Journal of Sound and Vibration**, London, v. 330, n. 5, p. 1018--1038, 2011. ISSN 0022-460X. Available from: http://www.sciencedirect.com/science/article/pii/S0022460X10006176. Access on: 22 Oct. 2016.

RÉBILLAT, M.; HMAD, O.; KADRI, F.; MECHBAL, N. Peaks over threshold-based detector design for structural health monitoring: Application to aerospace structures. **Structural Health Monitoring**, New York, v. 17, n. 1, p. 91--107, 2018. Available from: http://doi.org/10.1177/1475921716685039. Access on: 10 Dec. 2018.

RITTO, T. G.; SAMPAIO, R.; AGUIAR, R. R. Uncertain boundary condition Bayesian identification from experimental data: A case study on a cantilever beam. **Mechanical Systems and Signal Processing**, London, v. 68-69, p. 176--188, 2016. ISSN 0888-3270. Available from: http://www.sciencedirect.com/science/article/pii/S0888327015003714. Access on: 05 Mar. 2018.

ROSA, A. da; CAMPELLO, R. J. G. B.; AMARAL, W. C. Choice of free parameters in expansions of discrete-time Volterra models using Kautz functions. **Automatica**, Oxford, v. 43, n. 6, p. 1084--1091, 2007. ISSN 0005-1098. Available from: http://www.sciencedirect.com/science/article/pii/S0005109807000738. Access on: 18 Aug. 2017.

RUBINSTEIN, R. Y.; KROESE, D. P. **Simulation and the Monte Carlo Method**. 3rd. ed. [S.l.]: Wiley, 2016.

RYTTER, A. **Vibrational based inspection of civil engineering structures.** 1993. Thesis (Ph. D.) --- College, University of Aalborg, Denmark, 1993. Available from: http://vbn.aau.dk/en/publications/vibrational-based-inspection-of-civil-engineering-structures. Access on: 23 May 2016.

SANTOS, A.; FIGUEIREDO, E.; SILVA, M. F. M.; SALES, C. S.; COSTA, J. C. W. A. Machine learning algorithms for damage detection: Kernel-based approaches. **Journal of Sound and Vibration**, London, v. 363, p. 584--599, 2016. ISSN 0022-460X. Available from: http://www.sciencedirect.com/science/article/pii/S0022460X15009049. Access on: 05 Mar. 2018.

SCHETZEN, M. **The Volterra and Wiener theories of nonlinear systems**. [S.l.]: Wiley, 1980.

SCUSSEL, O.; SILVA, S. da. Output-only identification of nonlinear systems via Volterra series. **Journal of Vibration and Acoustics**, London, v. 138, n. 4, 2016. ISSN 1048-9002. 041012. Available from: http://doi.org/10.1115/1.4033458. Access on: 06 Oct. 2016.

SCUSSEL, O.; SILVA, S. da. The harmonic probing method for output-only nonlinear mechanical systems. **Journal of the Brazilian Society of Mechanical Sciences and Engineering**, Berlin, v. 39, n. 9, p. 3329--3341, set. 2017. ISSN 1806-3691. Available from: http://doi.org/10.1007/s40430-017-0723-y. Access on: 28 Aug. 2018.

SHIKI, S. B.; SILVA, S. da; TODD, M. D. On the application of discrete-time Volterra series for the damage detection problem in initially nonlinear systems. **Structural Health Monitoring**, New York, v. 16, n. 1, p. 62--78, 2017. Available from: http://dx.doi.org/10.1177/1475921716662142. Access on: 18 Aug. 2017.

SILVA, J. M. M. e; MAIA, N. M. M. **Modal analysis and testing**. [S.l.]: Springer Science & Business Media, 2012.

SILVA, S. da. Non-linear model updating of a three-dimensional portal frame based on Wiener series. **International Journal of Non-Linear Mechanics**, Amsterdam, v. 46, n. 1, p. 312--320, 2011. ISSN 0020-7462. Available from: http://www.sciencedirect.com/science/article/pii/S0020746210001472. Access on: 18 Aug. 2017.

SILVA, S. da. Non-parametric identification of mechanical systems by Kautz filter with multiple poles. **Mechanical Systems and Signal Processing**, London, v. 25, n. 4, p. 1103--1111, 2011. ISSN 0888-3270. Available from: http://www.sciencedirect.com/science/article/pii/S0888327010004139. Access on: 18 Aug. 2017.

SILVA, S. da; COGAN, S.; FOLTÊTE, E. Nonlinear identification in structural dynamics based on Wiener series and Kautz filters. **Mechanical Systems and Signal Processing**, London, v. 24, n. 1, p. 52--58, jan. 2010. ISSN 0888-3270. Available from: http://www.sciencedirect.com/science/article/pii/S0888327009001897. Access on: 20 Sep. 2016.

SILVERMAN, B. W. **Density estimation for statistics and data analysis**. [S.l.]: CRC, 1986.

SOHN, H. Effects of environmental and operational variability on structural health monitoring. **Philosophical Transactions of the Royal Society of London A: Mathematical, Physical and Engineering Sciences**, London, v. 365, n. 1851, p. 539--560, 2007. ISSN 1364-503X. Available from: http://rsta.royalsocietypublishing.org/content/365/1851/539. Access on: 10 Jan. 2017.

SOHN, H.; ALLEN, D. W.; WORDEN, K.; FARRAR, C. R. Structural damage classification using extreme value statistics. **Journal of Dynamic Systems, Measurement, and Control**, New York, v. 127, n. 1, p. 125--132, 05 2005. ISSN 0022-0434. Available from: http://doi.org/10.1115/1.1849240. Access on: 20 Apr. 2016.

SOIZE, C. A comprehensive overview of a non-parametric probabilistic approach of model uncertainties for predictive models in structural dynamics. **Journal of Sound and Vibration**, London, v. 288, n. 3, p. 623--652, 2005. ISSN 0022-460X. Uncertainty in structural dynamicsUncertainty in structural dynamics. Available from: http://www.sciencedirect.com/science/article/pii/S0022460X05004542. Access on: 18 Aug. 2018.

SOIZE, C. **Stochastic models of uncertainties in computational mechanics**. [S.l.]: Amer Society of Civil Engineers, 2012.

SOIZE, C. Stochastic modeling of uncertainties in computational structural dynamics -- recent theoretical advances. **Journal of Sound and Vibration**, London, v. 332, n. 10, p. 2379 -- 2395, 2013. ISSN 0022-460X. Available from: http://www.sciencedirect.com/science/article/pii/S0022460X11007966. Access on: 19 Jun. 2017.

SOIZE, C. **Uncertainty quantification:** an accelerated course with advanced applications in computational engineering. [S.l.]: Springer, 2017.

SOIZE, C.; CAPIEZ-LERNOUT, E.; OHAYON, R. Robust updating of uncertain computational models using experimental modal analysis. **AIAA Journal**, Reston, v. 46, n. 11, p. 2955--2965, 2008. Available from: http://doi.org/10.2514/1.38115. Access on: 11 Apr. 2016.

SUDRET, B. Probabilistic models for the extent of damage in degrading reinforced concrete structures. **Reliability Engineering & System Safety**, London, v. 93, n. 3, p. 410--422, 2008. ISSN 0951-8320. Probabilistic Modelling of Structural Degradation. Available from: http://www.sciencedirect.com/science/article/pii/S095183200700004X. Access on: 10 Oct. 2019.

SURACE, C.; RUOTOLO, R.; STORER, D. Detecting nonlinear behaviour using the Volterra series to assess damage in beam-like structures. **Journal of Theoretical and Applied Mechanics**, Sofia, v. 49, n. 3, p. 905--926, 2011.

TANG, B.; BRENNAN, M. J.; LOPES JUNIOR., V.; SILVA, S. da; RAMLAN, R. Using nonlinear jumps to estimate cubic stiffness nonlinearity: An experimental study. **Proceedings of the Institution of Mechanical Engineers, Part C: Journal of Mechanical Engineering Science**, London, v. 230, n. 19, p. 3575--3581, 2016. Available from: http://doi.org/10.1177/0954406215606746. Access on: 15 Feb. 2017.

TANG, H.; LIAO, Y. H.; CAO, J. Y.; XIE, H. Fault diagnosis approach based on Volterra models. **Mechanical Systems and Signal Processing**, London, v. 24, n. 4, p. 1099--1113, 2010. ISSN 0888-3270. Available from: http://www.sciencedirect.com/science/article/pii/S0888327009002611. Access on: 11 Nov. 2016.

TELOLI, R. O.; SILVA, S. da. A new way for harmonic probing of hysteretic systems through nonlinear smooth operators. **Mechanical Systems and Signal Processing**, London, v. 121, p. 856--875, 2019. ISSN 0888-3270. Available from: http://www.sciencedirect.com/science/article/pii/S0888327018307659. Access on: 21 Oct. 2019.

TELOLI, R. O.; VILLANI, L. G. G.; SILVA, S. d.; CUNHA JUNIOR, A. Uso do Método de Superfície de Resposta para Estimar um Modelo Estocástico de uma Viga Não Linear com Rigidez Cúbica. In: CONGRESSO NACIONAL DE ENGENHARIA MECÂNICA - CONEM 2016, 9., 2016, Fortaleza. **Proceedings** [...]. Fortaleza: [s.n.], 2016. Available from: https://hal.archives-ouvertes.fr/hal-01471297. Access on: 10 Sep. 2017.

VAMVOUDAKIS-STEFANOU, K. J.; SAKELLARIOU, J. S.; FASSOIS, S. D. Vibration-based damage detection for a population of nominally identical structures: Unsupervised Multiple Model (MM) statistical time series type methods. **Mechanical Systems and Signal Processing**, London, v. 111, p. 149 -- 171, 2018. ISSN 0888-3270. Available from: http://www.sciencedirect.com/science/article/pii/S0888327018301808. Access on: 20 Aug. 2019.

VILLANI, L. G. G.; SILVA, S. da; CUNHA JUNIOR, A. Identification of a nonlinear beam through a stochastic model based on a Duffing oscillator. In: INTERNATIONAL CONFERENCE ON NONLINEAR SCIENCE AND COMPLEXITY - NSC 2016, 6., 2016, São José dos Campos. **Proceedings** [...]. São José dos Campos? [s.n], 2016. Available from: https://hal.archives-ouvertes.fr/hal-01471296. Access on: 20 Oct. 2018.

VILLANI, L. G. G.; SILVA, S. da; CUNHA JUNIOR, A. Damage detection in an uncertain nonlinear beam. **Procedia Engineering**, Amsterdam, v. 199, p. 2090--2095, 2017. ISSN 1877-7058. Available from: http://www.sciencedirect.com/science/article/pii/S1877705817339759. Access on: 10 Oct. 2018.

VILLANI, L. G. G.; SILVA, S. da; CUNHA JUNIOR, A. Quantificação de Incertezas nos Núcleos de Volterra de um Oscilador de Duffing. In: CONGRESSO NACIONAL DE MATEMÁTICA APLICADA E COMPUTACIONAL - CNMAC 2016, 36., 2016, Gramado. **Proceedings** [...]. Gramado: [s.n.], 2017. v. 5, n. 1. (Series of the Brazilian Society of Computational and Applied Mathematics). Available from: https://proceedings.sbmac.org.br/sbmac/article/viewFile/1280/1294. Access on: 10 Nov. 2018.

VILLANI, L. G. G.; SILVA, S. da; CUNHA JUNIOR, A. Uncertainty quantification in Volterra series analysis of a nonlinear beam considering the noise effect. In: INTERNATIONAL SYMPOSIUM ON DYNAMIC PROBLEMS OF MECHANICS - DINAME 2017, 17., 2017, São Sebastião. **Proceedings** [...]. São Sebastião: [s.n.], 2017. Available from: https://hal.archives-ouvertes.fr/hal-01487344. Access on: 20 Sep. 2018.

VILLANI, L. G. G.; SILVA, S. da; CUNHA JUNIOR, A. Application of a stochastic version of the restoring force surface method to identify a Duffing oscillator. In: INTERNATIONAL NONLINEAR DYNAMICS CONFERENCE - NODYCON 2019, 1., 2019, Rome. **Proceedings** [...]. Rome: [s.n.], 2019. v. 1, p. 335--336.

VILLANI, L. G. G.; SILVA, S. da; CUNHA JUNIOR, A. Damage detection in uncertain nonlinear systems based on stochastic Volterra series. **Mechanical Systems and Signal Processing**, London, v. 125, p. 288--310, 2019. ISSN 0888-3270. Exploring nonlinear benefits in engineering. Available from: http://www.sciencedirect.com/science/article/pii/S0888327018304291. Access on: 10 Oct. 2019.

VILLANI, L. G. G.; SILVA, S. da; CUNHA JUNIOR, A.; TODD, M. D. Damage detection in an uncertain nonlinear beam based on stochastic Volterra series: An experimental application. **Mechanical Systems and Signal Processing**, London, v. 128, p. 463--478, 2019. ISSN 0888-3270. Available from: http://www.sciencedirect.com/science/article/pii/S0888327019302250. Access on: 15 Oct. 2019.

VILLANI, L. G. G.; SILVA, S. da; CUNHA JUNIOR, A.; TODD, M. D. On the detection of a nonlinear damage in an uncertain nonlinear beam using stochastic Volterra series. **Structural Health Monitoring**, New York, 2019. Available from: http://doi.org/10.1177/1475921719876086. Access on: 17 Oct. 2019.

VILLANI, L. G. G.; SILVA, S. da; CUNHA JUNIOR, A.; TODD, M. D. Structural health monitoring in uncertain nonlinear systems. In: INTERNATIONAL MODAL ANALYSIS CONFERENCE - IMAC, 37., 2019, Orlando. **Abstract Book**. Orlando: [s.n.], 2019.

VIRGIN, L. N. **Introduction to experimental nonlinear dynamics**. [S.l.]: Cambridge University, 2000.

WAHLBERG, B. System identification using Kautz models. **IEEE Transactions on Automatic Control**, Piscataway, v. 39, n. 6, p. 1276--1282, Jun 1994. ISSN 0018-9286.

WAHLBERG, B.; MAKILA, P. M. On approximation of stable linear dynamical systems using Laguerre and Kautz functions. **Automatica**, Oxford, v. 32, n. 5, p. 693--708, 1996. ISSN 0005-1098. Available from: http://www.sciencedirect.com/science/article/pii/0005109895001980. Access on: 18 Aug. 2017.

WASSERMANN, L. **All of nonparametric statistics**. [S.l.]: Springer, 2006. ISBN 9780387306230.

WORDEN, K.; CROSS, E. J. On switching response surface models, with applications to the structural health monitoring of bridges. **Mechanical Systems and Signal Processing**, London, v. 98, p. 139 -- 156, 2018. ISSN 0888-3270. Available from: http://www.sciencedirect.com/science/article/pii/S0888327017302170. Access on: 15 Jul. 2019.

WORDEN, K.; CROSS, E. J.; DERVILIS, N.; PAPATHEOU, E.; ANTONIADOU, I. Structural health monitoring: from structures to systems-of-systems. **IFAC-PapersOnLine**, London, v. 48, n. 21, p. 1--17, 2015. ISSN 2405-8963. 9th IFAC Symposium on Fault Detection, Supervision andSafety for Technical Processes SAFEPROCESS 2015. Available from: http://www.sciencedirect.com/science/article/pii/S2405896315016262. Access on: 26 Jun. 2017.

WORDEN, K.; FARRAR, C. R.; HAYWOOD, J.; TODD, M. A review of nonlinear dynamics applications to structural health monitoring. **Structural Control and Health Monitoring**, Oxford, v. 15, n. 4, p. 540--567, 2008. ISSN 1545-2263. Available from: http://dx.doi.org/10.1002/stc.215. Access on: 28 Mar. 2016.

WORDEN, K.; KERSCHEN, G.; VAKAKIS, A. F.; GOLINVAL, J.-C. Nonlinear system identification in structural dynamics: A short (and biased) history. In: CONFERENCE PROCEEDINGS OF THE SOCIETY FOR EXPERIMENTAL MECHANICS SERIES

- IMAC, 25., 2007, Orlando. **Proceedings** [...]. Orlando: [s.n.], 2007. p. 1996--2017. (Society for Experimental Mechanics Series).

WORDEN, K.; MANSON, G.; ALLMAN, D. Experimental validation of a structural health monitoring methodology: PART I. novelty detection on a laboratory structure. **Journal of Sound and Vibration**, London, v. 259, n. 2, p. 323--343, 2003. ISSN 0022-460X. Available from: http://www.sciencedirect.com/science/article/pii/S0022460X02951680. Access on: 16 Apr. 2016.

WORDEN, K.; MANSON, G.; FIELLER, N. R. J. Damage detection using outlier analysis. **Journal of Sound and Vibration**, London, v. 229, n. 3, p. 647--667, 2000. ISSN 0022-460X. Available from: http://www.sciencedirect.com/science/article/pii/S0022460X99925142. Access on: 12 Jan. 2016.

WORDEN, K.; TOMLINSON, G. R. **Nonlinearity in structural dynamics: detection, identification and modelling**. [S.l.]: CRC, 2000.

XIA, X.; ZHOU, J.; XIAO, J.; XIAO, H. A novel identification method of Volterra series in rotor-bearing system for fault diagnosis. **Mechanical Systems and Signal Processing**, London, v. 66-67, p. 557--567, 2016. ISSN 0888-3270. Available from: http://www.sciencedirect.com/science/article/pii/S0888327015002277. Access on: 22 Aug. 2017.

YAN, W.-J.; KATAFYGIOTIS, L. S. A novel Bayesian approach for structural model updating utilizing statistical modal information from multiple setups. **Structural Safety**, Amsterdam, v. 52, Part B, p. 260--271, 2015. ISSN 0167-4730. Available from: http://www.sciencedirect.com/science/article/pii/S0167473014000630. Access on: 20 Jun. 2017.

YEAGER, M.; GREGORY, B.; KEY, C.; TODD, M. On using robust Mahalanobis distance estimations for feature discrimination in a damage detection scenario. **Structural Health Monitoring**, New York, v. 18, n. 1, p. 245--253, 2019. Available from: https://doi.org/10.1177/1475921717748878. Access on: 14 Oct. 2019.

YUAN, Z.; LIANG, P.; SILVA, T.; YU, K.; MOTTERSHEAD, J. E. Parameter selection for model updating with global sensitivity analysis. **Mechanical Systems and Signal Processing**, London, v. 115, p. 483--496, 2019. ISSN 0888-3270. Available from: http://www.sciencedirect.com/science/article/pii/S0888327018303078. Access on: 15 Oct. 2019.

ZENG, M.; YANG, Y.; ZHENG, J.; CHENG, J. Normalized complex Teager energy operator demodulation method and its application to fault diagnosis in a rubbing rotor system. **Mechanical Systems and Signal Processing**, London, v. 50, p. 380 -- 399, 2015. ISSN 0888-3270. Available from: http://www.sciencedirect.com/science/article/pii/S0888327014001356. Access on: 14 Jun. 2017.